

The Golgi: a transition point in membrane lipid composition and topology

Quirine Lisman

The research presented in this thesis was performed at the Department of Cell Biology and Histology, Academic Medical Center, University of Amsterdam, and the Department of Membrane Enzymology, Faculty of Chemistry, Utrecht University. The research was financed by a grant from the Meelmeijer Foundation.

Published and distributed by Delft University Press

Cover design: Belia van der Giessen

Lay-out: Ingrid van Rooijen, AV-dienst, Faculteit Scheikunde, Universiteit Utrecht

ISBN: 90-407-2543-8

Keywords: Golgi, yeast, sphingolipids

Copyright © 2004 by Quirine Lisman

All rights reserved. No part of the material protected by this copyright notice may be reproduced or utilized in any form or by any means, electronic or mechanical, including photocopying, recording or by any information storage and retrieval system, without written permission from the publisher: Delft University Press, P.O. Box 98, 2600 MG Delft, The Netherlands. E-mail: info@library.tudelft.nl

The Golgi: a transition point in membrane lipid composition and topology

ACADEMISCH PROEFSCHRIFT

ter verkrijging van de graad van doctor aan de Universiteit van Amsterdam
op gezag van de Rector Magnificus prof. mr. P.F. van der Heijden
ten overstaan van een door het college voor promoties ingestelde commissie,
in het openbaar te verdedigen in de Aula der Universiteit

op vrijdag 17 december 2004, te 12.00 uur

door

Catherine Quirine Lisman

geboren te Oss

Promotiecommissie:

promotor: Prof. dr. G.E.B.P. van Meer

co-promotor: Dr. J.C.M. Holthuis

overige leden: Prof. dr. J.M.F.G. Aerts
Prof. dr. L.J. Braakman
Dr. B. Distel
Prof. dr. M.R. Egmond
Prof. dr. C.J.F. van Noorden
Prof. dr. R.P.J. Oude Elferink

Faculteit Geneeskunde

Pro Movere

Voor beweging
En vooruitgang
Voor beleving
En weest niet bang

Dat wetenschap
wordt bedreven
Maar weest gerust, bewust

En zonder dat
Het leven
Maar wordt gesust, geblust

Of belandt
In stilstand.

Nee,
Die onderzoekspracht
Dat zag ik meteen
Blijkt niet onverwacht
Een rollende steen

Traagheid gedijt
Info verspreidt

De steen versnelt
En is niet te keren
Vrees is hersteld
Men zal blijven leren

LJMF '04

Contents

Chapter 1	
General introduction	9
Chapter 2	
Protein sorting in the late Golgi of <i>Saccharomyces cerevisiae</i> does not require mannosylated sphingolipids	25
Chapter 3	
Sphingolipid mannosylation in yeast requires Csg2p-dependent manganese transport into the lumen of early secretory organelles	47
Chapter 4	
<i>HOR7</i>, a multicopy suppressor of the Ca²⁺-induced growth defect in sphingolipid mannosyltransferase-deficient yeast	61
Chapter 5	
Loss of the yeast <i>trans</i>-Golgi P-type ATPases Drs2p and Dnf3p disrupts aminophospholipid asymmetry in Pma1p-containing secretory vesicles	77
Chapter 6	
Summarizing discussion	91
Abbreviations	99
Samenvatting	101
Dankwoord	105
Curriculum vitae	109
List of Publications	111

Chapter 1

General introduction*

* Adapted from: van Meer G. and Lisman Q. (2002) Sphingolipid transport: rafts and translocators. *Journal of Biological Chemistry* 277, 25855-8

Until some 15 years ago, sphingolipids were generally believed to protect the cell surface against harmful factors in the environment by forming a mechanically stable and chemically resistant outer leaflet of the plasma membrane lipid bilayer. In addition, complex glycosphingolipids were found to be involved in more specific functions like recognition and signaling (1). Whereas the first feature would depend on the special physical properties of the sphingolipids, the signaling functions would depend on specific interactions of the complex glycan structures on the glycosphingolipids with similar lipids on neighboring cells or with proteins. Since then, two findings have revolutionized the field: (A) Simple sphingolipid metabolites, like ceramide and sphingosine-1-phosphate, have been found to be important mediators in signaling cascades of apoptosis, proliferation and stress responses (2, 3). (B) In addition, it has been realized that ceramide-based lipids self-aggregate in cellular membranes to form a separate phase that is less fluid (liquid-ordered) than the bulk of the cellular membranes that consists of liquid-disordered phospholipids based on diacylglycerol. These sphingolipid-based microdomains or “rafts” were originally proposed to sort membrane proteins along the cellular pathways of membrane transport (4). Presently, most excitement focuses on their organizing functions in signal transduction at the plasma membrane (5).

Sphingolipids are synthesized in the ER and in the Golgi complex, but they are enriched in plasma membrane and endosomes where they perform many of their functions. Some functions have been located to the mitochondria (2). Thus, sphingolipids travel between organelles. Transport occurs via transport vesicles, and in some cases via monomeric transport through the cytosol. Furthermore, as demonstrated below, some sphingolipids efficiently translocate across cellular membranes. That transport is not random is clear from the heterogeneous distribution of sphingolipids over the cell: whereas sphingolipids are virtually absent from mitochondria and the ER, they constitute 20–35 mol% of the total lipids of plasma membranes (Table I). Furthermore, signaling pools of sphingolipids do not freely mix with pools involved in biosynthesis and degradation (2, 3, 6). The specificity in sphingolipid transport is the topic of the present review.

Table 1. Sphingolipid content of various plasma membranes ¹.

mol/mol	sphingolipids	glycerophospholipids	sterol
Intestinal epithelium, apical ²	38	29	33
Intestinal epithelium, basolateral ²	19	56	25
Myelin ³	28	28	44
Yeast plasma membrane ⁴	16	36	48

¹ Plasma membranes are manifold enriched in sphingolipids and cholesterol as compared to the ER and the mitochondria (42, 104). This view has been confirmed by immunolocalization studies of the complex glycosphingolipid Forssman antigen: the labeling density in the plasma membrane was 10-fold higher than in the ER, with virtually no label over mitochondria and peroxisomes (68).

² In the intestinal epithelial cells 50% of the sphingolipids was GlcCer. The other 50% consisted of the complex glycosphingolipid globoside and of SM. The main glycerophospholipid is phosphatidylcholine which makes up 8 mol% of the lipids in the apical versus 29 mol% of the lipids in the basolateral membrane (105).

³ The major sphingolipid in myelin is GalCer followed by sulfated GalCer and SM (106).

⁴ Sphingolipids in *S. cerevisiae* consist of nearly equal fractions of inositolphosphoceramide (IPCer), MIPCer and M(IP)₂Cer (107). In addition, other yeasts generally contain GlcCer-based glycosphingolipids.

Biosynthetic traffic and lipid translocators

Ceramide

The first steps in sphingolipid synthesis are the condensation of L-serine and palmitoyl-CoA to ketosphinganine and its reduction to sphinganine in the ER membrane (6). In yeast, these lipids do not feed into signaling pools (7) and exogenous sphingoid bases need to go through a cycle of phosphorylation and dephosphorylation before they can be utilized for ceramide synthesis (8). This suggests that newly synthesized sphingoid bases are channeled through the pathway into ceramide without being able to escape. In yeast, ceramide is then converted to inositolphosphoceramide (IPCer)¹ and the mannosyl- and inositolphosphomannosyl-derivatives MIPCer and M(IP)₂Cer on the luminal surface of the Golgi complex (9). In mammals, ceramide is utilized for the synthesis of glucosylceramide (GlcCer) on the cytosolic side of the Golgi, sphingomyelin (SM) on the luminal surface of the Golgi, and, in specialized cells e.g. many epithelial cells, for galactosylceramide (GalCer) synthesis in the lumen of the ER (10) (Figure 1). Since ceramide synthesis occurs on the cytosolic side of the ER, the rate of ceramide translocation towards the lumina of ER and Golgi affects the relative synthesis of the various products. Indeed, if the half-time of the spontaneous transbilayer translocation of ceramide would be tens of minutes (11), this is rather slow compared to the vesicular transport between ER and Golgi (minutes). However, the translocation rate may be faster in the unsaturated lipid environment of the ER. In addition, it is unclear whether ER and Golgi possess proteins that stimulate ceramide translocation. Ceramide transport to the site of SM synthesis can be inhibited under conditions where transport to the site of GlcCer synthesis and ER-Golgi vesicle transport are normal (12), and, besides the vesicular pathway, a non-vesicular mechanism delivers ceramide to the Golgi in mammalian cells and yeast (13, 14). In yeast, this alternative pathway depends on ER-Golgi membrane contact and on a cytosolic factor and is energy-independent (14). Interestingly, close apposition of the ER to cisternae of the trans-Golgi has been observed in mammalian cells (15, 16). In the model of Figure 1, GlcCer synthase in the cis-Golgi receives ceramide via the vesicular pathway whereas GlcCer synthase and SM synthase in the trans-Golgi (17) receive ceramide from the ER via membrane contact sites. Similar contacts have often been observed between ER and mitochondria (16). These may be responsible for the transfer of signaling ceramide to mitochondria. A mitochondrial ceramidase has been identified (2).

Glucosylceramide

GlcCer synthesized on the cytosolic surface of the Golgi is partially converted to complex glycosphingolipids in the Golgi lumen (18). Experiments with brefeldin A, which fuses the cis-medial Golgi with the ER, have suggested that the enzymes that synthesize lactosylceramide (LacCer; Figure 1) and the first complex glycosphingolipids are present in the early Golgi. However, the bulk of these events are thought to occur in the trans Golgi or trans Golgi network (TGN) *in vivo* (19-21). GlcCer is probably translocated across the Golgi membrane by an energy-independent translocator (19, 22). Alternatively, GlcCer may be translocated towards the lumen by MDR1 P-glycoprotein, an ATP-binding cassette transporter that causes

multidrug resistance (23). However, so far, translocation of GlcCer by MDR1 P-glycoprotein has only been proven for short-chain analogs (24, 25). MDR1 P-glycoprotein is mostly found at the plasma membrane, where it may clear the cytosolic surface of GlcCer, and of other sphingolipids that leaked into this leaflet, by translocation towards the exoplasmic leaflet. GlcCer has access to the cytosolic surface of the plasma membrane after transport via the cytosolic side of transport vesicles or, alternatively, via monomeric transport through the cytosol (26). The latter may be mediated by the glycolipid transfer protein (27). An apical GlcCer translocator could thus enrich GlcCer on the apical as compared to the basolateral surface of epithelial cells (Figure 2). It is probably by a similar translocator, that sphingosine-1-phosphate after synthesis in the cytosol reaches the outside of the plasma membrane and is secreted.

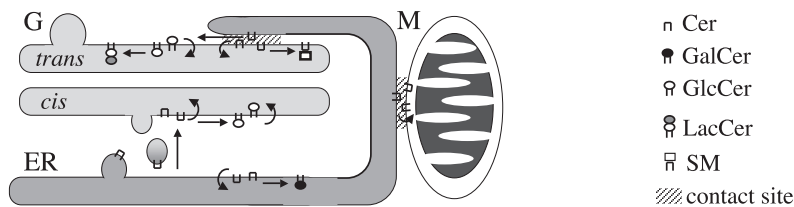
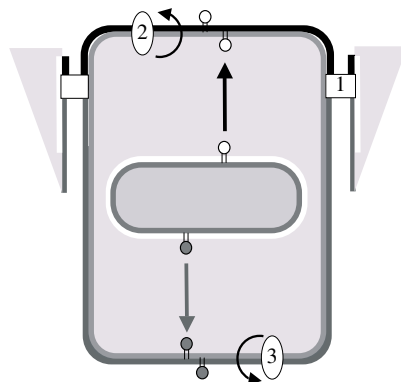


Figure 1. Spingolipid synthesis and translocation in the Golgi. Ceramide from the cytosolic surface of the ER is converted to GalCer in the ER lumen, or transported to the Golgi (G). The GlcCer synthase is found at two locations in the hepatocyte Golgi by sucrose gradient centrifugation (108). One peak colocalized with SM synthase, which was not relocated to the ER by brefeldin A in these cells (109). It is thus probably located in the trans Golgi/TGN (17). Ceramide reaches the cis-Golgi by vesicular transport whereas ER-TGN contacts allow ceramide transport by exchange. These contacts have been suggested to be sites of general lipid exchange (15), which also holds for similar contacts between ER and mitochondria (M). GlcCer translocates towards the lumen of the Golgi, where it is galactosylated to LacCer. LacCer is the precursor for the various complex glycosphingolipid series. For reasons of simplicity, the seven cisternae of the Golgi have been reduced to just two.

Figure 2. Generation of epithelial surface polarity of lipids by lipid translocators. (1) Tight junctions maintain the difference in lipid composition between the apical and basolateral domain of the epithelial plasma membrane by acting as a barrier to lipid diffusion in the outer leaflet of the lipid bilayer. Lipids freely diffuse through a continuous cytosolic leaflet (110). (2) An apical translocator with a specificity for GlcCer, the only sphingolipid synthesized on a cytosolic surface, would result in an enrichment of GlcCer on the apical surface. A candidate translocator is the uniformly expressed apical MDR1 P-glycoprotein. (3) A basolateral transporter with a specificity for PC would result in the enrichment of PC on the basolateral surface. Although one PC translocator has been identified (MDR3 P-glycoprotein), this is an apical protein.



Complex sphingolipids and sphingomyelin

GalCer synthesized in the ER lumen may flip towards the cytosolic surface (22), from where it has access to the same sites as GlcCer. In contrast, complex glycosphingolipids and SM synthesized in the lumen of the Golgi appear unable to translocate from the luminal towards the cytosolic surface (19, 22). As a consequence, they can only leave the Golgi via the luminal surface of transport vesicles (Figure 1). This has been confirmed for the complex glycosphingolipid GM3 (sialyl-LacCer; Ref. 28), SM (10), and for the yeast inositol sphingolipids (29). The enrichment of complex glycosphingolipids and SM in the exoplasmic leaflet of the apical plasma membrane of epithelial cells (10) as compared to the basolateral surface (Table 1) has led to the proposal that these sphingolipids self-aggregate at the site of budding of apical transport vesicles in the TGN (4, 30). Basolateral vesicles would have lower sphingolipid levels but the same high concentration of cholesterol. Sphingolipid and cholesterol concentrations are low in the ER. This implies that retrograde transport vesicles are essentially devoid of sphingolipids and cholesterol (31), which has been experimentally confirmed (32). These data lead to the simple model for sphingolipid sorting shown in Figure 3. Sphingolipid rafts are thought to occur in the early Golgi (33), possibly even in the ER (34).

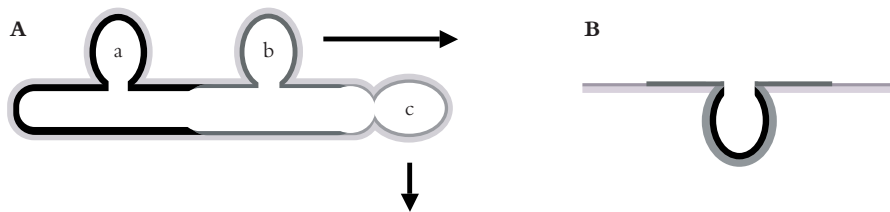


Figure 3. Lateral segregation of lipids into microdomains. (A), the Golgi complex of epithelial cells buds vesicles with at least three different lipid compositions: an apical composition, characterized by high levels of complex glycosphingolipids, SM, and cholesterol (a), a basolateral composition, having a high content of cholesterol (b), and an ER composition, with a low concentration of sphingolipids and cholesterol and a high concentration of unsaturated glycerophospholipids (42) (c). The three phases, displaying different thicknesses, must be recognized by the respective budding machineries in the cytosol, probably via membrane-spanning proteins. The segregation into three phases may occur in one single Golgi cisterna. (B), caveolae. In an environment of glycerophospholipids, sphingolipid/cholesterol domains enriched in GPI proteins may contain subdomains enriched in GM1, with lipid domains enriched in caveolin and dually acylated kinases oriented toward the cytosol.

Sphingolipid/cholesterol rafts

The notion that the lipids of eukaryotic plasma membranes display a heterogeneous lateral distribution is supported by a large body of evidence. Biophysical studies on model membranes have firmly established the principles by which mixtures of sphingolipids, unsaturated

glycerophospholipids and cholesterol can segregate into two fluid phases, where the sphingolipids and part of the cholesterol segregate into a “liquid-ordered” domain from the unsaturated lipids in a “liquid disordered” phase. At the same time, these studies have essentially validated the application of detergents in the cold to isolate the domains as detergent-insoluble remnants that float in sucrose gradients (5). Nevertheless, recently it has been suggested that Triton X100 (TX100) induces a strong perturbation of the bilayer at 4°C, but by coincidence reports a composition close to the one at 37°C (35). Thus, detergent resistance as an assay for rafts may not unequivocally report the distribution of proteins in the unperturbed cell. It has also been observed that TX100 promotes domain formation in single-phase membranes, thereby suggesting that ‘raft’ domains purified *in vitro* are an artifact of the detergent solubilization (36). Both observations underline the complexity of the relationship between DRMs and l_0 domains and still, a number of questions concerning the structural characteristics of the liquid-ordered domains remain to be solved:

A. What percentage of the cell surface is occupied by rafts? The diameter of sphingolipid/cholesterol rafts on the outer surface of the plasma membrane has been estimated by a number of different approaches to be small (tens to hundreds of nm) compared to that of cells (tens of μm), and to occupy some 10% of the cell surface (37, 38). In contrast, the sphingolipids constitute 20–50% of the polar lipids of the plasma membrane (Table 1). In addition, they are concentrated in the outer bilayer leaflet. Thus they completely cover the apical surface of epithelial cells, while the relative occupancy will be close to 40% in non-epithelial cells. In support of the latter, roughly half of the plasma membrane resisted extraction by cold detergent (39, 40). In a monolayer consisting of apical membrane lipids from kidney, only 50% was covered by liquid-ordered rafts whereas the outer leaflet of the apical membrane would consist exclusively of sphingolipids (41).

B. However, in the experimental monolayer the lipids of the outer and inner leaflets of the plasma membrane have been mixed, and the domain properties of the lipids of the cytosolic leaflet are unknown. From the fact that dually acylated proteins colocalize with the sphingolipid/cholesterol domains as measured by various techniques, it is assumed that liquid-ordered rafts exist in the cytosolic leaflet of the plasma membrane as well. There is some evidence to suggest that 70% of the phosphatidylserine, which is confined to the cytosolic leaflet by the activity of the aminophospholipid translocase, is disaturated (42), whereas in yeast only PI contained some 20% disaturated species (43). These lipids could thus form the basis for a liquid-ordered phase. In pure lipid membranes, rafts on one side of the membrane recognize and perfectly match rafts in the opposite leaflet (44). However, from the low concentration of potential raft-lipids in the cytosolic leaflet it is unlikely that rafts in the outer leaflet of the plasma membrane are fully complemented by rafts on the cytosolic surface (Figure 4 C–F).

C. If the rafts measured by biophysical techniques are different from the rafts as defined by detergent-insolubility (see under A.), does this imply that different types of raft exist within a single membrane? Indeed, studies locating the gangliosides GM1, GM3 and GD3, various proteins with a glycosylphosphatidylinositol (GPI) anchor, and caveolin have clearly established that various types of liquid-ordered domains co-exist on the cell surface (45–50). Small ganglioside-rich microdomains can exist within larger ordered domains in both natural and

model membranes (Figure 4 A, B; Ref. 51). Caveolae are examples where such “super” rafts are coupled to cytosolic rafts as defined by the acylated kinases. Coupling may involve proteins like caveolin or membrane spanning proteins, or may depend on phase-coupling between the opposed lipid domains.

D. By what mechanisms do membrane proteins locate to domains? One determinant may be a long transmembrane domain that would fit the thicker raft according to the principle originally described by M.S. Bretscher and S. Munro (52, 53). Membranes in cells occur in at least three thicknesses (Figure 3): The ER has the thickness of a pure phospholipid bilayer (hydrophobic thickness of some 3.5 nm), the liquid-disordered phase of the plasma membrane displays the thickness of phospholipid plus cholesterol (4 nm) and the sphingolipid rafts may be 4.5–5.5 nm thick (53). Since the thickness of a raft depends on whether the raft is matched by a raft on the cytosolic surface, and on the length of the amide-linked fatty acids, the various types of raft may display a distinct thickness and thereby recruit a unique set of proteins. Acylation is one other signal for raft localization on the cytosolic side (54). A glycosylphosphatidylinositol-anchor targets proteins to specific rafts. The mechanism is not clear. They can be displaced from rafts by gangliosides (41). Generally, a reduction of mobility by e.g. binding of a multivalent ligand also stimulates raft-association. In this light, recently a model has been suggested, that includes the presence of core proteins and low-affinity proteins (55). Core proteins have a high affinity for selected lipids and low affinity raft proteins need additional interactions for raft localization. Moreover, this model predicts that, depending on the oligomerization status of proteins, rafts can be created or disrupted. The mechanism of raft-association of proteins with multiple transmembrane domains and of protein-protein complexes is even more difficult to understand.

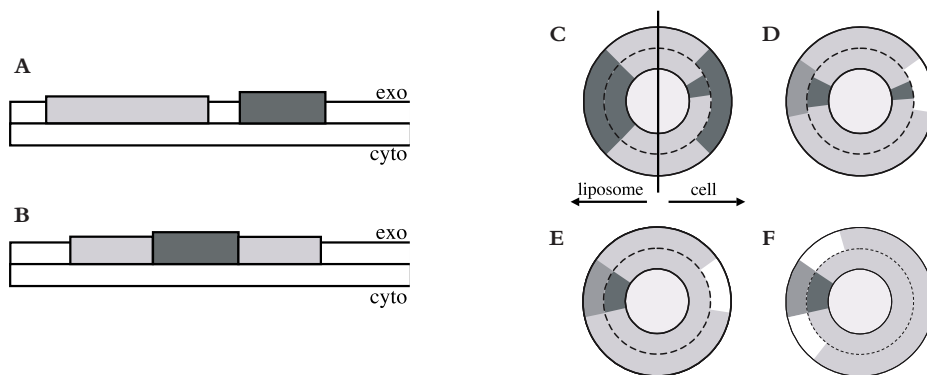


Figure 4. Lateral sphingolipid domains. Various types of domains with different physical properties (for example thickness) may be juxtaposed (A) or superimposed (B). In liposomes, liquid-ordered domains beautifully colocalize showing their capability of transbilayer recognition (C), whereas in cells the fraction of liquid-ordered lipids in the cytoplasmic leaflet seems far lower than in the outer leaflet (C). Domains in the inner leaflet may colocalize with each type of domain in the outer leaflet (D), or with only one of the various types of domains (E, F).

E. What are the physical properties that determine the affinity of a certain lipid for rafts? Although this question has been answered for model membranes of simple lipid compositions (5), biomembranes contain mixtures of 50–100 lipid species and various types of rafts. This means that many aspects of lipid-lipid immiscibility in biological membranes remain to be resolved. In many cases, fluorescent reporter molecules have been used to study rafts. Mostly, it is not very clear to what extent such a molecule mimics a natural lipid. For example, newly synthesized C_6 -NBD-SM is efficiently incorporated into transport vesicles from the Golgi to the plasma membrane, and has been used as an analog of SM, the typical marker of liquid-ordered domains, in numerous studies of domain-mediated sphingolipid sorting (10, 56). However, it has been used as a marker for the liquid-disordered phase in studies on plasma membrane rafts (40). Although fluorescent probes have been very helpful in spotting lipid sorting events, the raft partitioning coefficients of sphingolipids containing fluorescent fatty acids like C_6 -NBD and C_5 -DMB (also named Bodipy) are different from those of their natural counterparts (57). Results obtained with analogs can therefore not be directly extrapolated to natural lipids.

Uptake into the cell

Plasma membrane sphingolipids are continuously taken up into the cell via the membrane flux of endocytosis. In addition, lipids on the cytosolic surface may transfer to other membranes as monomers.

Non-vesicular traffic

The available evidence suggests that most sphingolipids reside in the exoplasmic leaflet of the plasma membrane bilayer and have no access to the cytosolic side under resting conditions. Exceptions are sphingosine and ceramide. After their generation in the outer leaflet of the plasma membrane, or after exogenous addition, sphingosine and ceramide spontaneously translocate to the cytosolic surface, from where sphingosine and short-chain ceramide can equilibrate with intracellular membranes. Ceramide may also be produced in the cytosolic leaflet via hydrolysis of SM by a neutral SMase (2), while also GlcCer may be degraded by a non-lysosomal enzyme (58). The resulting ceramide can be part of a signaling cascade (2). It is not fully clear how this ceramide reaches sites where it is reutilized for synthesis of SM and GlcCer. Surprisingly, a Golgi protein with some lipid transfer specificity for SM strongly stimulated SM resynthesis (59). Ceramide appears unable to leave the lumen of the lysosome (60), but this is presumably due to its inability to leave the internal membranes where it is produced. Exogenous sphingosine-1-phosphate, which binds to specific cell surface receptors (3), also appears to translocate to the cytosolic surface, possibly mediated by the ABC transporter CFTR, the cystic fibrosis transmembrane conductance regulator (61). In addition, galactosylsphingosine and glucosylsphingosine when added to cells are acylated (62, 63), probably after translocation towards the cytosolic surface. Whether they translocate at the plasma membrane or at some internal membrane has not been established. After translocation,

lysosphingolipids can freely move through the cell due to their high off-rate from membranes, while the resulting GalCer and GlcCer may fulfill functions on the cytosolic surface (63).

In one study, an exogenous fluorescent GlcCer (C_6 -NBD) was reported to flip towards the cytosolic surface of the plasma membrane (64). Such behavior was not observed for this and other N-acylated sphingolipids in many similar studies (10, 56). However, sphingolipids may appear in the cytosolic leaflet due to scrambling during signaling events (65). This may result in hydrolysis to ceramide. Alternatively, both lipids may be translocated back to the exoplasmic leaflet by ABC transporters, a notion supported by studies on short chain analogs of these lipids (24, 25). Finally, they may transfer to other membranes which step may be stimulated by a sphingomyelin transfer protein (e.g. Ref. 59) or by the glycolipid transfer protein (27). It is not clear whether complex glycosphingolipids ever reach the cytosolic surface of the plasma membrane and what would be their fate. Interestingly, specific interactions of glycosphingolipids with cytosolic proteins like calmodulin have been reported (66). In addition, if gangliosides can reach mitochondria during signaling events (67), they must first have reached the cytosolic surface. Translocation could occur at the plasma membrane or, alternatively, such lipids may be transported via the retrograde pathway to the ER, where translocation and transfer to the mitochondria can occur (Figure 1).

Endocytosis

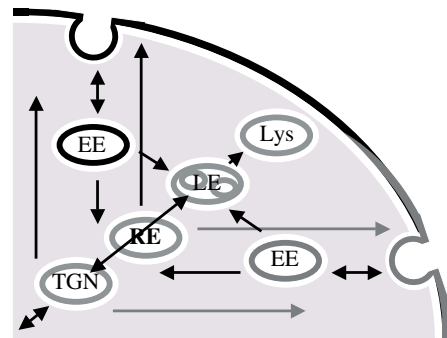
Like all other lipids, sphingolipids follow the bulk membrane flow through the exocytotic and endocytotic vesicular transport pathways. From studies on the transport of (mainly) membrane proteins a complex pattern of pathways and compartments in the endocytotic recycling pathways have been identified as illustrated in Figure 5. Sphingolipids have been shown to pass through each of these compartments. High concentrations of complex glycosphingolipids have been observed in the internal membranes of late endosomes, also referred to as multivesicular endosomes (68, 69), most likely the site of their degradation (70). On the other hand, studies on the Golgi glycosylation of exogenously added glycosphingolipids and on the transport of fluorescent analogs of sphingolipids have established that most sphingolipids recycle from the early (sorting) endosomes (71, 72), the late endosomes (73, 74), and from the recycling endosomes (72) to the plasma membrane. At the same time, a fraction of the complex sphingolipids, but particularly GlcCer, reaches the Golgi complex (63, 73, 75-78). The latter is also true for the glycolipid-binding toxins like Cholera toxin, Shiga toxin and E. coli verotoxin. From the Golgi, these toxin-glycolipid complexes follow the retrograde pathway all the way to the ER, where the active subunit is translocated across the membrane into the cytosol (see, for example Refs. 79, 80). Also in the absence of toxin, a small fraction of the complex glycosphingolipids reaches the ER (68).

The observation that GlcCer derived from LacCer hydrolysis in endosomes or lysosomes redistributed to the Golgi more efficiently than LacCer itself (LacCer cycles at 5-6% per hour (81) indicates that sorting had occurred but not by what mechanism (73). In contrast to LacCer, GlcCer may have translocated across the endosomal membrane and reached the Golgi by non-vesicular traffic. Alternatively, GlcCer and LacCer may have segregated into different lateral domains. Later studies have provided a large body of evidence for lipid sorting by

domains in the various endocytotic organelles. However, since most of this evidence is derived from the use of fluorescent lipid analogs, the study of toxins, antibodies and virus bound to glycosphingolipids, and the study of GPI-proteins as raft markers, the quantitative behavior of the natural lipids and the size of the various pathways remains to be established. Analogs of LacCer and globoside were endocytosed by a clathrin-independent subclass of the vesicles that took up SM, indicating sorting at the plasma membrane (78). The two pathways led to different classes of early endosomes, both of which had a connection to the Golgi. Both clathrin-dependent and -independent pathways are followed by glycolipid-bound toxins (78-80). The clathrin-independent pathway of toxin transport has been suggested to provide very efficient access to the Golgi for GPI-proteins (80), and might be a raft pathway. Interestingly, a rise in the cellular cholesterol concentration misrouted LacCer from this route to the lysosomes. The latter situation was also encountered in a number of sphingolipid storage diseases (78). Either, high cholesterol levels abolished the clathrin-independent pathway to the Golgi, or, alternatively, high cholesterol affected the partitioning of the LacCer analog into the proper membrane domain. In vivo, the properties of rafts and thereby their sorting potential maybe modulated by the production of, for example, small amounts of ceramide (82). Probes with a preference for raft and non-raft domains were found to be sorted in the early endosomes to late endosomes and to recycling endosomes, respectively (83). The late endosome, in turn, has been identified as a glycolipid sorting compartment (84), and the recycling endosomes were found to possess all components of a raft machinery (85).

Figure 5. Endocytotic recycling of sphingolipids.

Sphingolipids can be endocytosed via clathrin-dependent and -independent pathways. From early endosomes (EE) they are recycled to the plasma membrane, or shuttled to the recycling endosome (RE), the late endosome (LE) or the TGN. Endosomes and Golgi are connected via a bidirectional vesicular route. In epithelial cells, one leg of the system is connected to the apical and one to the basolateral surface, which are separated by tight junctions (see Figure 2).



Endocytotic lipid sorting is particularly interesting in epithelial cells, as they display a transcellular vesicular pathway but at the same time need to maintain the difference in apical and basolateral lipid composition. In initial studies in MDCK cells no specificity was observed in the transcytosis of different fluorescent SM and GlcCer analogs which allowed for their use as bulk membrane markers (86), as in non-epithelial cells (72, 87). However, sorting between these analogs was observed in hepatocyte-derived HepG2 cells. It was concluded that the lipids are sorted by lateral segregation in an apical endosome, termed the “sub-apical compartment” (88) or “apical recycling compartment” (85), which functionally resembles the recycling

endosome in non-epithelial cells. Under normal conditions in fully polarized hepatocytes, a GlcCer analog was recycled to the bile canalicular surface and SM to the basolateral surface (88), and evidence was provided for transient activation during polarity development of a pathway for SM to the bile canalicular surface by protein kinase A (89).

Role of sphingolipids and rafts in pathology

A number of diseases are initiated by the adherence of viruses, bacteria, or bacterial toxins to cell surface carbohydrates, of which several are components of glycosphingolipids. Since many glycosphingolipid-binding pathogens have been shown to bind 'multivalent' saccharides, and biotechnology has advanced in engineering bacteria that produce large quantities of specific oligosaccharides, it has become possible to design effective multivalent ligands capable of antagonizing pathogen-host interactions (93, 94).

Sphingolipidoses are inherited disorders characterized by excessive accumulation of one or multiple (glyco)sphingolipids, and form the most prevalent subgroup of the 'lysosomal storage disorders'. Approaches for therapeutic intervention have evolved and in type 1 Gaucher disease, a prototypical glycolipidosis, effective intervention has become available. For treating the symptoms, surgical removal of the spleen or bone-marrow transplantation has been carried out. Fortunately, nowadays there are several potential therapeutic options that deal directly with the case of the disease, either by replacing the defective gene or enzyme or by directly targeting the systems that are affected by the accumulation of undegraded metabolites (111). Nevertheless, the mechanism by which chronic accumulation of glycosphingolipids in lysosomes affects various cell types and triggers eventually pathology, remains unclear. One hypothesis is that the excessive extra-lysosomal glucosylceramide catabolism in Gaucher macrophages results in excessive production of cytosolic ceramide which may act as signaling molecule and cause abnormal cell behaviour (95).

Mucosal surfaces are the major site for HIV-1 entry (96). It has been shown that HIV-1 can cross the epithelium *in vitro* by transcytosis across epithelial cells, the most abundant cell type at mucosal surfaces (97, 98). Moreover, it has been demonstrated that both the binding of HIV-1 envelope glycoproteins to GalCer and the organization of GalCer in raft microdomains is required for effective HIV-1 transcytosis from the apical to the basolateral pole of the epithelial cell (99). Although there is substantial evidence that HIV and other retroviruses preferentially bud from lipid rafts in T-cells (100), recently the first test designed to differentiate between the lipid raft hypothesis of retroviral biogenesis and the 'Trojan exosome hypothesis' in macrophages was performed (101). The Trojan exosome hypothesis proposes that retroviruses exploit a pre-existing cellular pathway of intercellular vesicle trafficking, exosome exchange, for both the biogenesis of retroviral particles and a low-efficiency but mechanistically important mode of infection (102). Modeling HIV as a viral exosome, budding into multivesicular endosomes (MVEs; see figure 5) rather than at the plasma membrane, has important implications for viral pathogenesis and could explain many aspects of HIV biology. The phenomenon of HIV specifically infecting the very cells that respond to it calls out for caution to the practice of

structured therapy interruption (103).

The above examples all illustrate the fact that rafts are 'hot'...

New approaches

Several techniques have been developed to study the phenomenon 'raft'. As mentioned previously in this chapter, the physical basis for the extraction of lipids with detergents is poorly understood. Although DRM association defines a biochemical characteristic of raft components, DRMs do not resemble rafts as they occur in living cells in size, structure, composition, or even existence.

Many new approaches for detecting heterogeneity in cell membranes have emerged. Methods to measure lipid proximity, including chemical crosslinking and fluorescence resonance energy transfer (FRET), and methods to measure diffusion characteristics of raft components like Single-particle tracking (90) have given more insight into the raft issue. However, whether rafts are small sphingolipid/cholesterol-rich structures that recruit 'raft proteins' (91), or whether they are constructed of 'lipid shells' that target the protein they encase to preexisting rafts/caveolae domains (92), remains to be solved.

Perspectives and scope of this thesis

The exciting developments in the fields of sphingolipid-mediated signal transduction and sphingolipid-mediated protein sorting have led to a tremendous activity in the studies of sphingolipid organization in biomembranes, especially the structural role of sphingolipids in membrane rafts. It is now being realized that rafts may exist in many cellular membranes and that thus their functions are not limited to the plasma membrane. In order to fully grasp raft function, it will be necessary to identify and characterize the different types of raft, to follow their fate in time and to understand the role of the various sphingolipids in their structure.

In this chapter, a general introduction has been provided on the organization and transport of sphingolipids. It may be clear that, in order to nail down disease origin and development, first several fundamental questions must be answered. To this end, the yeast *Saccharomyces cerevisiae* serves as a great model system. It is easy to manipulate both sphingolipid structure and production levels in yeast, as the major enzymes involved in sphingolipid synthesis are known. Sphingolipids are primarily synthesized in the Golgi. An attractive hypothesis is that the self-organizing capacity of sphingolipids is exploited by the Golgi to boost its performance as the central sorting station of the cell (112). In order to test this possibility, we stripped sphingolipids of structural features that are considered important for microdomain formation and studied the effect this had on Golgi function. **Chapter 2** describes how we identified two sphingolipid mannosyltransferases, and studied the role of mannosylated sphingolipids in protein sorting in the late Golgi.

Because sphingolipid functions are governed by the enzymes that make, break and transport the sphingolipids, a major challenge will be to identify these enzymes and establish how their activity is regulated in the living cell. Although the protein Csg2p has been suggested to be involved in sphingolipid mannosylation (113), its precise role in this reaction has not been defined. In **Chapter 3** we set out to define the function of Csg2p, and come up with a very unexpected result.

While another important challenge will be to unravel the biophysical complexity of lipid mixtures, it will be most important to define the interactions between sphingolipids and proteins. These are proteins involved in vesicular traffic but also proteins involved in signaling. Except for structural functions, sphingolipids serve regulatory functions in their own right. Yeast cells lacking sphingolipid mannosyltransferases accumulate inositolphosphorylceramide, a sphingolipid that confers hypersensitivity towards calcium (113). We found that this Ca^{2+} -sensitive phenotype is suppressed by overexpression of *HOR7*, and further characterized this gene in **Chapter 4**.

The yeast Golgi not only contains enzymes involved in sphingolipid synthesis, but also putative lipid translocases that may regulate the transbilayer lipid distribution in this organelle (114, 115). Therefore, next to manipulating membrane lipid composition, we studied the effects of modifying the transbilayer lipid distribution in relation to Golgi function. In **Chapter 5** we studied the significance of two putative *trans*-Golgi aminophospholipid translocases in creating lipid asymmetry, and in the formation of post-Golgi secretory vesicles.

The implications of the findings presented in this thesis are discussed in **Chapter 6**.

References

1. Hakomori, S. (1990) *J. Biol. Chem.* **265**, 18713-18716
2. Hannun, Y. A., and Obeid, L. M. (2002) *J. Biol. Chem.* **277**, 25847-25850
3. Spiegel, S., and Milstien, S. (2002) *J. Biol. Chem.* **277**, 25851-25854
4. Simons, K., and van Meer, G. (1988) *Biochemistry* **27**, 6197-6202
5. Brown, D. A., and London, E. (2000) *J. Biol. Chem.* **275**, 17221-17224
6. Merrill, A. H., Jr. (2002) *J. Biol. Chem.* **277**, 25843-25846
7. Skrzypek, M. S., Nagiec, M. M., Lester, R. L., and Dickson, R. C. (1999) *J. Bacteriol.* **181**, 1134-1140
8. Zanolari, B., Friant, S., Funato, K., Sutterlin, C., Stevenson, B. J., and Riezman, H. (2000) *Embo J.* **19**, 2824-2833
9. Levine, T. P., Wiggins, C. A., and Munro, S. (2000) *Mol. Biol. Cell* **11**, 2267-2281
10. van Meer, G., and Holthuis, J. C. (2000) *Biochim. Biophys. Acta* **1486**, 145-170
11. Bai, J., and Pagano, R. E. (1997) *Biochemistry* **36**, 8840-8848
12. Yasuda, S., Kitagawa, H., Ueno, M., Ishitani, H., Fukasawa, M., Nishijima, M., Kobayashi, S., and Hanada, K. (2001) *J. Biol. Chem.* **276**, 43994-44002
13. Kok, J. W., Babia, T., Klappe, K., Egea, G., and Hoekstra, D. (1998) *Biochem. J.* **333**, 779-786
14. Funato, K., and Riezman, H. (2001) *J. Cell Biol.* **155**, 949-959
15. Ladinsky, M. S., Mastronarde, D. N., McIntosh, J. R., Howell, K. E., and Staehelin, L. A. (1999) *J. Cell Biol.*

- 144, 1135-1149
16. Marsh, B. J., Mastronarde, D. N., Buttle, K. F., Howell, K. E., and McIntosh, J. R. (2001) *Proc. Natl. Acad. Sci. U.S.A.* **98**, 2399-2406
 17. Sadeghlar, F., Sandhoff, K., and van Echten-Deckert, G. (2000) *FEBS Lett.* **478**, 9-12
 18. Kolter, T., Proia, R. L., and Sandhoff, K. (2002) *J. Biol. Chem.* **277**, 25859-25862
 19. Lannert, H., Gorgas, K., Meissner, I., Wieland, F. T., and Jeckel, D. (1998) *J. Biol. Chem.* **273**, 2939-2946
 20. Maccioni, H. J., Daniotti, J. L., and Martina, J. A. (1999) *Biochim. Biophys. Acta* **1437**, 101-118
 21. Allende, M. L., Li, J., Darling, D. S., Worth, C. A., and Young, W. W., Jr. (2000) *Glycobiology* **10**, 1025-1032
 22. Burger, K. N., van der Bijl, P., and van Meer, G. (1996) *J. Cell Biol.* **133**, 15-28
 23. Lala, P., Ito, S., and Lingwood, C. A. (2000) *J. Biol. Chem.* **275**, 6246-6251
 24. van Helvoort, A., Smith, A. J., Sprong, H., Fritzsche, I., Schinkel, A. H., Borst, P., and van Meer, G. (1996) *Cell* **87**, 507-517
 25. Borst, P., Zelcer, N., and van Helvoort, A. (2000) *Biochim. Biophys. Acta* **1486**, 128-144
 26. Warnock, D. E., Lutz, M. S., Blackburn, W. A., Young, W. W., Jr., and Baenziger, J. U. (1994) *Proc. Natl. Acad. Sci. U.S.A.* **91**, 2708-2712
 27. Lin, X., Mattjus, P., Pike, H. M., Windebank, A. J., and Brown, R. E. (2000) *J. Biol. Chem.* **275**, 5104-5110
 28. Young, W. W., Jr., Lutz, M. S., and Blackburn, W. A. (1992) *J. Biol. Chem.* **267**, 12011-12015
 29. Hechtberger, P., and Daum, G. (1995) *FEBS Lett.* **367**, 201-204
 30. van Meer, G., Stelzer, E. H., Wijnaendts-van-Resandt, R. W., and Simons, K. (1987) *J. Cell Biol.* **105**, 1623-1635
 31. van Meer, G. (1989) *Annu. Rev. Cell Biol.* **5**, 247-275
 32. Brugger, B., Sandhoff, R., Wegehingel, S., Gorgas, K., Malsam, J., Helms, J. B., Lehmann, W. D., Nickel, W., and Wieland, F. T. (2000) *J. Cell Biol.* **151**, 507-518
 33. Gkantiragas, I., Brugger, B., Stuken, E., Kaloyanova, D., Li, X. Y., Lohr, K., Lottspeich, F., Wieland, F. T., and Helms, J. B. (2001) *Mol. Biol. Cell* **12**, 1819-1833
 34. Bagnat, M., Keranen, S., Shevchenko, A., and Simons, K. (2000) *Proc. Natl. Acad. Sci. U.S.A.* **97**, 3254-3259
 35. de Almeida, R. F., Fedorov, A., and Prieto, M. (2003) *Biophys. J.* **85**, 2406-2416
 36. Heerklotz, H., Szadkowska, H., Anderson, T., and Seelig, J. (2003) *J. Mol. Biol.* **329**, 793-799
 37. Schutz, G. J., Kada, G., Pastushenko, V. P., and Schindler, H. (2000) *Embo J.* **19**, 892-901
 38. Suzuki, K., Sterba, R. E., and Sheetz, M. P. (2000) *Biophys. J.* **79**, 448-459
 39. Mayor, S., and Maxfield, F. R. (1995) *Mol. Biol. Cell* **6**, 929-944
 40. Hao, M., Mukherjee, S., and Maxfield, F. R. (2001) *Proc. Natl. Acad. Sci. U.S.A.* **98**, 13072-13077
 41. Dietrich, C., Volovyk, Z. N., Levi, M., Thompson, N. L., and Jacobson, K. (2001) *Proc. Natl. Acad. Sci. U.S.A.* **98**, 10642-10647
 42. Keenan, T. W., and Morre, D. J. (1970) *Biochemistry* **9**, 19-25
 43. Schneider, R., Brugger, B., Sandhoff, R., Zellnig, G., Leber, A., Lampl, M., Athenstaedt, K., Hrastnik, C., Eder, S., Daum, G., Paltauf, F., Wieland, F. T., and Kohlwein, S. D. (1999) *J. Cell Biol.* **146**, 741-754
 44. Dietrich, C., Bagatolli, L. A., Volovyk, Z. N., Thompson, N. L., Levi, M., Jacobson, K., and Gratton, E. (2001) *Biophys. J.* **80**, 1417-1428
 45. Iwabuchi, K., Handa, K., and Hakomori, S. (1998) *J. Biol. Chem.* **273**, 33766-33773
 46. Madore, N., Smith, K. L., Graham, C. H., Jen, A., Brady, K., Hall, S., and Morris, R. (1999) *Embo J.* **18**, 6917-6926
 47. Chigorno, V., Palestini, P., Sciannamblo, M., Dolo, V., Pavan, A., Tettamanti, G., and Sonnino, S. (2000) *Eur. J. Biochem.* **267**, 4187-4197
 48. Kenworthy, A. K., Petranova, N., and Edidin, M. (2000) *Mol. Biol. Cell* **11**, 1645-1655

49. Gomez-Mouton, C., Abad, J. L., Mira, E., Lacalle, R. A., Gallardo, E., Jimenez-Baranda, S., Illa, I., Bernad, A., Manes, S., and Martinez, A. C. (2001) *Proc. Natl. Acad. Sci. U.S.A.* **98**, 9642-9647
50. Vyas, K. A., Patel, H. V., Vyas, A. A., and Schnaar, R. L. (2001) *Biol. Chem.* **382**, 241-250
51. Yuan, C., and Johnston, L. J. (2001) *Biophys. J.* **81**, 1059-1069
52. Bretscher, M. S., and Munro, S. (1993) *Science* **261**, 1280-1281
53. Sprong, H., van der Sluijs, P., and van Meer, G. (2001) *Nat. Rev. Mol. Cell Biol.* **2**, 504-513
54. Melkonian, K. A., Ostermeyer, A. G., Chen, J. Z., Roth, M. G., and Brown, D. A. (1999) *J. Biol. Chem.* **274**, 3910-3917
55. Helms, J. B., and Zurzolo, C. (2004) *Traffic* **5**, 247-254
56. Hoekstra, D., and van, I. S. C. (2000) *Curr. Opin. Cell Biol.* **12**, 496-502
57. Wang, T. Y., and Silvius, J. R. (2000) *Biophys. J.* **79**, 1478-1489
58. van Weely, S., Brandsma, M., Strijland, A., Tager, J. M., and Aerts, J. M. (1993) *Biochim. Biophys. Acta* **1181**, 55-62
59. Van Tiel, C. M., Luberto, C., Snoek, G. T., Hannun, Y. A., and Wirtz, K. W. (2000) *Biochem. J.* **346**, 537-543
60. Chatelut, M., Leruth, M., Harzer, K., Dagan, A., Marchesini, S., Gatt, S., Salvayre, R., Courtoy, P., and Levade, T. (1998) *FEBS Lett.* **426**, 102-106
61. Boujaoude, L. C., Bradshaw-Wilder, C., Mao, C., Cohn, J., Ogretmen, B., Hannun, Y. A., and Obeid, L. M. (2001) *J. Biol. Chem.* **276**, 35258-35264
62. Farrer, R. G., and Dawson, G. (1990) *J. Biol. Chem.* **265**, 22217-22222
63. Sprong, H., Degroote, S., Claessens, T., van Drunen, J., Oorschot, V., Westerink, B. H., Hirabayashi, Y., Klumperman, J., van der Sluijs, P., and van Meer, G. (2001) *J. Cell Biol.* **155**, 369-380
64. Martin, O. C., and Pagano, R. E. (1994) *J. Cell Biol.* **125**, 769-781
65. Tepper, A. D., Ruurs, P., Wiedmer, T., Sims, P. J., Borst, J., and van Blitterswijk, W. J. (2000) *J. Cell Biol.* **150**, 155-164
66. Higashi, H., Omori, A., and Yamagata, T. (1992) *J. Biol. Chem.* **267**, 9831-9838
67. Rippo, M. R., Malisan, F., Ravagnan, L., Tomassini, B., Condo, I., Costantini, P., Susin, S. A., Rufini, A., Todaro, M., Kroemer, G., and Testi, R. (2000) *Faseb J.* **14**, 2047-2054
68. van Genderen, I. L., van Meer, G., Slot, J. W., Geuze, H. J., and Voorhout, W. F. (1991) *J. Cell Biol.* **115**, 1009-1019
69. Mobius, W., Herzog, V., Sandhoff, K., and Schwarzmann, G. (1999) *J. Histochem. Cytochem.* **47**, 1005-1014
70. Schuette, C. G., Pierstorff, B., Huettler, S., and Sandhoff, K. (2001) *Glycobiology* **11**, 81R-90R
71. Kok, J. W., Eskelinen, S., Hoekstra, K., and Hoekstra, D. (1989) *Proc. Natl. Acad. Sci. U.S.A.* **86**, 9896-9900
72. Hao, M., and Maxfield, F. R. (2000) *J. Biol. Chem.* **275**, 15279-15286
73. Trinchera, M., Carrettoni, D., and Ghidoni, R. (1991) *J. Biol. Chem.* **266**, 9093-9099
74. Kok, J. W., Hoekstra, K., Eskelinen, S., and Hoekstra, D. (1992) *J. Cell Sci.* **103**, 1139-1152
75. Kok, J. W., Babia, T., and Hoekstra, D. (1991) *J. Cell Biol.* **114**, 231-239
76. Gordon, C. M., and Lloyd, K. O. (1994) *Arch. Biochem. Biophys.* **315**, 339-344
77. Babia, T., Ledesma, M. D., Saffrich, R., Kok, J. W., Dotti, C. G., and Egea, G. (2001) *Traffic* **2**, 395-405
78. Puri, V., Watanabe, R., Singh, R. D., Dominguez, M., Brown, J. C., Wheatley, C. L., Marks, D. L., and Pagano, R. E. (2001) *J. Cell Biol.* **154**, 535-547
79. Torgersen, M. L., Skretting, G., van Deurs, B., and Sandvig, K. (2001) *J. Cell Sci.* **114**, 3737-3747
80. Nichols, B. J., Kenworthy, A. K., Polishchuk, R. S., Lodge, R., Roberts, T. H., Hirschberg, K., Phair, R. D., and Lippincott-Schwartz, J. (2001) *J. Cell Biol.* **153**, 529-541
81. Sillence, D. J., and Allan, D. (1998) *Mol. Membr. Biol.* **15**, 229-235
82. Xu, X., Bittman, R., Duportail, G., Heissler, D., Vilcheze, C., and London, E. (2001) *J. Biol. Chem.* **276**,

- 33540-33546
83. Mukherjee, S., Soe, T. T., and Maxfield, F. R. (1999) *J. Cell Biol.* **144**, 1271-1284
 84. Zhang, M., Dwyer, N. K., Neufeld, E. B., Love, D. C., Cooney, A., Comly, M., Patel, S., Watari, H., Strauss, J. F., 3rd, Pentchev, P. G., Hanover, J. A., and Blanchette-Mackie, E. J. (2001) *J. Biol. Chem.* **276**, 3417-3425
 85. Gagescu, R., Demaurex, N., Parton, R. G., Hunziker, W., Huber, L. A., and Gruenberg, J. (2000) *Mol. Biol. Cell* **11**, 2775-2791
 86. van Genderen, I., and van Meer, G. (1995) *J. Cell Biol.* **131**, 645-654
 87. Koval, M., and Pagano, R. E. (1989) *J. Cell Biol.* **108**, 2169-2181
 88. van IJzendoorn, S. C., and Hoekstra, D. (1999) *Mol. Biol. Cell* **10**, 3449-3461
 89. van IJzendoorn, S. C., and Hoekstra, D. (2000) *Mol. Biol. Cell* **11**, 1093-1101
 90. Dietrich, C., Yang, B., Fujiwara, T., Kusumi, A., and Jacobson, K. (2002) *Biophys. J.* **82**, 274-284
 91. Simons, K., and Ikonen, E. (1997) *Nature* **387**, 569-572
 92. Anderson, R. G., and Jacobson, K. (2002) *Science* **296**, 1821-1825
 93. Kitov, P. I., Sadowska, J. M., Mulvey, G., Armstrong, G. D., Ling, H., Pannu, N. S., Read, R. J., and Bundle, D. R. (2000) *Nature* **403**, 669-672
 94. Thompson, J. P., and Schengrund, C. L. (1997) *Glycoconj. J.* **14**, 837-845
 95. Aerts, J. M., Hollak, C., Boot, R., and Groener, A. (2003) *Philos. Trans. R. Soc. Lond. B. Biol. Sci.* **358**, 905-914
 96. Nicolosi, A., Musicco, M., Saracco, A., and Lazzarin, A. (1994) *J. Acquir. Immune Defic. Syndr.* **7**, 296-300
 97. Bomsel, M. (1997) *Nat. Med.* **3**, 42-47
 98. Bomsel, M., Heyman, M., Hocini, H., Lagaye, S., Belec, L., Dupont, C., and Desgranges, C. (1998) *Immunity* **9**, 277-287
 99. Alfsen, A., Iniguez, P., Bouguyon, E., and Bomsel, M. (2001) *J. Immunol.* **166**, 6257-6265
 100. Nguyen, D. H., and Hildreth, J. E. (2000) *J. Virol.* **74**, 3264-3272
 101. Nguyen, D. G., Booth, A., Gould, S. J., and Hildreth, J. E. (2003) *J. Biol. Chem.* **278**, 52347-52354
 102. Gould, S. J., Booth, A. M., and Hildreth, J. E. (2003) *Proc Natl. Acad. Sci. U.S.A.* **100**, 10592-10597
 103. Douek, D. C., Brenchley, J. M., Betts, M. R., Ambrozak, D. R., Hill, B. J., Okamoto, Y., Casazza, J. P., Kuruppu, J., Kunstman, K., Wolinsky, S., Grossman, Z., Dybul, M., Oxenius, A., Price, D. A., Connors, M., and Koup, R. A. (2002) *Nature* **417**, 95-98
 104. Lange, Y., Swaisgood, M. H., Ramos, B. V., and Steck, T. L. (1989) *J. Biol. Chem.* **264**, 3786-3793
 105. Kawai, K., Fujita, M., and Nakao, M. (1974) *Biochim. Biophys. Acta* **369**, 222-233
 106. Morell, P., Quarles, R. H., and Norton, W. T. (1994) *Basic Neurochemistry. Molecular, Cellular, and Medical aspects, 4th ed.* (Siegel, G.J., Agranoff, B.W., Albers, R.W., and Molinoff, P.B., eds.) Raven Press, New York, 117-143
 107. Patton, J. L., and Lester, R. L. (1991) *J. Bacteriol.* **173**, 3101-3108
 108. Jeckel, D., Karrenbauer, A., Burger, K. N., van Meer, G., and Wieland, F. (1992) *J. Cell Biol.* **117**, 259-267
 109. van Meer, G., and van 't Hof, W. (1993) *J. Cell Sci.* **104**, 833-842
 110. van Meer, G., and Simons, K. (1986) *Embo J.* **5**, 1455-1464
 111. Futerman, A.H., and van Meer, G. (2004) *Nat. Rev. Mol. Cell Biol.* **5**, 554-65
 112. Holthuis, J. C., Pomorski, T., Raggars, R. J., Sprong, H., and van Meer, G. (2001) *Physiol. Rev.* **81**, 1689-1723
 113. Beeler, T. J., Fu, D., Rivera, J., Monaghan, E., Gable, K., and Dunn, T. M. (1997) *Mol. Gen. Genet.* **255**, 570-579
 114. Chen, C. Y., Ingram, M. F., Rosal, P. H., and Graham, T. R. (1999) *J. Cell Biol.* **147**, 1223-1236
 115. Pomorski, T., Lombardi, R., Riezman, H., Devaux, P.F., van Meer, G., and Holthuis, J. C. (2003) *Mol. Biol. Cell* **14**, 1240-1254

Chapter 2

Protein sorting in the late Golgi of *Saccharomyces cerevisiae* does not require mannosylated sphingolipids*

* Lisman Q., Pomorski T., Vogelzangs C., Urli-Stam D., de Cocq van Delwijnen W., and Holthuis J.C.M. (2004). *Journal of Biological Chemistry* 279, 1020-9

Summary

Glycosphingolipids are widely viewed as integral components of the Golgi-based machinery by which membrane proteins are targeted to compartments of the endosomal/lysosomal system and to the surface domains of polarized cells. The yeast *Saccharomyces cerevisiae* creates glycosphingolipids by transferring mannose to the head group of inositolphosphorylceramide (IPC), yielding mannosyl-IPC (MIPC). Addition of an extra phosphoinositol group onto MIPC generates mannosyl-di-IPC (M(IP)₂C), the final and most abundant sphingolipid in yeast. Mannosylation of IPC is partially dependent on *CSG1*, a gene encoding a putative sphingolipid-mannosyltransferase. Here we show that open reading frame *YBR161w*, renamed *CSH1*, is functionally homologous to *CSG1* and that deletion of both genes abolishes MIPC and M(IP)₂C synthesis without affecting protein mannosylation. Csg1p and Csh1p are closely related polytopic membrane proteins that co-localize with IPC synthase in the *medial* Golgi. Loss of Csg1p and Csh1p has no effect on clathrin- or AP-3 adaptor-mediated protein transport from the Golgi to the vacuole. Moreover, segregation of the periplasmic enzyme invertase, the plasma membrane ATPase Pma1p and the glycosylphosphatidylinositol-anchored protein Gas1p into distinct classes of secretory vesicles occurs independently of Csg1p and Csh1p. Our results indicate that protein sorting in the late Golgi of yeast does not require production of mannosylated sphingolipids.

Introduction

Correct sorting of membrane proteins and lipids is essential for establishing and maintaining the identity and function of the different cellular organelles. Although much progress has been made in uncovering the transport machinery for delivering endosomal/lysosomal proteins (1, 2), the mechanisms for cargo sorting to the cell surface are still poorly defined. Exocytic cargo can reach the cell surface by multiple pathways in most, if not all eukaryotic cells (3). For example, the polarized organization of epithelial cells relies on the sorting of both proteins and lipids into distinct classes of Golgi-derived vesicles that are targeted to the apical or basolateral surface (4). Apical and basolateral proteins expressed in fibroblasts are also sorted into different vesicles (5) and it appears that the Golgi-based sorting machinery for apical and basolateral cargo operates both in polarized and non-polarized cell types (6). Characterization of secretory vesicles that accumulate in late (post-Golgi-blocked) secretory yeast mutants has identified two vesicle populations with different densities and unique cargo proteins (7-9). Hence, transport of exocytic cargo by independent routes seems a conserved feature of eukaryotic cells.

There are numerous indications that lipid microheterogeneity plays a role in cargo sorting along the secretory pathway. Importantly, sphingolipids and in particular glycosphingolipids have the propensity to segregate from glycerolipids and to cluster with sterols into lateral microdomains with physicochemical properties distinct from those of the bulk membrane (10).

Glycosphingolipid/sterol-rich microdomains were first conceived in polarized MDCK cells as Golgi-based sorting platforms for apically directed proteins and lipids (11, 12). In support of this model, inhibition of sphingolipid synthesis with fumonisin B randomises the cell surface distribution of apical GPI-anchored proteins in MDCK cells (13). A similar glycosphingolipid-based sorting mechanism is held responsible for axonal delivery of GPI-anchored proteins in neurons (14), regulated apical secretion of zymogens from pancreatic acinar cells (15), apical trafficking of thyroglobulin in thyrocytes (16), and cell surface delivery of plasma membrane ATPase, Pma1p, and diverse GPI-anchored proteins in yeast (17-19). Glycosphingolipids are also required for transport of melanosomal proteins from the Golgi to melanosomes in melanoma cells (20), but the underlying mechanism remains to be elucidated. The ubiquitous expression of glycosphingolipids suggests that they exert organizing functions in all eukaryotic cells.

Animals as well as some plants and fungi generate glycosphingolipids by transferring glucose or galactose to the C1 hydroxyl group of ceramide. These additions can be further decorated by additional sugars and sometimes sulfates to yield hundreds of different glycosphingolipid species (21). In the yeast *Saccharomyces cerevisiae*, however, the direct precursor for glycosphingolipid synthesis is not ceramide but inositolphosphorylceramide (IPC; (22). IPC is formed by addition of phosphoinositol released from phosphatidylinositol to ceramide, a reaction catalysed by IPC synthase in a *medial* compartment of the yeast Golgi (23). IPC is then mannosylated to yield mannosyl-IPC (MIPC), which in turn can receive a second phosphoinositol group from phosphatidylinositol to generate the final and by far most abundant sphingolipid, M(IP)₂C (22). MIPC and M(IP)₂C synthesis occurs in the lumen of the Golgi (22, 24). Whereas IPC is highly enriched in Golgi and vacuolar membranes, the largest amounts of MIPC and M(IP)₂C are found in the plasma membrane (25). Hence, the yeast Golgi seems to be a branching point in sphingolipid trafficking from where mannosylated sphingolipids selectively migrate to the cell surface and sphingolipids without the sugar moiety reach the vacuole. However, direct evidence that mannosylated sphingolipids play a role in cargo sorting to the cell surface is lacking.

Addressing the biological function of mannosylated sphingolipids in yeast is hampered by the fact that little is known about the enzyme(s) responsible for their synthesis. Three structurally unrelated genes have been implicated in the mannosylation of IPC. The *VRG4* gene encodes a nucleotide sugar transporter that mediates GDP-mannose import into the Golgi lumen (24). Besides being essential for IPC mannosylation, *VRG4* also affects *N*-linked and *O*-linked glycoprotein modifications (24). Null mutations in either the *CSG1* or *CSG2* gene cause a reduction in, but do not completely eliminate MIPC synthesis (26, 27). Csg1p is predicted to have a catalytic function since it contains a region of 93 amino acids with homology to the yeast α -1,6-mannosyltransferase, Och1p (27). The function of Csg2p is less obvious. Csg2p contains an EF-Ca²⁺-binding domain and has been localized to the ER where it may play a role in Ca²⁺ homeostasis (28). The recent finding that Csg2p forms a complex with Csg1p raises the possibility that IPC mannosyltransferase activity in yeast is regulated by Ca²⁺ through Csg2p (29).

Yeast open reading frame *YBR161w*, recently renamed *CSH1*, encodes a protein

exhibiting strong similarity to the putative sphingolipid mannosyltransferase, Csg1p (27). Here we report that Csh1p is functionally homologous to Csg1p and provide evidence that Csg1p and Csh1p function as two independent sphingolipid mannosyltransferases. Loss of Csg1p and Csh1p had no effect on the delivery of vacuolar proteins or on the packaging of cell surface components into distinct classes of secretory vesicles. From these results, we conclude that the organization of the various post-Golgi delivery pathways in yeast does not depend on production of mannosylated sphingolipids.

Experimental Procedures

Strains and plasmids

Unless indicated otherwise, yeast strains were grown at 28°C to mid-logarithmic phase (0.5–1.0 OD₆₀₀) in synthetic dextrose (SD) medium or in yeast extract-peptone-dextrose (YEPD) medium. Yeast transformations were carried out as described (30). The yeast mutants *Apep12Δvam3*, *Δanp1*, *Δmnn10* and *Δvan1* were all derived from the strain SEY6210 (*MATα ura3-52 his3 Δ200 leu2-3-112 trp-Δ901 suc2-Δ9 lys2-801*) and have been described elsewhere (31, 32). All other gene deletion phenotypes were characterized in the strain EHY227 (*MATα sec6-4 TPI1::SUC2::TRP1 ura3-52 his3-Δ200 leu2-3-112 trp1-1*). For the deletion of *CSG1*, *CSH1* and *IPT1* genes, 450–550 base-pair fragments of the promoter and ORF 3'-end of each gene were amplified by PCR from yeast genomic DNA. The gene promoters and ORF ends were cloned into *NotI/EcoRI* and *SpeI/MluI* sites located on either side of a *loxP-HIS3-loxP* cassette that was ligated into the *EcoRI/SpeI* sites of a pBluescript KS⁻ vector (Stratagene, La Jolla, CA; the *loxP-HIS3-loxP* plasmid was a gift of T. Levine, University College London, UK). Gene deletion constructs were linearized with *NotI* and *MluI* and transformed into EHY227 to generate *Δcsg1* (JHY075), *Δcsh1* (JHY088) and *Δipt1* (JHY079) strains. Double deletions were performed sequentially in EHY227 by repeated use of the *loxP-HIS3-loxP* cassette and subsequent removal of the *HIS3* marker by excisive recombination using Cre recombinase (33), yielding the *Δcsg1Δcsh1* strain (JHY090). In each case, the correct integration or excision event was confirmed by PCR.

Aur1p was tagged at its carboxy-terminus with three copies of the hemagglutinin (HA) epitope using the PCR knock-in approach (34) and plasmid p3xHA₃-HIS5 (S. Munro, MRC-LMB, Cambridge, UK). Pma1p was tagged at its amino-terminus with one copy of the HA epitope using integration plasmid pRS305Δ51 as described (35). Vam3p was tagged at its amino-terminus with three copies of the HA epitope using integration plasmid pRS405(HA)₃VAM3 (B. Nichols, MRC-LMB, Cambridge, UK). Expression plasmids encoding Myc-tagged invertase, Myc-tagged Mnt1p and GFP-tagged Sed5p have been described previously (23).

Promotor regions (650 bp) and open reading frames of *CSG1* and *CSH1* were PCR amplified from yeast genomic DNA and subsequently ligated into single-copy vector pRS413 (CEN, *HIS3*) or multi-copy vector pRS425 (2μ, *LEU2*; (36)). A second version of these constructs was prepared, but then with 3 copies of the HA epitope fused to the

carboxy-termini of *CSG1* and *CSH1*, using PCR.

Lipid analysis

Exponentially grown cells (0.5 OD₆₀₀) were inoculated in 5 ml SD medium containing 10 µCi *myo*-[³H]inositol (16 Ci/mmol; ICN Biomedicals, Eschwege) and grown for 16 h at 30°C. Cells were harvested by centrifugation, washed twice with 10 mM NaN₃ and lipids extracted by bead bashing in H₂O/methanol/chloroform (5:16:16). The organic extracts were dried and subjected to butanol/water partitioning. Lipids recovered from the butanol phase were deacylated by mild base treatment using 0.2 N NaOH in methanol. After neutralizing with 1 M acetic acid, lipids were extracted with chloroform and separated by TLC using chloroform/methanol/4.2 M NH₃ (9:7:2). The TLC plate was dipped in 0.4% 2,5 diphenyloxazol dissolved in 2-methylnaphthalene supplemented with 10% xylene (37) and ³H-labeled lipids detected by fluorography using Kodak X-Omat S films exposed at -80°C. Alternatively, ³H-labeled lipids were detected by exposure to BAS-TR2040 imaging screens (Fuji, Japan) and read out on a BIO-RAD Personal Molecular Imager (BioRad, Hercules, CA).

Analysis of IPC mannosyltransferase activity in cell extracts

Exponentially grown *Δcsg1Δcsh1* cells (2.5 OD₆₀₀) were inoculated in 50 ml SD medium containing 100 µCi *myo*-[³H]inositol and then grown for 16 hrs at 30°C. Cells were harvested by centrifugation, washed twice with 10 mM NaN₃ and lysed by bead bashing in lysis buffer (50 mM Hepes, pH 7.2, 1 mM MnCl₂, 1 mM NEM) in the presence of fresh protease inhibitors. After removal of unbroken cells (500 g, 10 min), membranes were collected (100.000 g, 60 min) and solubilized in 1 ml lysis buffer containing 1% and fresh protease inhibitors. After incubation for 60 min at room temperature, the extract was centrifuged (100.000 g, 60 min), and 50 µl aliquots were stored at -80°C. In addition, 400 OD₆₀₀ of non-radiolabeled, exponentially-grown wild type or *Δcsg1Δcsh1* cells transformed with multicopy *CSG1*, *CSH1* or control plasmids were lysed by bead bashing in 4 ml ice-cold lysis buffer containing fresh protease inhibitors. Upon removal of unbroken cells, total membranes were collected, resuspended in 1 ml ice-cold lysis buffer containing 1% TritonX-100 and rotated at 4°C for 60 min.

For IPC mannosyltransferase assays, 50 µl of radio-labeled extract was mixed with 150 µl of unlabeled extract and then pre-incubated with 10 mM GDP-mannose (Sigma-Aldrich, St. Louis, MO) for 10 min at 30°C. Reactions were diluted 10-fold in lysis buffer and then incubated for 2 hrs at 30°C. Reactions were stopped by adding 6.4 ml chloroform:methanol (1:2.2). Lipids were extracted, deacylated and separated by TLC as above.

Antibodies and immunoblotting

Peptides corresponding to carboxy-terminal regions of Csg1p and Csh1p (Figure 1) were synthesized and then coupled to a carrier before immunization of rabbits. The resulting antisera were affinity-purified against peptides coupled to NHS-activated Sepharose 4 Fast Flow according to instructions of the manufacturer (Pharmacia, Piscataway, NJ). Affinity-

purified antibodies were used at a dilution of 1:1000 for immunoblot analysis and at 1:250 for immunofluorescence microscopy. Rabbit polyclonal antibodies to CPY, Gos1p, Pep12p, Tlg1p and Tlg2p were described previously (38). Rabbit polyclonal antibodies to Sso2p were provided by S. Keränen, (Biotechnology and Food Research, Espoo, Finland) and to Gas1p by H. Riezman (Sciences II, Geneva, Switzerland). The Myc epitope was detected with mouse monoclonal antibody 9E10 or with rabbit polyclonal antibodies (Santa Cruz Biotechnology, CA) and the HA epitope with rat monoclonal antibody 3F10, mouse monoclonal antibody 12CA5 (Boehringer-Mannheim, Germany) or rabbit polyclonal antibodies (Santa Cruz). For immunoblotting, all antibody incubations were carried out in PBS containing 5% dried milk and 0,5% Tween-20. After incubation with peroxidase-conjugated secondary antibodies (Biorad), blots were developed using a chemiluminescent substrate kit (Pierce, Rockford, USA). Chemiluminescent bands were quantified using a GS-710 calibrating imaging densitometer (BioRad) with QuantityOne software.

Enzyme assays

ATPase assays were performed on equal amounts of 10-fold diluted fraction at 30°C in a volume of 25 µl (10 mM Hepes-KOH, pH 7.2, 0.8 M sorbitol, 2 mM ATP, 5 mM MgCl₂). Reactions were stopped after 30 minutes with 175 µl 40 mM H₂SO₄. Then 50 µl 6 M H₂SO₄ containing 0.001% malachite green was added and after 30 min incubation at room temperature, the absorbance was measured at 595 nm. For determining the invertase activity, fractions were diluted 10–20 fold and assayed by the method described by Goldstein and Lampen (39), and the absorbance was measured at 540 nm.

Immunofluorescence microscopy

Exponentially-grown cells were fixed and mounted on glass-slides as described previously (38). All antibody incubations were performed in PBS supplemented with 2% dried milk and 0.1% saponin for 2h at room temperature. Primary polyclonal antibodies to Csg1p, Csh1p and the rat monoclonal 9F10 to HA were used at a dilution of 1:400, 1:150 and 1:250 respectively. Fluorescein- or Cy3-conjugated secondary antibodies (Amersham, Arlington Heights, IL) were used at a dilution of 1:100. Fluorescence microscopy and image acquisition were carried out using a Leica DMRA microscope (Leitz, Wetzlar, Germany) equipped with a cooled CCD camera (KX85, Apogee Instruments Inc., Tucson, AZ) driven by Image-Pro Plus software (Media Cybernetics, Silver Spring, MD).

Fractionation of secretory vesicles

Exponentially grown *sec6-4* cells expressing HA-tagged Pma1p (2.0 OD₆₀₀) were inoculated into YEPD medium (500 ml culture per gradient) and then grown for 14–16 h at 25°C to 0.7 OD₆₀₀/ml. Next, cells were collected (500 g, 5 min) resuspended in 250 ml YEPD and then shifted to 38°C for 60 min to induce the *sec6-4* secretory block. Spheroplasting, cell lysis and collection of membrane pellet enriched in secretory vesicles (SVs) were performed essentially as described (7) except that SVs were collected on a 60% Nycodenz cushion in lysis buffer. SVs were resuspended in 1.5 ml lysis buffer adjusted to 30% Nycodenz and then

loaded at the bottom of a 11 ml linear 16–26% Nycodenz/0.8 M sorbitol gradient. Following centrifugation at 100,000 g_{av} for 16 h min at 4°C in a Beckman SW41Ti rotor, 0.6-ml fractions were collected from the top of the gradient. Fraction densities were determined by reading refractive indices on a Bausch and Lomb refractometer. Equal amounts per fraction were subjected to immunoblotting and analysed for ATPase and invertase enzyme activity as described (7).

Immuno-isolation of secretory vesicles

Immuno-isolations of Pma1p-HA-containing SVs were performed using magnetic Dynabeads protein G (DynaL Biotech GmbH, Hamburg, Germany) loaded with mouse anti-HA (12CA5) or anti-Myc (9E10) monoclonal antibodies. Beads were incubated with antibodies for 40 min at room temperature and antibodies bound quantified by SDS-PAGE. Anti-HA beads contained 0.35 μ g 12CA5/ μ l bead-slurry and control beads contained 0.1 μ g 9E10/ μ l bead-slurry. For immuno-isolation of Pma1p-containing vesicles, a 300- μ l reaction was prepared in lysis buffer containing 126 μ l Dynabeads slurry, 5 mg/ml BSA and 15 μ l membranes from Nycodenz gradient PM-ATPase peak fractions obtained by fractionating membranes derived from 1 g of cells. The reactions were rotated gently at 4°C for 2 h. Supernatants were subjected to centrifugation (100.000 g , 1 h, 4°C) and membrane pellets were resuspended in 100 μ l SDS sample buffer. Beads were washed twice for 30 min in 1 ml of BSA-containing lysis buffer, twice in lysis buffer and resuspended in 75 μ l SDS sample buffer. Bound and unbound membranes were analyzed by immunoblotting.

Results

CSH1 encodes a novel putative IPC mannosyltransferase

Comparative sequence analysis revealed that Csh1p is 67% identical to Csg1p and has the same predicted protein topology, namely a putative NH₂-terminal signal sequence and two potential transmembrane segments localized to the carboxy-terminal half of the protein (Figure 1). Between the signal sequence and first transmembrane segment there is a region of 93 residues sharing 29% identity with the luminal portion (residues 96–197) of the yeast α -1,6-mannosyltransferase, Och1p (40). This region contains a conserved DXD motif that occurs in a wide range of glycosyltransferase families and likely forms part of a catalytic site (41).

Csg1p is required for accumulation of mannosylated sphingolipids in yeast and its similarity to Och1p suggests that the protein serves as an IPC mannosyltransferase (27). However, loss of Csg1p is not sufficient to abolish IPC mannosylation (see also below), raising the possibility that Csh1p represents an alternative IPC mannosyltransferase that functions independently of Csg1p. To investigate this possibility, we constructed yeast strains in which the ORFs of *CSG1*, *CSH1* or both were removed. TLC analysis of alkaline-treated lipid extracts prepared from *myo*-[³H]inositol-labeled cells showed that, compared to the wild type strain, the Δ *csg1* mutant produced greatly reduced levels of the mannosylated sphingolipids MIPC and M(IP)₂C, and accumulated IPC-C and IPC-D (Figure 2 A, lanes 1 and 2; note that IPC-C contains a

monohydroxylated C26 fatty acid whereas the C26 fatty acid in IPC-D is dihydroxylated; (42). Unlike $\Delta csg1$ cells, the $\Delta csh1$ mutant produced IPC and mannosylated IPC species at ratios similar to those in wild type cells (Figure 2 A, lanes 1 and 3). In the $\Delta csg1\Delta csh1$ double mutant, however, production of MIPC and $M(IP)_2C$ was completely abolished (Figure 2 A, lane 4). These results are consistent with those reported in a recent study (29) and indicate that Csg1p and Csh1p have redundant functions in IPC mannosylation.

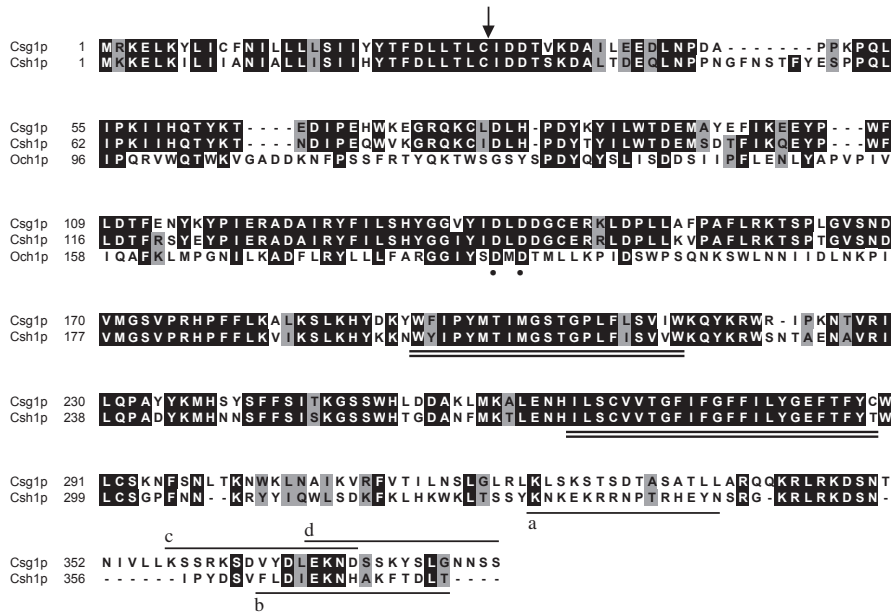


Figure 1. Alignment of the amino acid sequences of Csg1p, Csh1p and Och1p. Sequences were aligned with CLUSTAL W. Conserved (black) or related residues (gray) are boxed. A putative signal peptide cleavage site is indicated by an arrow. Two potential transmembrane domains are doubly underlined. A conserved DXD motif found in many glycosyltransferases is marked by dots. Single lines (a-d) mark peptide sequences used to raise specific antibodies.

The block in MIPC and $M(IP)_2C$ synthesis observed in $\Delta csg1\Delta csh1$ cells can be explained by a complete loss of IPC mannosyltransferase activity, but may also be due to a defective delivery of IPC or GDP-mannose to the transferase-containing compartment. To explore these possibilities, we analyzed the IPC mannosyltransferase activity in detergent extracts derived from wild type and $\Delta csg1\Delta csh1$ cells. To this end, Triton-X100 extracts prepared from *myo*- $[^3H]$ inositol-labeled $\Delta csg1\Delta csh1$ cells were mixed with extracts from unlabeled wild type or mutant cells, and then incubated in the presence or absence of externally added GDP-mannose. When extracts from inositol-labeled $\Delta csg1\Delta csh1$ cells were incubated with unlabeled wild type cell extracts, radioactive IPC was converted to MIPC and $M(IP)_2C$ in a GDP-mannose-dependent manner (Figure 2 B, lanes 2 and 3). In contrast, addition of GDP-mannose to $\Delta csg1\Delta csh1$ cell extracts was not sufficient to support MIPC and $M(IP)_2C$ synthesis (Figure 2 B,

lanes 1 and 4). However, when inositol-labeled $\Delta csg1\Delta csh1$ extracts were incubated with extracts from unlabeled $\Delta csg1\Delta csh1$ cells transformed with the *CSG1* or *CSH1* gene on a multicopy plasmid, the GDP-mannose-dependent mannosylation of IPC was restored (Figure 2 B, lanes 5 and 6; our unpublished data). These results indicate that $\Delta csg1\Delta csh1$ cells are defective in IPC mannosyltransferase activity rather than in IPC or GDP-mannose transport.

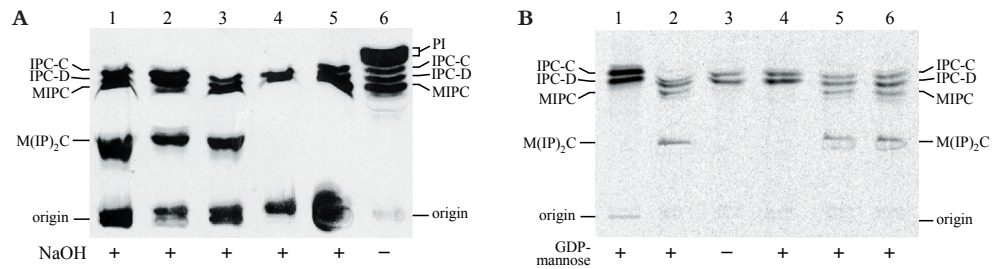
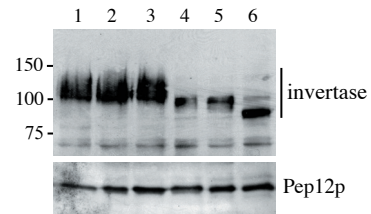


Figure 2. Csg1p and Csh1p have redundant functions in sphingolipid mannosylation. (A) Deletion of *CSG1* and *CSH1* abolishes IPC mannosylation. Yeast cells were labeled overnight with *myo*-[³H]inositol and the lipid extracts either deacylated by mild alkaline hydrolysis with NaOH (+) or control incubated (-). Lipids were extracted, separated by TLC, and then visualized by autoradiography as described under Experimental Procedures. Lane 1: wild type; lane 2: $\Delta csg1$; lane 3: $\Delta csh1$; lane 4: $\Delta csg1\Delta csh1$; lanes 5 and 6: $\Delta ipt1$. Note that *IPT1* is known to have an essential function in M(IP)₂C synthesis. (B) Analysis of IPC mannosyltransferase activity in TritonX-100 extracts derived from wild type and $\Delta csg1\Delta csh1$ cells. Extracts prepared from *myo*-[³H]inositol-labeled $\Delta csg1\Delta csh1$ cells were either control incubated (lane 1) or mixed with extracts of unlabeled wild type cells (lanes 2 and 3), $\Delta csg1\Delta csh1$ cells (lane 4) or $\Delta csg1\Delta csh1$ cells transformed with a multicopy vector containing *CSG1* (lane 5) or *CSH1* (lane 6). Incubations were performed in the presence (+) or absence (-) of 1 mM GDP-mannose as described under Experimental Procedures. Lipids were extracted, deacylated and then separated by TLC before autoradiography.

To investigate whether loss of Csg1p and Csh1p also affects protein mannosylation, we next examined the glycosylation state of invertase produced in wild type and mutant strains. This periplasmic enzyme undergoes extensive outer chain mannan addition on 8-10 of its *N*-linked glycans while passing through the Golgi (43). Consequently, its electrophoretic mobility is increased when enzymes responsible for mannan synthesis are removed (32, 44). Immunoblot analysis of cells expressing Myc-tagged invertase showed that the gel mobility of the protein produced in the $\Delta csg1\Delta csh1$ mutant was indistinguishable from that in wild type cells (Figure 3, lanes 1 and 3). In contrast, loss of mannosyltransferases involved in the initiation (Van1p) or elongation (Anp1p, Mnn10p) of the mannan backbone caused a substantial increase in the gel mobility of invertase (Figure 3, lanes 4-6). These results demonstrate that protein mannosylation occurs independently of Csg1p and Csh1p, and that the defect in sphingolipid mannosylation in $\Delta csg1\Delta csh1$ cells is specific.

Collectively, our results suggest that yeast contains two independent IPC mannosyltransferases: one encoded by *CSG1* and likely responsible for producing the bulk of mannosylated IPC, and the second one encoded by *CSH1* and corresponding to a minor IPC mannosyltransferase activity.

Figure 3. Loss of Csg1p and Csh1p does not affect protein mannosylation. An immunoblot of total protein extracts prepared from wild type and various mannosyltransferase mutant cells expressing Myc-tagged invertase was stained with a monoclonal antibody to the Myc epitope. The blot was reprobbed with polyclonal antibodies to the endosomal t-SNARE, Pep12p, to control for equal loading. The positions of size markers (kDa) are indicated. Lane 1: wild type; lane 2: $\Delta csg1$; lane 3: $\Delta csg1\Delta csh1$; lane 4: $\Delta amp1$; lane 5: $\Delta mnn10$; lane 6: $\Delta van1$.



Membrane topology of Csg1p and Csh1p

Golgi-associated glycosyltransferases generally have a type II topology with a short cytoplasmic tail and a large catalytic domain in the lumen (e.g. Mnt1p). Csg1p and Csh1p, on the other hand, contain a putative N-terminal signal sequence and two potential membrane spans that predict a different membrane topology where both termini of the protein are situated in the lumen (Figure 4 A). To test this prediction, we introduced three copies of the HA epitope at the carboxy-terminus of Csg1p. Attachment of the epitope did not inactivate the enzyme since expression of Csg1p-HA restored production of mannosylated sphingolipids in $\Delta csg1\Delta csh1$ cells (data not shown). Expression of Csg1p-HA resulted in the appearance of two major protein bands of approximately 48 and 54 kDa on blots of total yeast extracts probed with anti-HA antibody (Figure 4 B, lane 2). Pre-treatment of extracts with endoglycosidase F (Endo F) abolished the 54-kDa band and increased the intensity of the 48-kDa band (Figure 4 B, lane 3), indicating that a portion of Csg1p is glycosylated on one or more asparagine residues. Since all 5 potential N-linked glycosylation sites of Csg1p occur within its hydrophilic carboxy-terminus (see Figure 1), this region would be luminal. Indeed, when membranes from cells expressing Csg1p-HA were treated with trypsin, the 48-kDa and 54-kDa protein bands were degraded and a major HA-tagged product of 24 kDa appeared in the absence of detergent (Figure 4 C). Under these conditions, the *medial* Golgi v-SNARE Gos1p was degraded whereas removal of a luminal, carboxy-terminal Myc-tag fusion to the type II Golgi enzyme Mnt1p was observed only after detergent treatment. Together, these findings demonstrate that the carboxy-terminus of Csg1p is luminal, hence consistent with the topology depicted in Figure 4 A.

Csg1p and Csh1p co-localize with IPC synthase to the medial Golgi

To investigate the subcellular distribution of Csg1p and Csh1p, we raised polyclonal antibodies against synthetic peptides corresponding to areas with the least sequence homology (see Figure 1). Antibodies against Csg1p-derived peptides detected 45- and 52-kDa protein bands on immunoblots of wild type yeast extracts. These bands were absent in extracts from $\Delta csg1$ mutant strains while their levels increased 10-fold in cells expressing Csg1p from a multicopy vector (Figure 5 A). Antibodies against Csh1p-derived peptides detected a 48-kDa band, but only in extracts of cells over-expressing Csh1p from a multicopy vector (Figure 5 A). We initially investigated the subcellular distribution of Csg1p and Csh1p

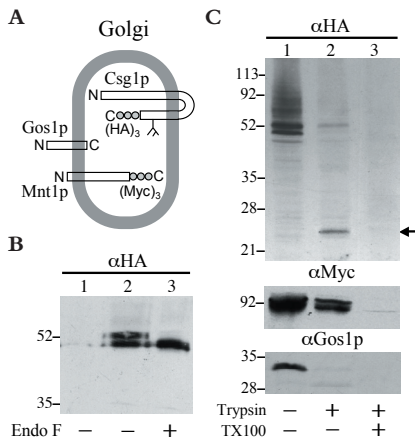


Figure 4. Membrane topology of Csg1p. (A) Schematic view of the (predicted) membrane topologies of Golgi v-SNARE, Gos1p, glycosyltransferase, Mnt1p, and putative sphingolipid mannosyltransferase, Csg1p. (B) Total protein extracts from cells in which Csg1p was either tagged with three copies of the HA epitope (lanes 2 and 3) or not (lane 1) were treated for 24 h at 37°C with 80 mU EndoF (Boehringer, Mannheim) per 60 μ g protein, as indicated. Proteins were resolved by SDS-PAGE and subjected to Western blot analysis using anti-HA antibodies. (C) Immunoblot of membranes from yeast cells expressing Csg1p and Mnt1p tagged with three copies of the HA (Csg1p) or Myc epitope (Mnt1p) at the carboxy-terminus. Membranes were pretreated for 30 min at 30°C with 8 mM trypsin and 0.4% TritonX-100 (TX100), as indicated. Each lane contains membranes prepared from 33 OD (600 nm) units of log-phase grown cells, as described previously (38). The immunoblot was stained with polyclonal antibodies against the HA epitope, the myc epitope or the Golgi v-SNARE, Gos1p.

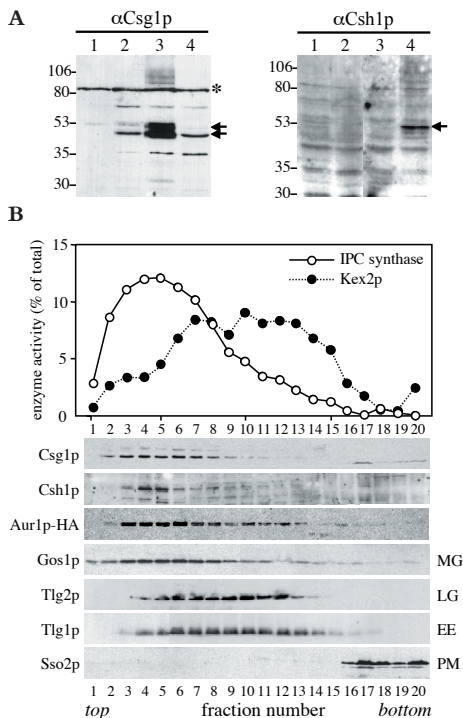


Figure 5. Subcellular fractionation of Csg1p and Csh1p. (A) Immunoblots containing equal amounts of total protein extracts prepared from Δ *csg1* cells (lane 1), Δ *csh1* cells (lane 2) or wild type cells transformed with a multicopy vector containing *CSG1* (lane 3) or *CSH1* (lane 4). Blots were stained with polyclonal anti-Csg1p or anti-Csh1p antibodies that were raised against synthetic peptides corresponding to areas with the least sequence homology (see Figure 1). (B) Sucrose gradient fractionation of membranes. A high-speed membrane pellet (100,000 g) prepared from yeast cells expressing HA-tagged Aurlp was fractionated on a sucrose density gradient. Fractions were assayed for IPC synthase and Kex2p enzyme activities as described under Experimental Procedures. Fractions were also analysed by immunoblotting using polyclonal antibodies against Csg1p, Csh1p and several organellar markers. A mouse monoclonal anti-HA antibody was used to detect HA-tagged Aurlp. MG: medial Golgi; LG: late Golgi; EE: early endosomes; PM: plasma membrane.

by fractionating organelles from wild type yeast on equilibrium sucrose density gradients and blotting the gradient fractions with the specific antibodies. Csg1p and Csh1p clearly separated from markers for late Golgi/early endosomes (Kex2p, Tlg1p, Tlg2p), vacuoles (Vam3p) and plasma membrane (Sso2p; Figure 5 B and data not shown). In contrast, Csg1p and Csh1p co-fractionated with the *medial* Golgi v-SNARE Gos1p, with IPC synthase activity and with HA-tagged Aur1p, a protein required for IPC synthesis and localized to the *medial* Golgi (23, 45).

Since the different compartments of the yeast Golgi are not well resolved on sucrose gradients, the localization of Csg1p and Csh1p was further investigated by immunofluorescence microscopy. Staining of wild type cells with anti-Csg1p antibodies produced a punctate pattern characteristic of the yeast Golgi apparatus that was absent in $\Delta csg1$ cells (Figure 6 A). A similar pattern was observed when cells were stained with anti-Csh1p antibodies, but only when Csh1p was overexpressed from a multi-copy vector. These Csh1p-positive structures showed extensive co-localization with HA-tagged Csg1p, indicating that the two proteins occupy the same subcompartment of the Golgi (Figure 6 B). There was no significant co-localization of Csg1p/Csh1p-labeled spots with GFP-tagged Sed5p, a marker of the *cis* Golgi (Figure 7). However, Csg1p/Csh1p-positive structures showed substantial co-localization with HA-tagged Aur1p (Figure 7) and with the *medial* Golgi marker Mnt1p (data not shown).

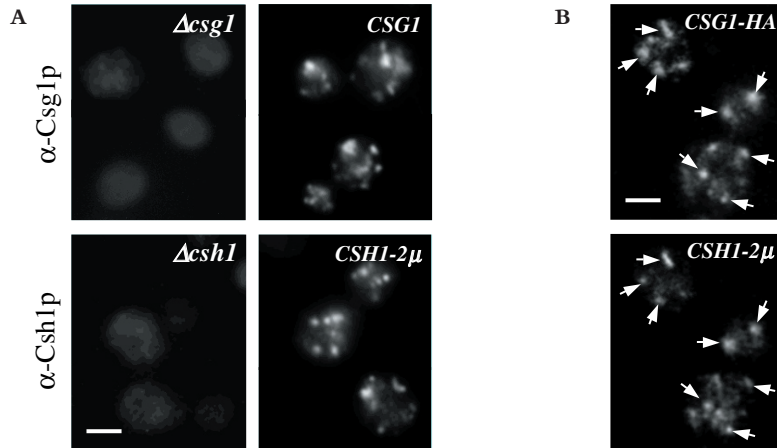


Figure 6. Colocalization of Csg1p and Csh1p by immunofluorescence. (A) Immunofluorescence confocal micrographs of yeast cells stained with affinity-purified rabbit polyclonal antibodies directed against Csg1p (α -Csg1p) or Csh1p (α -Csh1p). Note that anti-Csg1p fluorescence is observed in wild type (*CSH1*), but not in $\Delta csg1$ cells, whereas anti-Csh1p fluorescence occurs only in cells overexpressing Csh1p from a multi-copy plasmid (*CSH1-2 μ*). (B) Double-label immunofluorescence confocal micrographs comparing the localization of HA-tagged Csg1p (*CSH1-HA*) with Csh1p expressed from a multi-copy plasmid (*CSH1-2 μ*). Anti-HA staining was with rat monoclonal antibody 3F10. Most of the Csg1p-positive structures were also positive for Csh1p (arrows). Bars, 3 μ m.

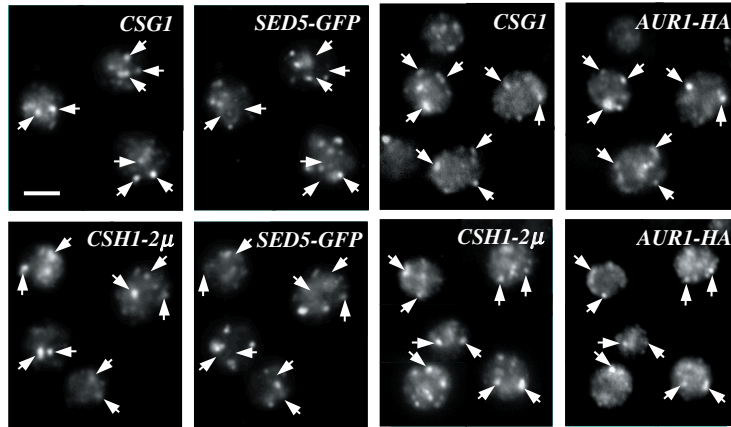


Figure 7. Csg1p and Csh1p colocalize with Aur1p by immunofluorescence. Double-label immunofluorescence confocal micrographs comparing the localization of Csg1p and Csh1p with that of GFP-tagged Sed5p (*cis* Golgi) or HA-tagged Aur1p (*medial* Golgi). Staining of Csg1p and Csh1p was performed as in Figure 6 with Csh1p expressed from a multicopy plasmid (*CSH1-2 μ*). Staining of HA-tagged Aur1p was with the rat mAb, 3F10. Csg1p and Csh1p positive structures were often positive for Aur1p, but not for Sed5p. Bar, 5 μ m.

To verify co-localization of Csg1p/Csh1p and Aur1p by a complementary method, cells expressing Aur1p with three copies of the HA epitope inserted at its cytosolic carboxy-terminus were lysed and Aur1p-containing membranes immunisolated using anti-HA antibodies bound to magnetic beads. This method allowed the isolation of nearly 20% of the Aur1p-HA containing membranes from a cell lysate (Figure 8 A). Strikingly, a similar fraction of Csg1p containing membranes was bound to the beads. Binding of Aur1p-HA and Csg1p containing membranes was strictly dependent on the presence of anti-HA antibodies on the beads. Membranes containing the ER marker Dpm1p did not bind. As additional control, the immunoisolation procedure was repeated on lysates of cells expressing the HA-tag on the cytosolic amino-terminus of the vacuolar t-SNARE, Vam3p. As shown in Figure 8 B, anti-HA beads brought down nearly half of the Vam3p-containing membranes. Under these conditions, neither Csg1p- nor Dpm1p-containing membranes did bind.

Collectively, our results indicate that Csg1p and Csh1p primarily reside with the IPC synthase in a *medial* compartment of the yeast Golgi.

Golgi-to-vacuole transport pathways are unaffected in mutants deficient in mannosylated sphingolipids

In mammals, glycosphingolipids have been implicated in targeting membrane proteins from the Golgi to compartments of the endosomal/lysosomal system (20) and to the surface domains of polarized cells (12-15). To investigate whether mannosylated sphingolipids in yeast serve a similar role, the Δ *csg1* Δ *csh1* mutant was analysed for possible defects in post-Golgi delivery pathways.

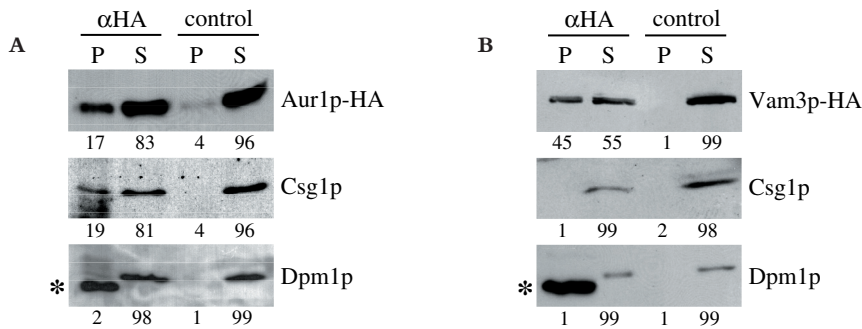


Figure 8. Membranes immunoprecipitated by Aur1p contain Csg1p. High speed membrane pellets (100,000 g) prepared from cells expressing 3 copies of the HA epitope on the cytosolic carboxy-terminus of Aur1p (**A**) or amino-terminus of vacuolar t-SNARE Vam3p (**B**) were subjected to immunoprecipitation using Dynabeads protein G preincubated with (α HA) or without (control) mouse anti-HA monoclonal antibody, 12CA5. Percentages of immunoprecipitated Aur1p, Vam3p, Csg1p and the ER marker, Dpm1p, were determined by Western blot analysis using rabbit polyclonal antibodies against the HA-epitope or Smt1p, and a mouse monoclonal antibody against Dpm1p. Note that immunostaining against Dpm1p led to cross-reactivity with the 12CA5-derived IgG light chain (asterisk). B: beads; S: supernatant.

In yeast, biosynthetic transport of proteins from the Golgi to the vacuole proceeds through two separate pathways, the carboxypeptidase Y (CPY) pathway and the alkaline phosphatase (ALP) pathway. Whereas the CPY pathway mediates a clathrin-dependent delivery of vacuolar proteins via late (prevacuolar) endosomes, the ALP pathway provides an alternative, clathrin-independent route that bypasses late endosomes and requires the AP-3 adaptor protein complex (2). The vacuolar protease CPY is synthesized as a p1 precursor in the ER, modified to a slightly larger p2 form in the Golgi, and then passes through late endosomes to reach the vacuole where it is proteolytically processed to its mature form (46). Pulse-chase immunoprecipitation analysis revealed that CPY maturation in the $\Delta csg1\Delta csh1$ mutant is unaffected (Figure 9). The efficient processing of CPY indicated that there was little mis-sorting to the cell surface, and indeed we failed to detect any radio-labeled CPY released from $\Delta csg1\Delta csh1$ cells. This is in contrast to cells lacking the endosomal/vacuolar syntaxins Pep12p and Vamp3p where CPY is diverted to the cell surface in the p2 form (Figure 9). The vacuolar membrane protein ALP is synthesized as a precursor that undergoes proteolytic processing in the vacuole yielding a smaller mature form (47). As shown in Figure 9, $\Delta csg1\Delta csh1$ cells displayed no significant delay in ALP maturation. In the $\Delta pep12\Delta vam3$ mutant, on the other hand, ALP maturation was abolished. These results show that mannosylated sphingolipids in yeast do not serve a critical function in clathrin- or AP-3-mediated protein transport from the Golgi to the vacuole. Moreover, the efficient processing of newly synthesized CPY and ALP in $\Delta csg1\Delta csh1$ cells indicates that blocking sphingolipid mannosylation has no general effect on forward transport through the Golgi apparatus. Consistent with this notion, $\Delta csg1\Delta csh1$ and wild type cells contain similar amounts of Golgi-modified invertase (Figure 3).

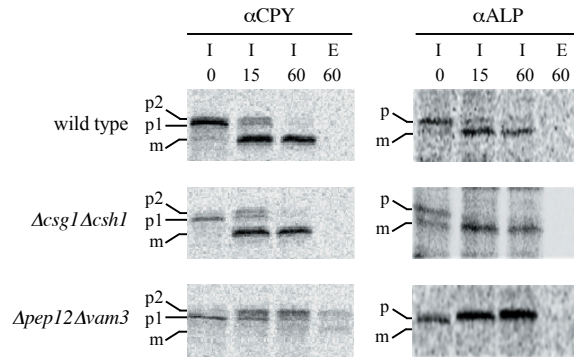


Figure 9. Vacuolar protein sorting and processing in the $\Delta csg1\Delta csh1$ mutant. Wild type, $\Delta csh1\Delta csg1$ and $\Delta pep12\Delta vam3$ cells were pulse-labeled with ^{35}S -labeled amino acids for 10 min, and then chased with nonradioactive methionine and cysteine for the indicated time points (min) at 26°C as described previously (55). Carboxypeptidase Y (CPY) and alkaline phosphatase (ALP) were immunoprecipitated from lysed cells (I) and the medium (E), resolved by SDS-PAGE and visualized on a PhosphorImager. Precursor (p) and mature forms (m) of CPY and ALP are indicated.

Mannosylated sphingolipids are not required for sorting cell surface proteins into distinct classes of secretory vesicles

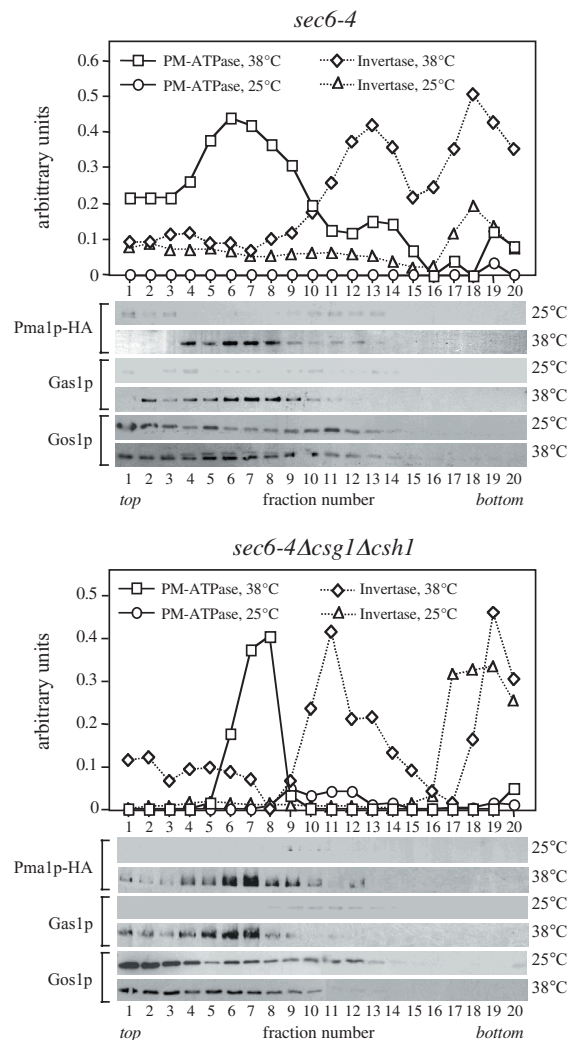
The characterization of secretory vesicles that accumulate in late exocytic yeast mutants (e.g. *sec1*, *sec6*) has identified two vesicle populations with different densities and distinct cargo proteins, indicating the existence of two parallel routes from the Golgi to the plasma membrane (7-9). The more abundant, lighter density vesicles contain the major plasma membrane ATPase Pma1p whereas the denser vesicles contain the periplasmic enzymes invertase and acidic phosphatase. Sorting invertase into the dense class of vesicles requires clathrin and an intact Golgi-to-late endosome transport pathway (9, 48). From these observations, it has been suggested that invertase is sorted from Pma1p at the late Golgi for delivery to late endosomes, from where high-density vesicles bud that carry invertase to the cell surface.

To investigate whether mannosylated sphingolipids play a role in the organisation of membrane trafficking to the cell surface, we disrupted the *CSG1* and *CSH1* genes in the late secretory mutant *sec6-4* and analysed the strain for defects in secretory cargo sorting. The *sec6-4* strain harbours a temperature-sensitive mutation in a component of the ‘exocyst’ protein complex that is required for polarized fusion of exocytic vesicles with the plasma membrane (49). The *sec6-4* mutant grows like wild type cells at 25°C, but growth ceases at 38°C and cells accumulate plasma membrane ATPase- and invertase-containing vesicles that can be separated by equilibrium isodensity centrifugation on Nycodenz gradients (7). To this end, *sec6-4* cells were grown at 25°C, shifted to 38°C for 90 min, lysed and then subjected to a 13,000-*g* spin to remove most of the ER, nuclei, vacuoles, mitochondria and plasma membrane. Next, a high-speed (100,000 *g*) membrane pellet enriched in secretory vesicles was collected and loaded at the bottom of a linear 16-26% Nycodenz gradient in 0.8 M sorbitol. As shown in Figure 10, gradient fractionation of membranes from 38°C-

shifted cells resulted in two peaks of enzyme activities that were absent when fractionation was performed on 25°C-grown cells: a low density peak (fractions 4-9) containing ATPase activity and a higher density peak (fractions 10-15) containing invertase activity (note that the invertase peak found near the bottom of the gradient (fractions 17-20) likely corresponds to the cytoplasmic, non-glycosylated form of the enzyme). Western blot analysis revealed that Pma1p co-fractionates with the lower density membranes, confirming that the detected ATPase activity is due to this protein. In contrast, markers for the ER (Dpm1p) and Golgi (Gos1p) did not peak with either vesicle population and their levels in gradients of 25°C-grown and 38°C-shifted cells were very similar (Figure 10 and data not shown). This indicates that the detected ATPase and invertase peaks are not due to the accumulation or fragmentation of the ER or Golgi apparatus.

Figure 10. Gradient fractionation of secretory vesicles accumulated in *sec6-4* and *sec6-4Δcsg1Δcsh1* cells.

Membrane pellets (100,000 g) enriched in secretory vesicles were prepared from temperature-shifted (38°C) and non-shifted (25°C) cells, loaded on the bottoms of linear 16–26% Nycodenz/0.8 M sorbitol gradients and then floated to equilibrium by centrifugation. Fractions were collected from the top and analyzed for enzyme activities and by immunoblotting. Enzyme activities are expressed in arbitrary units based upon the absorbance measured at 820 nm (PM-ATPase) or 540 nm (invertase) as described under Experimental Procedures. Immunoblots were stained with a monoclonal antibody against the HA epitope to detect HA-tagged Pma1p and with polyclonal antibodies against the GPI-anchored protein, Gas1p, or the medial Golgi v-SNARE, Gos1p. The density profiles were similar for all gradients (not shown).



The fractionation profiles of ATPase activity, Pma1p and invertase in gradients of 38°C-shifted *sec6-4Δcsg1Δcsh1* cells closely resembled those found for *sec6-4* cells (Figure 10). This shows that mannosylated sphingolipids are required neither for the biogenesis of the light or the dense class of secretory vesicles, nor for segregating Pma1p and invertase into these different vesicle populations. Since glycosphingolipids have previously been implicated in the sorting of GPI-linked proteins (13-15), we wished to determine which of the two secretory vesicle classes in yeast mediates transport of the GPI-anchored cell surface protein Gas1p. Western blot analysis revealed that Gas1p co-fractionates with Pma1p and ATPase activity in gradients of 38°C-shifted *sec6-4* cells, regardless of whether Csg1p and Csh1p were present (Figure 10). A similar fractionation profile was observed for the GPI-linked protein Ysp1p (data not shown). The co-fractionation of GPI-linked proteins and Pma1p suggests that these proteins are packaged into a common carrier. However, it is also possible that GPI-linked proteins are sorted into a different class of vesicles with fractionation properties similar to that of Pma1p-transporting vesicles. To distinguish between these possibilities, we immuno-isolated Pma1p-containing vesicles from 38°C-shifted *sec6-4* and *sec6-4Δcsg1Δcsh1* cells, and assessed whether these vesicles contained Gas1p. Immuno-isolations were performed with membranes derived from 38°C-shifted cells expressing Pma1p with three copies of the HA epitope inserted at its cytosolic amino-terminus. Membranes were fractionated on a Nycodenz gradient as above and Pma1p-HA containing vesicles isolated from the ATPase peak fraction (fraction 7) using anti-HA monoclonal antibodies bound to magnetic beads. This allowed the isolation of about 70% of Pma1p-HA and 50% of Gas1p present in the *sec6-4* ATPase peak fraction (Figure 11). Immuno-isolation of Pma1p-HA from the *sec6-4Δcsg1Δcsh1*-derived ATPase peak was less efficient (24% of total), but brought down a similar portion of Gas1p (16%). In both cases, binding of Pma1p-HA and Gas1p containing membranes was strictly dependent on the presence of anti-HA antibodies on the beads. It therefore appears that Pma1p and Gas1p are packaged into a common transport carrier for delivery to the cell surface. Moreover, our findings demonstrate that sorting of GPI-linked proteins in the late secretory pathway of yeast essentially occurs independently of mannosylated sphingolipids.

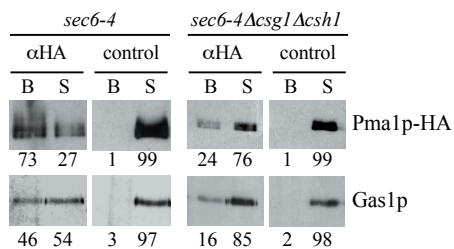


Figure 11. Pma1p and Gas1p are packaged into a common secretory vesicle species.

Aliquots from the PM-ATPase peak fractions derived from temperature-shifted, Pma1p-HA-expressing *sec6-4* or *sec6-4Δcsg1Δcsh1* cells (Figure 10) were used to immunoisolate Pma1p-containing vesicles with anti-HA monoclonal antibodies (αHA) bound to Dynabeads protein G. Immunoisolations with Dynabeads containing anti-Myc monoclonal antibodies served as control. The percentage of immunoprecipitated Pma1p and Gas1p was determined by Western blot analysis. B: beads; S: supernatant.

Discussion

The results presented in this study indicate that the yeast genes *CSG1* and *CSH1* encode proteins with a primary and redundant function in the mannosylation of phosphoinositol-containing sphingolipids. Our finding that $\Delta csg1\Delta csh1$ cells exhibit a specific and complete block in sphingolipid mannosylation offered an opportunity to explore the potential role of mannosylated sphingolipids in secretory cargo sorting in yeast.

A primary function of Csg1p and Csh1p as sphingolipid mannosyltransferases is supported by the following observations. First, removal of Csg1p and Csh1p suffices to abolish MIPC and $M(IP)_2C$ synthesis, resulting in accumulation of MIPC precursor, IPC. Second, biochemical characterization of the IPC mannosyltransferase activity in cell extracts revealed that the inability of $\Delta csg1\Delta csh1$ cells to generate MIPC and $M(IP)_2C$ can not be attributed to a defective delivery of GDP-mannose or IPC to the transferase-containing compartment. Third, Csg1p and Csh1p share a region of homology with the yeast α -1,6-mannosyltransferase Och1p and contain a conserved DXD motif which is part of a catalytic site found in many known glycosyltransferases (41). Fourth, Csg1p and Csh1p are localized to the yeast Golgi where sphingolipid mannosylation is known to occur (50). Fifth, protease protection analysis and the utilization of *N*-linked glycosylation sites in Csg1p predict a membrane topology with the Och1p-homology domain and DXD motif positioned in the Golgi lumen, hence in keeping with the fact that sphingolipid mannosylation takes place on the luminal aspect of the Golgi (24).

Whether Csg1p and Csh1p are IPC mannosyltransferases or represent catalytic subunits of two distinct IPC mannosyltransferase complexes remains to be established. Recent work revealed that Csg1p and Csh1p occur in a complex with Csg2p, a putative Ca^{2+} -binding membrane protein lacking homology to glycosyltransferases. Several lines of evidence suggest that the role of Csg2p in these complexes is regulatory rather than enzymatic (29). In any case, the latter study and our present findings point to the existence of two independent IPC mannosyltransferases in yeast. So why would yeast need two distinct sphingolipid mannosyltransferases? We found that Csg1p and Csh1p are co-localized with IPC synthase to a *medial* compartment of the Golgi. Hence, the expression of two sphingolipid mannosyltransferases unlikely serves to accommodate a need for synthesizing mannosylated sphingolipids at different cellular locations. It should be noted that yeast IPC is not a monomolecular lipid species, but represents a mixture of molecules that differ in the chain length and the extent of hydroxylation of both the sphingoid base and fatty acid (22). This raises the possibility that the two IPC mannosyltransferases differ in substrate specificity. Indeed, metabolic labeling of $\Delta csg1$ and $\Delta csh1$ cells with [3H]-dihydrosphingosine revealed some differences in activity between Csg1p and Csh1p toward particular molecular species of IPC (29). The biological implications of this finding remain to be established.

A key function attributed to sphingolipids is their ability to self-associate into membrane microdomains/rafts, especially when sterols are present. Formation of sphingolipid/sterol-rich microdomains is important for lateral sorting of membrane proteins, in particular those containing a GPI anchor (51, 52). Previous work in yeast has shown that sphingolipid

depletion affects both raft association and cell surface delivery of Pma1p and GPI-anchored proteins, i.e. Gas1p (17-19). In these studies, sphingolipid synthesis was blocked using a conditional allele of serine palmitoyltransferase activity, which catalyses the first committed step of sphingolipid synthesis (22). Precisely what structural determinants on sphingolipids are critical for a correct delivery of cell surface components has remained an open issue. The availability of a yeast strain with a primary block in IPC mannosylation led us to investigate whether maturation of the sphingolipid head group serves a role in organizing membrane trafficking to the plasma membrane.

Yeast harbours two transport routes from the Golgi to the plasma membrane. One route mediates delivery of Pma1p while the other one carries the secretory enzyme invertase among its cargo (7). Our data show that the GPI-anchored protein, Gas1p, segregates from the invertase route and is packaged with Pma1p into a common transport carrier for delivery to the plasma membrane. Blocking sphingolipid mannosylation by disrupting *CSG1* and *CSH1* had no effect on the sorting of these cargo molecules and we observed that temperature-shifted *sec6-4Δcsg1Δcsh1* cells accumulate two populations of secretory vesicles with characteristics indistinguishable from those generated in *sec6-4* cells. Moreover, thin-section electron microscopy revealed that both cell types accumulate very similar amounts of secretory vesicles (data not shown). Hence, mannosylated sphingolipids appear fully dispensable for the biogenesis of the two classes of secretory vesicles that mediate cell surface transport in yeast.

Also transport through the Golgi seems unaffected by a block in sphingolipid mannosylation. This can be inferred from the fact that *Δcsg1Δcsh1* cells deliver newly synthesized vacuolar proteins at wild type kinetics and do not contain higher levels of Golgi-modified invertase than wild type cells. Collectively, our data indicate that the plasma membrane trafficking defects previously reported for mutants blocked in the first committed step of sphingolipid synthesis cannot be ascribed to a deficiency in complex mannosylated sphingolipids (17-19). In fact, we found no evidence for a critical function of mannosylated sphingolipids in any of the known post-Golgi delivery pathways in yeast.

It has been shown that GDP-mannose transport into the Golgi lumen is essential for cell growth (24). Since mannosylation of proteins in the Golgi does not appear to be essential, it has been suggested that the strict requirement of GDP-mannose transport involves its effect on sphingolipid mannosylation (24). This idea is inconsistent with our present findings. Mannosylated sphingolipids are abundant components of the yeast plasma membrane, accounting for up to 8% of its total mass (25, 53). Therefore, it is somewhat surprising that a complete block in their synthesis has little if any effect on cell growth, at least under standard growth conditions (YEPA or synthetic medium at 30°C). Strains deleted for *CSG1* are hypersensitive for calcium (27) and we and others found that this phenotype is aggravated upon additional loss of *CSH1* (29). This calcium sensitivity is likely due to accumulation and/or mislocalization of IPC (more specifically IPC-C) rather than depletion of MIPC or M(IP)₂C (27). Interestingly, recent work suggests that M(IP)₂C synthesis is controlled in coordination with multidrug resistance in yeast, and that this lipid serves a role in determining the activity of drug transporters in and/or the permeability properties of the plasma membrane (54). How mannosylated sphingolipids

contribute to the functional organization of the plasma membrane poses an intriguing problem for future research.

Acknowledgements

This work is dedicated to Chantal Vogelzangs who set the basis of this study until her untimely death (June 24th, 2000). We are grateful to Edina Harsay, Amy Chang, Howard Riezman, Sirkka Keränen, Timothy Levine, Ben Nichols, Sean Munro and Steve Nothwehr for generously providing strains, plasmids or antibodies, to Sigrún Hrafnisdóttir and Juergen Stolz for helpful advice, and to Maurice Jansen for expert technical assistance. Q.L. is supported by a grant from the Meelmeijer foundation, and J.H. by a grant from the Royal Netherlands Academy of Arts and Sciences.

References

1. Mellman, I. (1996) *Annu. Rev. Cell Dev. Biol.* **12**, 575-625
2. Burd, C. G., Babst, M., and Emr, S. D. (1998) *Semin. Cell Dev. Biol.* **9**, 527-533
3. Keller, P., and Simons, K. (1997) *J. Cell Sci.* **110 (Pt 24)**, 3001-3009
4. Mostov, K. E., Verges, M., and Altschuler, Y. (2000) *Curr. Opin. Cell Biol.* **12**, 483-490
5. Yoshimori, T., Keller, P., Roth, M. G., and Simons, K. (1996) *J. Cell Biol.* **133**, 247-256
6. Musch, A., Xu, H., Shields, D., and Rodriguez-Boulan, E. (1996) *J. Cell Biol.* **133**, 543-558
7. Harsay, E., and Bretscher, A. (1995) *J. Cell Biol.* **131**, 297-310
8. David, D., Sundarababu, S., and Gerst, J. E. (1998) *J. Cell Biol.* **143**, 1167-1182
9. Harsay, E., and Schekman, R. (2002) *J. Cell Biol.* **156**, 271-285
10. Brown, D. A., and London, E. (2000) *J. Biol. Chem.* **275**, 17221-17224
11. van Meer, G., Stelzer, E. H. K., Wijnaendts-van-Resandt, R. W., and Simons, K. (1987) *J. Cell Biol.* **105**, 1623-1635
12. Simons, K., and van Meer, G. (1988) *Biochem.* **27**, 6197-6202
13. Mays, R. W., Siemers, K. A., Fritz, B. A., Lowe, A. W., van Meer, G., and Nelson, W. J. (1995) *J. Cell Biol.* **130**, 1105-1115
14. Ledesma, M. D., Simons, K., and Dotti, C. G. (1998) *Proc. Natl. Acad. Sci. U.S.A.* **95**, 3966-3971
15. Schmidt, K., Schrader, M., Kern, H. F., and Kleene, R. (2001) *J. Biol. Chem.* **276**, 14315-14323
16. Martin-Belmonte, F., Alonso, M. A., Zhang, X., and Arvan, P. (2000) *J. Biol. Chem.* **275**, 41074-41081
17. Skrzypek, M., Lester, R. L., and Dickson, R. C. (1997) *J. Bacteriol.* **179**, 1513-1520
18. Bagnat, M., Keranen, S., Shevchenko, A., and Simons, K. (2000) *Proc. Natl. Acad. Sci. U.S.A.* **97**, 3254-3259
19. Bagnat, M., Chang, A., and Simons, K. (2001) *Mol. Biol. Cell* **12**, 4129-4138
20. Sprong, H., Degroote, S., Claessens, T., van Drunen, J., Oorschot, V., Westerink, B. H., Hirabayashi, Y., Klumperman, J., van der Sluijs, P., and van Meer, G. (2001) *J. Cell Biol.* **155**, 369-380
21. Merrill Jr., A. H., and Sweeley, C. C. (1996) in: *Biochemistry of Lipids, Lipoproteins and Membranes*. D. Vance and J.E. Vance, eds., pp. 309-339
22. Dickson, R. C., and Lester, R. L. (1999) *Biochim. Biophys. Acta* **1438**, 305-321

23. Levine, T. P., Wiggins, C. A., and Munro, S. (2000) *Mol. Biol. Cell* **11**, 2267-2281
24. Dean, N., Zhang, Y. B., and Poster, J. B. (1997) *J. Biol. Chem.* **272**, 31908-31914
25. Hechtberger, P., Zinser, E., Saf, R., Hummel, K., Paltauf, F., and Daum, G. (1994) *Eur. J. Biochem.* **225**, 641-649
26. Beeler, T., Gable, K., Zhao, C., and Dunn, T. (1994) *J. Biol. Chem.* **269**, 7279-7284
27. Beeler, T. J., Fu, D., Rivera, J., Monaghan, E., Gable, K., and Dunn, T. M. (1997) *Mol. Gen. Genet.* **255**, 570-579
28. Tanida, I., Takita, Y., Hasegawa, A., Ohya, Y., and Anraku, Y. (1996) *FEBS Lett.* **379**, 38-42
29. Uemura, S., Kihara, A., Inokuchi, J., and Igarashi, Y. (2003) *J. Biol. Chem.* **278**, 45049-45055
30. Elble, R. (1992) *Biotechniques* **13**, 18-20
31. Holthuis, J. C. M., Nichols, B. J., and Pelham, H. R. B. (1998) *Mol. Biol. Cell* **9**, 3383-3397
32. Jungmann, J., Rayner, J. C., and Munro, S. (1999) *J. Biol. Chem.* **274**, 6579-6585
33. Sauer, B. (1987) *Mol. Cell. Biol.* **7**, 2087-2096
34. Wach, A., Brachat, A., Alberti-Segui, C., Rebischung, C., and Philippsen, P. (1997) *Yeast* **13**, 1065-1075
35. Ziman, M., Chuang, J. S., and Schekman, R. W. (1996) *Mol. Biol. Cell* **7**, 1909-1919
36. Sikorski, R. S., and Hieter, P. (1989) *Genetics* **122**, 19-27
37. Bonner, W. M., and Stedman, J. D. (1978) *Anal. Biochem.* **89**, 247-256
38. Holthuis, J. C., Nichols, B. J., Dhruvakumar, S., and Pelham, H. R. (1998) *EMBO J.* **17**, 113-126
39. Nakayama, K., Nagasu, T., Shimma, Y., Kuromitsu, J., and Jigami, Y. (1992) *EMBO J.* **11**, 2511-2519
40. Wiggins, C. A., and Munro, S. (1998) *Proc. Natl. Acad. Sci. U.S.A.* **95**, 7945-7950
41. Haak, D., Gable, K., Beeler, T., and Dunn, T. (1997) *J. Biol. Chem.* **272**, 29704-29710
42. Ziegler, F. D., Maley, F., and Trimble, R. B. (1988) *J. Biol. Chem.* **263**, 6986-6992
43. Rayner, J. C., and Munro, S. (1998) *J. Biol. Chem.* **273**, 26836-26843
44. Nagiec, M. M., Nagiec, E. E., Baltisberger, J. A., Wells, G. B., Lester, R. L., and Dickson, R. C. (1997) *J. Biol. Chem.* **272**, 9809-9817
45. Stack, J. H., DeWald, D. B., Takegawa, K., and Emr, S. D. (1995) *J. Cell Biol.* **129**, 321-334
46. Cowles, C. R., Snyder, W. B., Burd, C. G., and Emr, S. D. (1997) *EMBO J.* **16**, 2769-2782
47. Gurunathan, S., David, D., and Gerst, J. E. (2002) *EMBO J.* **21**, 602-614
48. TerBush, D. R., Maurice, T., Roth, D., and Novick, P. (1996) *EMBO J.* **15**, 6483-6494
49. Puoti, A., Desponds, C., and Conzelmann, A. (1991) *J. Cell Biol.* **113**, 515-525
50. Brown, D. A., and Rose, J. K. (1992) *Cell* **68**, 533-544
51. Simons, K., and Ikonen, E. (1997) *Nature* **387**, 569-572
52. Patton, J. L., and Lester, R. L. (1991) *J. Bacteriol.* **173**, 3101-3108
53. Hallstrom, T. C., Lambert, L., Schorling, S., Balzi, E., Goffeau, A., and Moye-Rowley, W. S. (2001) *J. Biol. Chem.* **276**, 23674-23680
54. Stepp, J. D., Huang, K., and Lemmon, S. K. (1997) *J. Cell Biol.* **139**, 1761-1774

Chapter 3

Sphingolipid mannosylation in yeast requires Csg2p-dependent manganese transport into the lumen of early secretory organelles*

* Lisman Q., Alferts, A.P., Staffhorst R., and Holthuis J.C.M. (2004).
Manuscript in preparation

Summary

The Golgi apparatus of the yeast *Saccharomyces cerevisiae* harbors a diverse group of luminal mannosyltransferases that catalyze the terminal glycosylation of proteins and sphingolipids. These enzymes utilize GDP-mannose as carbohydrate donor and require divalent cations, usually Mn^{2+} , for activity. Glycosphingolipid synthesis in yeast involves the transfer of a mannose residue onto the head group of inositolphosphoryl ceramide (IPC), yielding mannosyl-IPC. This reaction is catalyzed by two independent IPC mannosyltransferases, Csg1p and Csh1p, that each are supposed to form a complex with a polytopic membrane protein, Csg2p. Although removal of Csg2p severely perturbs IPC mannosylation, its precise role in this reaction has not been defined. Here we show that IPC mannosyltransferase activity in yeast requires Mn^{2+} and that cells lacking Csg2p are defective in the luminal uptake of Mn^{2+} . Moreover, the IPC mannosylation defect in a $\Delta csg2$ mutant is suppressed when cells are grown in Mn^{2+} -supplemented medium. Our findings suggest that Csg2p is an Mn^{2+} transporter with a critical role in supplying Mn^{2+} to the IPC mannosyltransferases in the Golgi lumen.

Introduction

The Golgi apparatus is the site where the terminal glycosylation of both proteins and lipids occurs. Unlike the situation in mammalian cells, glycoproteins and sphingolipids in the Golgi of the yeast *Saccharomyces cerevisiae* are exclusively modified by the addition of mannose residues. Glycoproteins can undergo two types of modifications in which oligosaccharides are attached to either asparagine residues (*N*-linked) or serine/threonine residues (*O*-linked; Ref. 1). Both of these pathways are initiated in the endoplasmic reticulum (ER). After transport of the protein to the Golgi, most *N*-linked oligosaccharides are elongated by a series of different mannosyltransferases to form mannoproteins with outer chains of 50 or more mannose residues. *O*-linked sugars can receive up to five mannoses upon addition of the first mannose in the ER. Sphingolipids in yeast are formed by the transfer of phosphoinositol from phosphatidylinositol (PI) onto the C1 hydroxyl group of ceramide, yielding inositol phosphorylceramide (2). This reaction requires Aur1p, a putative IPC synthase residing in a *medial* compartment of the Golgi (3, 4). IPC is then mannosylated to form mannosyl-IPC (MIPC), which in turn can receive a second phosphoinositol group from PI to create $M(IP)_2C$, the final and most abundant sphingolipid in yeast (2).

Both protein and sphingolipid mannosylation require transport of the critical mannosyl donor, GDP-mannose, from the cytoplasm into the Golgi lumen by a nucleoside sugar transporter, Vrg4p (5). The sequential reactions involved in the synthesis of mannoproteins are catalyzed by a diverse group of mannosyltransferases that form distinct oligomeric complexes compartmentalized from one another within the individual Golgi cisternae (6, 7). MIPC production is catalyzed by two structurally-related IPC mannosyltransferases, Csg1p and Csh1p, that co-localize with Aur1p in the *medial* cisternae of the Golgi (8–10). Csg1p and Csh1p each form a complex with Csg2p (9), a protein lacking the structural hallmarks of

glycosyltransferases. Removal of *Csg2p* severely affects IPC mannosylation (9, 11, 12), yet its precise role in this reaction is not understood. *Csg2p* is an integral membrane protein with ten putative transmembrane segments that, when overexpressed, localizes to the ER (13, 14). *Csg2p* also contains an EF- Ca^{2+} -binding domain and has been implicated in the regulation of an exchangeable, intracellular Ca^{2+} pool (12, 15). Since calcium has been shown to stimulate the conversion of IPC to MIPC *in vivo*, IPC mannosyltransferase activity in yeast may be regulated by Ca^{2+} through *Csg2p* (9).

Csg1p and *Csh1p* share a luminal region of homology with the α -1,6-mannosyltransferase, *Och1p* (8). This homology domain contains a conserved sequence motif, DXD, found in a wide range of glycosyltransferase families. Mutagenesis of one of the members of these families, the yeast α -1,3-mannosyltransferase *Mnn1p*, revealed that altering either of these aspartates eliminates all enzymatic activity (16). Different mannosyltransferases involved in creating the carbohydrate outer chain of yeast mannoproteins have been reported to require Mn^{2+} for activity (16, 17). Crystal structures of different glycosyltransferases revealed that the two aspartic residues in the DXD motif bind a Mn^{2+} ion needed to position the GDP-mannose in the active site (18-20).

In this study, we report that the yeast IPC mannosyltransferases, *Csg1p* and *Csh1p*, require Mn^{2+} for activity and that *Csg2p* likely functions as a Mn^{2+} transporter with a critical role in supplying the Golgi lumen with Mn^{2+} required for efficient MIPC synthesis.

Experimental Procedures

Strains and Plasmids

Yeast strains were routinely grown at 28°C to mid-logarithmic phase (0.5-1.0 OD_{600}) in synthetic dextrose (SD) medium. Yeast transformations were carried out as described (21). The wild type (EHY227) and $\Delta\text{csg1}\Delta\text{csh1}$ mutant strain (JHY090) have been described elsewhere (10). For deletion of *CSH1*, *CSG1* and *CSG2*, 450-550 base-pair fragments of the promotor and ORF 3'-end of each gene were amplified by PCR from yeast genomic DNA and cloned on either site of a *loxP-HIS3-loxP* cassette in a pBluescript KS⁻ vector, as described (10). The deletion constructs were linearized with *NotI* and *MluI* and then transformed into EHY227 (*MAT α sec6-4 TPI1::SUC2::TRP1 ura3-52 his3- Δ 200 leu2-3 -122 trp1-1*) to generate Δcsh1 (JHY088), Δcsg1 (JHY075) and Δcsg2 (JHY104) strains. Double and triple deletions were performed sequentially in EHY227 by repeated use of the *loxP-HIS3-loxP* cassette and subsequent removal of the *HIS3* marker by excisive recombination using Cre recombinase (22), yielding the $\Delta\text{csh1}\Delta\text{csg1}$ (JHY090) and $\Delta\text{csh1}\Delta\text{csg1}\Delta\text{csg2}$ (QLY019) strains. In each case, the correct integration or excision event was confirmed by PCR.

Promotor regions (650 bp) and complete ORFs of *CSH1*, *CSG1* and *CSG2* and were PCR amplified from yeast genomic DNA and subsequently ligated into multi-copy vector, pRS425 (2 μ , *LEU2*) or pRS426 (2 μ , *URA3*; Ref. 23). A N-terminally *myc*-tagged construct containing the ORF of *GOS1* was generated by PCR amplification of yeast genomic DNA and subsequent ligation into vector JS209 (2 μ , *URA3*; Ref. 24) behind the *TPI1* promotor.

Subcellular Membrane Fractionation

Wild type and $\Delta csg2$ cells transformed with the *CSH1*-pRS426 construct were grown in 500 ml SD medium, harvested, spheroplasted, and then lysed in a hypo-osmotic buffer as described (25). Subcellular membranes were collected at 100,000 g_{av} (60 min, 4°C) and loaded on top of a sucrose step gradient prepared in gradient buffer (10 mM Hepes-KOH, pH 7.2, 1 mM EDTA, 0.8 M sorbitol) using the following steps: 0.5 ml 60%, 1 ml 40%, 1 ml 37%, 1.5 ml 34%, 2 ml 32%, 2 ml 29%, 1.5 ml 27% and 1.5 ml 22% (w/w) sucrose. After centrifugation at 130,000 g_{av} in a Beckman SW40Ti rotor (18 hrs, 4°C), 20 x 0.6 ml fractions were collected from the top. Equal amounts per fraction were subjected to immunoblotting using affinity-purified rabbit polyclonal antibodies against Csg1p and Csh1p (10). Other antibodies were directed against Gos1p (25) and Dpm1p (Molecular Probes, Eugene, OR). For immunoblotting, all antibody incubations were carried out in PBS containing 5% dried milk and 0.5% Tween-20. After incubation with peroxidase-conjugated secondary antibodies (BioRad, Hercules, CA), blots were developed using a chemiluminescent substrate kit (Pierce, Rockford, USA).

Immunofluorescence Microscopy

Exponentially-grown cells were fixed and mounted on poly-lysine-coated glass-slides as described (25). All antibody incubations were performed in PBS supplemented with 2% dried milk and 0.1% saponin for 2h at room temperature. Mouse anti-*myc* monoclonal antibody, 9E10 (Santa Cruz Biotechnology, CA) and affinity-purified rabbit anti-Csg1p polyclonal antibodies were used at a dilution of 1:100. Fluorescein- or Cy3-conjugated secondary antibodies (Amersham, Arlington Heights, IL) were used at a dilution of 1:100. Fluorescence microscopy and image acquisition were carried out using a Leica DMRA microscope (Leitz, Wetzlar, Germany) equipped with a cooled CCD camera (KX85, Apogee Instruments Inc., Tucson, AZ) driven by Image-Pro Plus software (Media Cybernetics, Silver Spring, MD).

Analysis of IPC Mannosyltransferase Activity in Cell Extracts

Exponentially grown $\Delta csg1\Delta csh1\Delta csg2$ cells (2.5 OD₆₀₀) were inoculated in 50 ml SD medium containing 100 μ Ci *myo*-[³H]inositol and then grown for 16 hrs at 30°C. Cells were harvested by centrifugation, washed twice with 10 mM NaN₃ and lysed by bead bashing in lysis buffer (50 mM Hepes, pH 7.2, 1 mM NEM) in the presence of fresh protease inhibitors. After removal of unbroken cells (500 g, 10 min), membranes were collected (100,000 g, 60 min) and solubilized in 1 ml lysis buffer containing 1% Triton X-100 and fresh protease inhibitors (10). After incubation for 60 min at room temperature, the extract was centrifuged (100,000 g, 60 min), and 50 μ l aliquots were stored at -80°C. In addition, 400 OD₆₀₀ of non-radiolabeled, exponentially-grown wild type, $\Delta csg1\Delta csh1$ and $\Delta csg2$ cells were lysed by bead bashing in 4 ml ice-cold lysis buffer containing 2 mM EDTA and fresh protease inhibitors. Upon removal of unbroken cells, total membranes were collected, resuspended in 1 ml ice-cold lysis buffer containing 1% Triton X-100 and rotated at 4°C for 60 min.

For IPC mannosyltransferase assays, 50 μ l of radio-labeled extract was mixed with 150 μ l of unlabeled extract and then pre-incubated with or without 10 mM GDP-mannose (Sigma-

Aldrich, St. Louis, MO), 4 mM CaCl₂ and/or 4 mM MnCl₂ for 10 min at 30°C. Reactions were diluted 10-fold in lysis buffer containing 1 mM EDTA, 4 mM CaCl₂ and/or 4 mM MnCl₂, and then incubated for 2 hrs at 30°C. Reactions were stopped by adding 6.4 ml chloroform:methanol (1:2.2). The organic extracts were dried and subjected to butanol/water partitioning. Lipids recovered from the butanol phase were deacylated by mild base treatment using 0.2 N NaOH in methanol. After neutralizing with 1 M acetic acid, lipids were extracted with chloroform and separated by TLC using chloroform/methanol/4.2 M NH₃ (9:7:3). ³H-labeled lipids were detected by exposure to BAS-TR2040 imaging screens (Fuji, Japan) and read out on a BIO-RAD Personal Molecular Imager (BioRad).

Preparation of Permeabilized Yeast Cells

Permeabilized yeast cells (PYC) were prepared as described (26) with some modifications. Cells were grown in SD medium at 30°C to a density of 1 OD₆₀₀/ml. After harvesting, cells were resuspended at 50 OD₆₀₀/ml in 10 mM DTT, 100 mM Tris-HCl (pH 9.4). After 5 min at room temperature, cells were centrifuged and resuspended at 50 OD₆₀₀/ml in 0.75 x YP (1% Bacto-Yeast extract and 2% Bacto-Peptone; Difco Laboratories Inc.), 0.5% glucose, 0.7 M sorbitol, 10 mM Tris-HCl (pH 7.5) and 1 unit of zymolyase per 1 OD₆₀₀ of cells. After 20 min incubation at 30°C, over 90% of the yeast cells were converted to spheroplasts. Spheroplasts were centrifuged at 1,500 x g for 3 min and resuspended in 0.75 x YPA containing 0.7 M sorbitol and 1% glucose at 2.5 OD₆₀₀/ml. After incubating at 30°C for 20 min to allow metabolic recovery, cells were washed with lysis buffer (400 mM sorbitol, 20 mM HEPES, pH 6.8, 150 mM potassium acetate, 2 mM magnesium acetate) and resuspended in lysis buffer at 300 OD₆₀₀/ml. Aliquots of PYCs (200 µl) were slowly frozen in the vapors above liquid nitrogen for 1 h and immediately transferred to -80 °C.

Luminal Manganese Transport Assay

Luminal manganese transport was measured in permeabilized cells (PYCs). PYCs were thawed quickly and washed three times with 1 ml of ice-cold reaction buffer (20 mM HEPES, pH 6.8, 150 mM potassium acetate, 250 mM sorbitol, 5 mM magnesium acetate) to remove cytosol and endogenous manganese. Two volumes of reaction buffer were added to the PYC-pellet. Reactions were initiated by mixing 5 µl of membranes (containing 20–30 µg of protein) with 20 µl of reaction buffer containing 500 µM MnCl₂, bringing the final protein concentration to 0.8–1.2 mg/ml. Protein concentrations were determined using the BCA reagent (Pierce). After incubation at 30°C for 0, 5, 10, 15 and 20 min, the reaction was stopped by adding 0.5 ml of ice-cold reaction buffer, and samples were placed on ice. Membranes were pelleted by centrifugation at 100,000 g in a Beckman Optima TL ultracentrifuge and pellets were washed twice with 1.0 ml of ice-cold reaction buffer. Pellets were resuspended in 200 µl 65% nitric acid and heated at 70°C for 2 h. Then, 1 ml of H₂O was added and samples were diluted 2- to 4-fold in 0.1% nitric acid. The manganese content of each sample was determined by Atomic Absorption Spectroscopy, using a SpectrAA model 400 Plus spectrophotometer (Varian PtY Ltd., Mulgrave, Australia) with a GTA-96 graphite furnace and pyrolytically coated partitioned graphite tube. The amount of endogenous manganese present before addition of MnCl₂ was

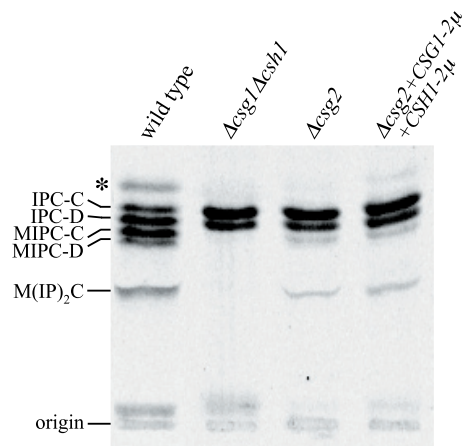
determined by measuring at zero time of incubation; this value was then subtracted from the measurements. The amount of Mn^{2+} transported was normalized for the amount of PYC-associated protein and then expressed in pmoles per mg protein.

Results

Overexpression of Csg1p and Csh1p does not Suppress the IPC Mannosylation Defect in $\Delta csg2$ Mutant Cells

Addition of mannose to IPC in yeast requires the putative IPC mannosyltransferases Csg1p and Csh1p (10). Consistent with previous work (9, 27), TLC analysis of alkaline-treated lipid extracts from *myo*- 3H]inositol labeled yeast cells revealed that Csg2p is critical but not essential for IPC mannosylation (Figure 1). Overexpression of Csg1p and Csh1p from multi-copy vectors in $\Delta csg2$ mutant cells did not suppress the partial defect in MIPC synthesis (Figure 1). Collectively, these data indicate that the primary function of Csg2p is distinct from that of Csg1p or Csh1p.

Figure 1. The IPC mannosylation defect in $\Delta csg2$ cells cannot be overcome by overexpression of CSG1 and CSH1. Wild type, $\Delta csg1\Delta csh1$, $\Delta csg2$ and $\Delta csg2$ yeast cells harboring multicopy plasmids containing *CSG1* and *CSH1* (*CSG1-2 μ* , *CSH1-2 μ*) were labeled overnight with *myo*- 3H]inositol. Lipid extracts were deacylated by mild alkaline hydrolysis, separated by TLC, and then visualized by autoradiography as described under Experimental Procedures. Note that due to incomplete deacylation, a small amount of phosphatidylinositol was sometimes visible (asterisk).



Loss of Csg2p Does Not Affect the Subcellular Distribution of Csg1p and Csh1p

Csg2p has been reported to form a complex with both Csg1p and Csh1p (9). Even though formation of these complexes is not absolutely required for MIPC synthesis (Figure 1), it is feasible that association with Csg2p is necessary for efficient export of newly-synthesized Csg1p and Csh1p from the ER to the Golgi where MIPC synthesis occurs. GDP-mannose transport into the Golgi-lumen is essential for IPC mannosylation and requires Vrg4p, a putative Golgi-associated GDP-mannose transporter (5). Hence, a failure to deliver Csg1p and Csh1p to the Golgi would likely affect MIPC production levels. To determine whether loss of Csg2p prevents Csg1p and Csh1p from reaching the Golgi, we initially examined their subcellular distribution

in wild type or $\Delta csg2$ cells by fractionating total cellular membranes on equilibrium sucrose density gradients. As shown in Figure 2 A, Csg1p and Csh1p displayed a fractionation profile similar to that of the *medial*-Golgi v-SNARE, Gos1p (peak fractions: 6 and 7), but distinct from that of ER marker, Dpm1p (peak fractions: 4 and 5). This was regardless of whether fractionated membranes were derived from wild type or $\Delta csg2$ cells. As a complementary approach, we next investigated the localization of Csg1p by immunofluorescence microscopy. Staining of wild type and $\Delta csg2$ cells with anti-Csg1p antibodies in each case produced a punctuate pattern characteristic of the yeast Golgi (Figure 2 B). In both cell types, these Csg1p-positive structures displayed extensive co-localization with the *medial*-Golgi marker, Gos1p. Hence, Csg2p unlikely serves a critical role in the delivery of Csg1p and Csh1p to the Golgi.

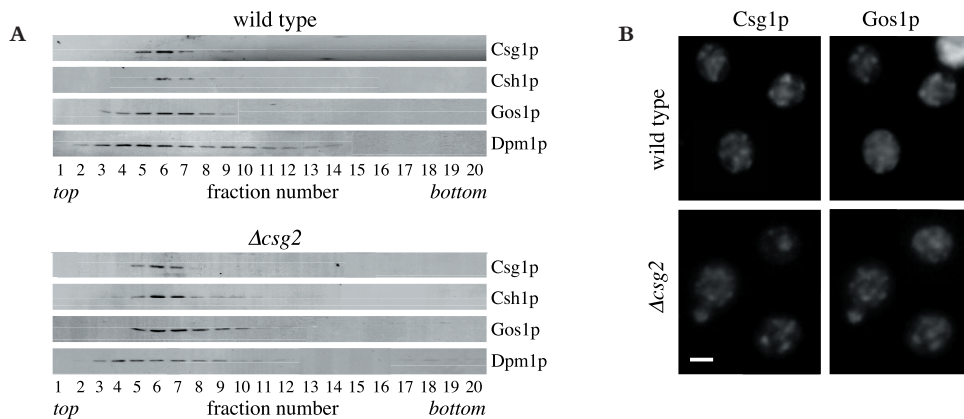


Figure 2. Association of Csg1p and Csh1p with the *medial* Golgi is independent of Csg2p. (A) Subcellular fractionation of Csg1p and Csh1p. High-speed membrane pellets (100,000 g) prepared from wild type and $\Delta csg2$ yeast cells were fractionated on a sucrose step gradient. Fractions were analyzed by immunoblotting using antibodies directed against Csg1p, Csh1p, the ER marker Dpm1p and the *medial* Golgi marker Gos1p. (B) Double-label immunofluorescence micrographs of wild type and $\Delta csg2$ cells comparing the localization of Csg1p and *myc*-tagged Gos1p. Staining of Csg1p was with rabbit polyclonal anti-Csg1p antibodies. *Myc*-tagged Gos1p was detected with mouse monoclonal anti-*myc* antibody, 9E10. Note that most of the Csg1p-positive structures were also positive for *myc*-tagged Gos1p. Bar, 3 μ m.

IPC Mannosyltransferase Activity Requires Manganese and is Unaffected by Calcium

Csg2p is a polytopic membrane protein with an EF-hand Ca^{2+} -binding domain (12). Based on the observation that Ca^{2+} causes a change in sphingolipid composition and stimulates the conversion of IPC to MIPC in yeast, Uemura *et al.* (9) proposed that IPC mannosyltransferase activity may be regulated by Ca^{2+} through Csg2p. In addition, glycosyltransferases using nucleoside diphosphate sugars as carbohydrate donors often require divalent cations, usually manganese (16, 17, 28). Therefore, we decided to investigate the effects of Ca^{2+} and Mn^{2+} on IPC mannosyltransferase activity in the absence or presence of Csg2p. To this end, we

used a previously established *in vitro* IPC mannosyltransferase assay (10). In brief, Triton X-100 extracts prepared from *myo*-[^3H]inositol-labeled $\Delta csh1\Delta csg1\Delta csg2$ cells were mixed with extracts from unlabeled wild-type or $\Delta csg2$ cells and then incubated with or without externally added metal ions. When extracts from the inositol-labeled triple mutant were mixed with extracts from unlabeled wild-type cells, radioactive IPC was converted to MIPC and $\text{M(IP)}_2\text{C}$ in a GDP-mannose- and Mn^{2+} -dependent manner (Figure 3 A). Unlike Mn^{2+} , Ca^{2+} had no significant effect on IPC mannosyltransferase activity, regardless of whether or not Mn^{2+} was present. Essentially the same results were obtained when extracts from the inositol-labeled triple mutant were mixed with $\Delta csg2$ cell extracts (Figure 3 B). These findings demonstrate that IPC mannosyltransferase activity in yeast requires Mn^{2+} . However, they do not support a direct stimulatory effect of Ca^{2+} .

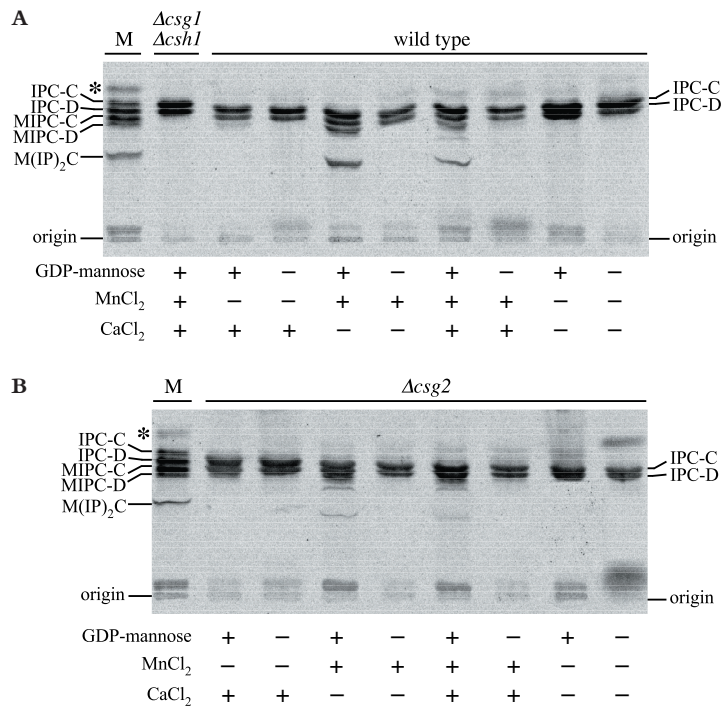


Figure 3. Manganese is required for IPC mannosyltransferase activity *in vitro*. Analysis of IPC mannosyltransferase activity in extracts derived from wild type, $\Delta csg1\Delta csh1$ and $\Delta csg2$ cells. Triton X-100 extracts prepared from *myo*-[^3H]inositol-labeled $\Delta csg1\Delta csh1\Delta csg2$ cells were mixed with extracts of unlabeled wild type, $\Delta csg1\Delta csh1$ or $\Delta csg2$ cells, and then incubated for 30 min at 30°C in the presence (+) or absence (-) of 1 mM GDP-mannose, 4 mM CaCl_2 and/or 4 mM MnCl_2 , as indicated. Extracts prepared from *myo*-[^3H]inositol-labeled wild type cells served as positive control (M). Lipid extracts were deacylated by mild alkaline hydrolysis and then separated by TLC before autoradiography. Note that due to incomplete deacylation, a small amount of phosphatidylinositol was sometimes visible (asterisk).

Acs2 Cells Are Defective in the Luminal Uptake of Manganese

Csg1p and Csh1p share a region of homology with the α -1,6-mannosyltransferase, Och1p. This domain is positioned in the Golgi lumen (10) and contains a conserved sequence motif, DXD, which may bind a divalent cation required for positioning the nucleoside diphosphate sugar in the active site. Csg2p has tentatively been classified as a Ca^{2+} membrane transporter (29). Our finding that IPC mannosylation requires Mn^{2+} but not Ca^{2+} raises an alternative possibility, namely that Csg2p is needed to translocate Mn^{2+} into the lumen of the ER or Golgi. Searching the Protein Data Bank for Csg2p homologues revealed hypothetical proteins of unknown function in *Candida glabrata*, *Neurospora crassa* and various other fungi. No clear homologues were found in higher organisms. However, we noticed that Csg2p contains a region (residues 128–370) sharing 22% identity (42% similarity) with the permease component of a bacterial ABC-type $\text{Mn}^{2+}/\text{Zn}^{2+}$ transport system (Figure 4). Hence, we decided to investigate a role for Csg2p in Mn^{2+} transport.

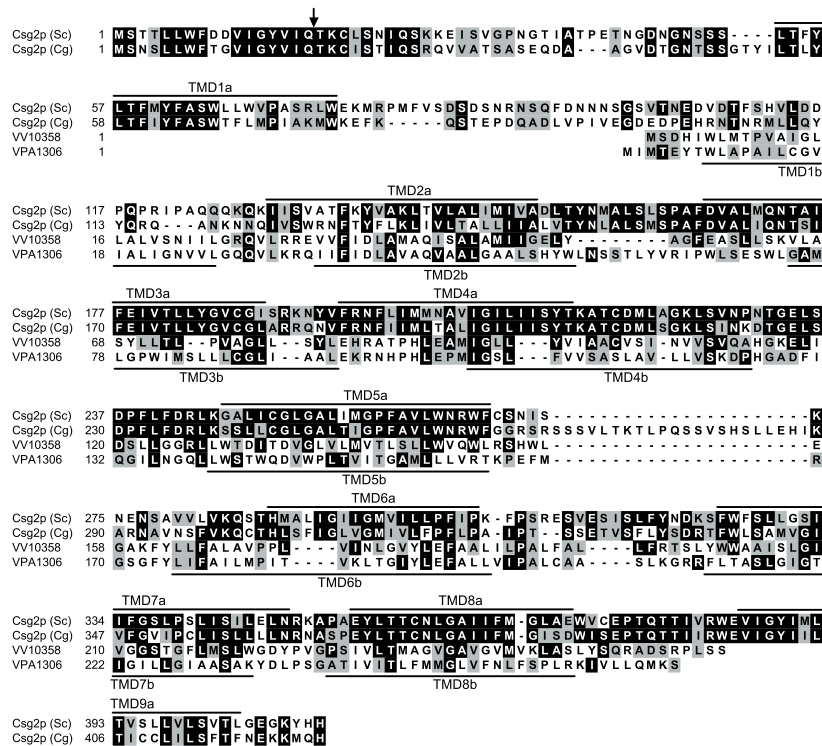


Figure 4. Csg2p shares a region of homology with the permease component of bacterial $\text{Mn}^{2+}/\text{Zn}^{2+}$ transporters. Alignment of the amino acid sequences of Csg2p from *S. cerevisiae* (Sc), a Csg2p homologue from *Candida glabrata* (Cg), and the permease component of an ABC-type $\text{Mn}^{2+}/\text{Zn}^{2+}$ transport system found in *Vibrio vulnificus* (VV10358; Swiss-Prot/TrEMBL accession number: Q8DF65) and in *Vibrio parahaemolyticus* (VPA1306; Swiss-Prot/TrEMBL accession number: Q87GK9). Sequences were aligned with ClustalW. Conserved (black) or related residues (grey) are boxed. A putative signal peptide cleavage site is indicated by an arrow. Potential transmembrane domains are underlined.

For this purpose, a method previously developed for measuring luminal GDP-mannose transport in permeabilized yeast cells (PYC; Refs. 5,26) was modified and applied to analyse the Mn^{2+} transport activity in wild type and $\Delta csg2$ cells. Thus, PYCs prepared from wild type and $\Delta csg2$ cells were washed in reaction buffer to remove cytosol and endogenous Mn^{2+} , and then incubated at 30°C in the presence of 400 μM Mn^{2+} ($MnCl_2$). After incubation, PYCs were washed extensively to remove non-translocated Mn^{2+} and the amount of PYC-associated Mn^{2+} was determined by atomic absorption spectrometry. A time course of Mn^{2+} uptake by wild type PYCs indicated that transport of Mn^{2+} was quite efficient, with 2 pmol of Mn^{2+} taken up per min per mg of PYC-associated protein (Figure 4). The accumulation rate was linear with time up to 10 min. Mn^{2+} uptake was abolished by the addition of detergent (0.1% Triton X-100), indicating that it required intact vesicles. Addition of ATP had no effect, suggesting that Mn^{2+} transport occurred independently of metabolic energy (data not shown). Removal of Csg2p, on the other hand, caused a 4- to 5-fold reduction in the Mn^{2+} transport rate (from 2 to < 0.5 pmol Mn^{2+} per min per mg protein; Figure 4). Mn^{2+} transport was fully restored when $\Delta csg2$ cells were transformed with a multicopy plasmid bearing the *CSG2* gene. In fact, cells expressing *CSG2* from the multicopy plasmid showed a higher rate of Mn^{2+} transport than wild type cells (Figure 4). From these data we conclude that Csg2p is required for luminal Mn^{2+} transport.

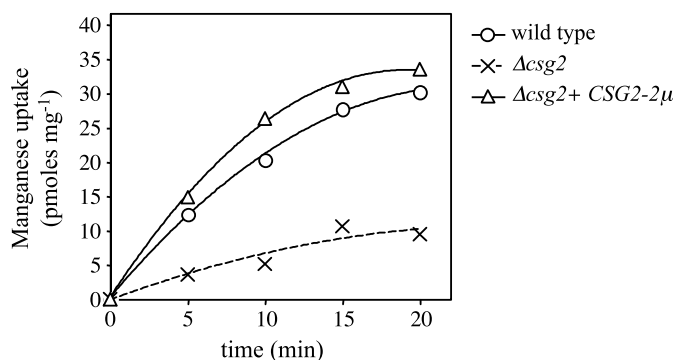


Figure 5. $\Delta csg2$ cells are defective in luminal Mn^{2+} transport. Permeabilized yeast cells (PYCs) prepared from wild type, $\Delta csg2$ and $\Delta csg2$ strains transformed with *CSG2* on a multicopy plasmid were washed to remove all cytosol and then incubated at 30°C in reaction buffer containing 400 μM $MnCl_2$. At the indicated time points, PYCs were diluted in ice-cold reaction buffer, washed, and the amount of Mn^{2+} taken up quantified by atomic absorption spectroscopy as described under Experimental Procedures. The amount of Mn^{2+} transported was normalized for the amount of PYC-associated protein and then expressed in pmoles per mg protein. The experiment was repeated twice with similar results.

The IPC Mannosylation Defect in $\Delta csg2$ Cells is Partially Suppressed by Externally Added Mn^{2+}

Our finding that $\Delta csg2$ cells are defective in the luminal uptake of Mn^{2+} suggests that Csg2p has a critical role in supplying Mn^{2+} to the IPC mannosyltransferases in the Golgi lumen. If so,

addition of Mn^{2+} to the culture medium may help overcome the IPC mannosylation defect in $\Delta csg2$ cells. To test this possibility, wild type, $\Delta csg2$ and $\Delta csg1\Delta csh1$ cells were labeled with *myo*- $[^3H]$ inositol in the presence or absence of 1mM $MnCl_2$. As shown in Figure 6, externally added $MnCl_2$ was unable to restore IPC mannosylation in $\Delta csg1\Delta csh1$ cells. In contrast, $MnCl_2$ had a stimulating effect on MIPC and $M(IP)_2C$ formation in $\Delta csg2$ cells. These data support a critical role for *Csg2p* in the luminal transport of Mn^{2+} .

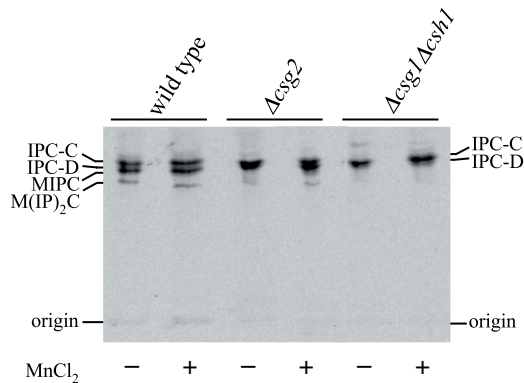


Figure 6. The IPC mannosylation defect in $\Delta csg2$ cells is partially suppressed by externally added Mn^{2+} . Wild type, $\Delta csg2$ and $\Delta csg1\Delta csh1$ cells were labeled overnight with *myo*- $[^3H]$ inositol in the presence (+) or absence (-) of 1 mM $MnCl_2$. Lipids were extracted, deacylated by mild alkaline hydrolysis and then separated by TLC before autoradiography.

Discussion

Although previous work has suggested the involvement of *Csg2p* in IPC mannosylation (11, 12), its precise role in that reaction has not been defined. Here we provide evidence that Mn^{2+} is required for IPC mannosylation and that *Csg2p* is a Mn^{2+} transporter with a critical role in supplying Mn^{2+} ions to the IPC mannosyltransferases in the Golgi lumen. A primary function for *Csg2p* in Mn^{2+} transport is supported by the following observations: (i) $\Delta csg2$ cells accumulate under-mannosylated sphingolipids *in vivo*; (ii) membranes from $\Delta csg2$ cells are defective in the luminal uptake of Mn^{2+} *in vitro*; (iii) the IPC mannosylation defect in the $\Delta csg2$ mutant can be partially suppressed by growing cells in Mn^{2+} supplemented medium; (iv) *Csg2p* shares a region of homology with the permease component of a bacterial ABC-type Mn^{2+}/Zn^{2+} transport system.

Our findings are remarkable with respect to previous work on the role of the *medial*-Golgi ion pump, *Pmr1p*, in supplying the yeast secretory pathway with Ca^{2+} and Mn^{2+} . *Pmr1p* belongs to the group of Secretory Pathway Ca^{2+} ATPases (SPCAs), an emerging family of Golgi-resident, Ca^{2+} -transporting P-type ATPases with inhibitor and transport characteristics different from the well-studied sarcoendoplasmic reticulum (SERCA) and plasma membrane (PMCA) Ca^{2+} -ATPases (30). A distinctive feature of SPCA pumps is their apparent ability to transport Mn^{2+} with high affinity. Several lines of evidence indicate that SPCAs function as high affinity Mn^{2+} pumps. First, $\Delta pmr1$ cells in yeast accumulate cytosolic Mn^{2+} that can serve

as an inorganic scavenger of superoxide radicals, thus bypassing the requirement for cytosolic superoxidase dismutase in aerobic growth (31). Second, $\Delta pmr1$ cells exhibit defects in *N*-linked and *O*-linked protein glycosylation that can be alleviated by supplying Mn^{2+} , but not Ca^{2+} , to the growth medium (32). Third, Mn^{2+} is a potent inhibitor of Pmr1p-mediated $^{45}Ca^{2+}$ -transport in isolated Golgi vesicles (33, 34). Fourth, Mn^{2+} stimulates Pmr1p-mediated ATP hydrolysis and formation of the phosphoenzyme intermediate (35, 36). Consequently, Pmr1p is widely viewed as a dual transporter responsible for maintaining the intralumenal Ca^{2+} and Mn^{2+} concentrations in the early secretory pathway of yeast. Our present findings indicate that early secretory organelles in yeast are equipped with an additional, Csg2p-dependent Mn^{2+} -uptake system. Csg2p, when over-expressed, localizes to the ER (13, 14) yet affects an Mn^{2+} -dependent process in the Golgi lumen. In an analogous situation, Pmr1p, the only known Ca^{2+} -pump in the early secretory pathway of yeast, resides in the *medial* Golgi (37, 38) yet affects Ca^{2+} -dependent processes in the ER (32). We propose that the Mn^{2+} content of the Golgi is determined, at least in part, by Csg2p-dependent Mn^{2+} -transport into the ER lumen.

While Csg2p-dependent Mn^{2+} transport is critical for sustaining normal levels of IPC mannosylation, loss of Csg2p did not seem to have any obvious effect on the mannosylation of invertase (data not shown). This is in contrast to the situation in $\Delta pmr1$ cells that produce and secrete a form of invertase essentially lacking the high-mannose outer chains (32). Perhaps transferases involved in sphingolipid mannosylation require higher levels of intralumenal Mn^{2+} for optimal activity than can be provided by Pmr1p when Csg2p is absent. In addition, it should be noted that Pmr1p function in protein glycosylation was investigated using $\Delta pmr1$ cells grown in Mn^{2+} -depleted culture media (32). In contrast, the $\Delta csg2$ cells analysed in this study were grown in regular culture media that may have contained Mn^{2+} in amounts sufficient to alleviate a requirement for Csg2p in protein mannosylation. Whether loss of Pmr1p affects sphingolipid mannosylation remains to be established.

The mechanism of Csg2p-dependent Mn^{2+} -transport is presently unclear. The low level of homology between Csg2p and the permease component of a group of bacterial ABC-type Mn^{2+}/Zn^{2+} transporters suggests that Csg2p directly participates in Mn^{2+} transport and perhaps forms the channel through which the Mn^{2+} ions travel. Csg2p-dependent Mn^{2+} -transport occurs in the absence of ATP, hence in contrast to the cation transport catalysed by P-type ATPases like Pmr1p. Csg2p contains ten putative membrane spans and a EF-hand Ca^{2+} binding domain in the second predicted extramembrane loop (12). Whether the Ca^{2+} binding domain is exposed to the cytosol or ER lumen remains to be established. Ca^{2+} has been reported to stimulate IPC mannosylation in yeast (9). Rather than stimulating IPC mannosyltransferase activity directly, Ca^{2+} may regulate the supply of Mn^{2+} ions required for this reaction by activating Csg2p-mediated Mn^{2+} transport. At present, final proof for a direct role of the Ca^{2+} -ATPase Pmr1p in lumenal Mn^{2+} transport is lacking. A challenging prospect is that uptake of Mn^{2+} by early secretory organelles in yeast is controlled by Pmr1p through Csg2p. This possibility is currently under investigation.

Acknowledgements

We wish to thank Hein Sprong, Maarten Egmond, Gerrit van Meer and Chantal Christis for valuable advice. Q.L. is supported by a grant from the Meelmeijer foundation, and J.H. by a VIDI grant from the Netherlands Organization for Scientific Research (NWO).

References

1. Herscovics, A., and Orlean, P. (1993) *Faseb J.* **7**, 540-550
2. Dickson, R. C., and Lester, R. L. (1999) *Biochim. Biophys. Acta* **1426**, 347-357
3. Nagiec, M. M., Nagiec, E. E., Baltisberger, J. A., Wells, G. B., Lester, R. L., and Dickson, R. C. (1997) *J. Biol. Chem.* **272**, 9809-9817
4. Levine, T. P., Wiggins, C. A., and Munro, S. (2000) *Mol. Biol. Cell* **11**, 2267-2281
5. Dean, N., Zhang, Y. B., and Poster, J. B. (1997) *J. Biol. Chem.* **272**, 31908-31914
6. Jungmann, J., and Munro, S. (1998) *Embo J.* **17**, 423-434
7. Jungmann, J., Rayner, J. C., and Munro, S. (1999) *J. Biol. Chem.* **274**, 6579-6585
8. Beeler, T. J., Fu, D., Rivera, J., Monaghan, E., Gable, K., and Dunn, T. M. (1997) *Mol. Gen. Genet.* **255**, 570-579
9. Uemura, S., Kihara, A., Inokuchi, J., and Igarashi, Y. (2003) *J. Biol. Chem.* **278**, 45049-45055
10. Lisman, Q., Pomorski, T., Vogelzangs, C., Urli-Stam, D., de Cocq van Delwijnen, W., and Holthuis, J. C. (2004) *J. Biol. Chem.* **279**, 1020-1029
11. Zhao, C., Beeler, T., and Dunn, T. (1994) *J. Biol. Chem.* **269**, 21480-21488
12. Beeler, T., Gable, K., Zhao, C., and Dunn, T. (1994) *J. Biol. Chem.* **269**, 7279-7284
13. Takita, Y., Ohya, Y., and Anraku, Y. (1995) *Mol. Gen. Genet.* **246**, 269-281
14. Huh, W. K., Falvo, J. V., Gerke, L. C., Carroll, A. S., Howson, R. W., Weissman, J. S., and O'Shea, E. K. (2003) *Nature* **425**, 686-691
15. Tanida, I., Takita, Y., Hasegawa, A., Ohya, Y., and Anraku, Y. (1996) *FEBS Lett.* **379**, 38-42
16. Wiggins, C. A., and Munro, S. (1998) *Proc. Natl. Acad. Sci. U.S.A* **95**, 7945-7950
17. Nakajima, T., and Ballou, C. E. (1975) *Proc. Natl. Acad. Sci. U.S.A* **72**, 3912-3916
18. Gastinel, L. N., Bignon, C., Misra, A. K., Hindsgaul, O., Shaper, J. H., and Joziase, D. H. (2001) *Embo J.* **20**, 638-649
19. Persson, K., Ly, H. D., Dieckelmann, M., Wakarchuk, W. W., Withers, S. G., and Strynadka, N. C. (2001) *Nat. Struct. Biol.* **8**, 166-175
20. Lobsanov, Y. D., Romero, P. A., Sleno, B., Yu, B., Yip, P., Herscovics, A., and Howell, P. L. (2004) *J. Biol. Chem.* **279**, 17921-17931
21. Elble, R. (1992) *Biotechniques* **13**, 18-20
22. Sauer, B. (1987) *Mol. Cell Biol.* **7**, 2087-2096
23. Sikorski, R. S., and Hieter, P. (1989) *Genetics* **122**, 19-27
24. Semenza, J. C., Hardwick, K. G., Dean, N., and Pelham, H. R. (1990) *Cell* **61**, 1349-1357
25. Holthuis, J. C., Nichols, B. J., Dhruvakumar, S., and Pelham, H. R. (1998) *Embo J.* **17**, 113-126
26. Baker, D., Hicke, L., Rexach, M., Schleyer, M., and Schekman, R. (1988) *Cell* **54**, 335-344
27. Haak, D., Gable, K., Beeler, T., and Dunn, T. (1997) *J. Biol. Chem.* **272**, 29704-29710

28. Haselbeck, A., and Schekman, R. (1986) *Proc. Natl. Acad. Sci. U.S.A.* **83**, 2017-2021
29. Paulsen, I. T., Sliwinski, M. K., Nelissen, B., Goffeau, A., and Saier, M. H., Jr. (1998) *FEBS Lett.* **430**, 116-125
30. Sorin, A., Rosas, G., and Rao, R. (1997) *J. Biol. Chem.* **272**, 9895-9901
31. Lapinskas, P. J., Cunningham, K. W., Liu, X. F., Fink, G. R., and Culotta, V. C. (1995) *Mol. Cell Biol.* **15**, 1382-1388
32. Durr, G., Strayle, J., Plemper, R., Elbs, S., Klee, S. K., Catty, P., Wolf, D. H., and Rudolph, H. K. (1998) *Mol. Biol. Cell* **9**, 1149-1162
33. Wei, Y., Marchi, V., Wang, R., and Rao, R. (1999) *Biochemistry* **38**, 14534-14541
34. Wei, Y., Chen, J., Rosas, G., Tompkins, D. A., Holt, P. A., and Rao, R. (2000) *J. Biol. Chem.* **275**, 23927-23932
35. Mandal, D., Woolf, T. B., and Rao, R. (2000) *J. Biol. Chem.* **275**, 23933-23938
36. Van Baelen, K., Vanoevelen, J., Missiaen, L., Raeymaekers, L., and Wuytack, F. (2001) *J. Biol. Chem.* **276**, 10683-10691
37. Antebi, A., and Fink, G. R. (1992) *Mol. Biol. Cell* **3**, 633-654
38. Schroder, S., Schimmoller, F., Singer-Kruger, B., and Riezman, H. (1995) *J. Cell Biol.* **131**, 895-912

Chapter 4

***HOR7*, a multicopy suppressor of the Ca²⁺-induced
growth defect in sphingolipid
mannosyltransferase-deficient yeast***

* Lisman Q., Urli-Stam D., and Holthuis J.C.M. (2004).
Journal of Biological Chemistry 279, 36390-6

Summary

Yeast mutants defective in sphingolipid mannosylation accumulate inositol phosphorylceramide C (IPC-C), which renders cells Ca^{2+} sensitive. A screen for loss of function suppressors of the Ca^{2+} -sensitive phenotype previously led to the identification of numerous genes involved in IPC-C synthesis. To better understand the molecular basis of the Ca^{2+} -induced growth defect in IPC-C overaccumulating cells, we searched for genes whose overexpression restored Ca^{2+} tolerance in a mutant lacking the IPC mannosyltransferases Csg1p and Csh1p. Here we report the isolation of *HOR7* as a multicopy suppressor of the Ca^{2+} -sensitive phenotype of $\Delta\text{csg1}\Delta\text{csh1}$ cells. *HOR7* belongs to a group of hyperosmolarity-responsive genes and encodes a small (59 residues) type I membrane protein that localizes at the plasma membrane. Hor7p is not required for high Ca^{2+} or Na^+ tolerance. Instead, we find that Hor7p-overproducing cells display an increased resistance to high salt, sensitivity to low pH and a reduced uptake of methylammonium, an indicator of the plasma membrane potential. These phenotypes are induced through a mechanism independent of the plasma membrane H^+ -ATPase, Pma1p. Our findings suggest that induction of Hor7p causes a depolarization of the plasma membrane that may counteract a Ca^{2+} -induced influx of toxic cations in IPC-C overaccumulating cells.

Introduction

Sphingolipids are abundant components of eukaryotic plasma membranes with important functions in bilayer stability, stress adaptation, signaling and possibly the formation of lipid microdomains (1-3). They consist of a ceramide linked through either a glucosyl or phosphodiester bond to a polar head group. Ceramides are comprised of an sphingoid base joined in amide linkage to a fatty acid and can be classified according to the level of hydroxylation of the sphingoid and fatty acid moieties. The yeast *Saccharomyces cerevisiae* produces phytoceramide based on C4-hydroxylated phytosphingosine and a C_{26} fatty acid that is usually hydroxylated on C2 (4, 5). Aur1p is required for transferring phosphoinositol from phosphatidylinositol onto the C1 hydroxyl group of phytoceramide, yielding inositol phosphorylceramide (IPC; Ref. 6). IPC is mannosylated to form mannosyl-IPC (MIPC), which in turn can receive a second phosphoinositol group from phosphatidylinositol to generate the final and most abundant yeast sphingolipid, $\text{M}(\text{IP})_2\text{C}$ (7). MIPC production requires the IPC mannosyltransferases Csg1p and Csh1p (8-10) as well as an EF- Ca^{2+} -binding domain-containing membrane protein, Csg2p (11). Csg2p interacts with Csg1p and Csh1p (9), but its precise role in MIPC production is unclear. Whereas Csg1p and Csh1p contain a region of homology with the yeast α -1,6-mannosyltransferase Och1p, Csg2p does not share this sequence and is not absolutely required for MIPC synthesis, suggesting that Csg2p serves a regulatory rather than a catalytic function.

Csg1p and Csg2p play an important role in Ca^{2+} tolerance since *csg1* and *csg2* mutants have been identified as Ca^{2+} -sensitive, Sr^{2+} -resistant mutants (12). The Ca^{2+} -sensitive phenotype

appears to be due to the accumulation of IPC-C, which contains a phytosphingosine and a monohydroxylated C₂₆-fatty acid. Indeed, the Ca²⁺-sensitivity of *csg2* mutant cells is suppressed by mutations causing either a reduction in IPC-C levels or a change in its structure. Thus, suppressor mutations have been found in genes involved in sphingoid base synthesis (*LCB1*, *LCB2*, *TSC10*), palmitoyl-CoA synthesis (*FAS2*), fatty acid chain elongation (*TSC13*), conversion of dihydrosphingosine to phytosphingosine (*SUR2*), and hydroxylation of the C₂₆ fatty acid (*SCS7*) (Figure 1; Refs. 4, 8). Why IPC-C overaccumulating cells become Ca²⁺-sensitive is unknown. Several intermediates of sphingolipid metabolism have been reported to function as signaling molecules. For example, sphingoid base 1-phosphate is involved in heat stress resistance, diauxic shift and Ca²⁺ mobilization (13-15) while accumulation of ceramide causes cell growth arrest (16, 17). Hence, one possibility is that Ca²⁺ activates hydrolysis of IPC-C resulting in the formation of toxic levels of ceramide. Alternatively, IPC-C itself may act as a signaling molecule in a Ca²⁺-signaling pathway. Suppressors of the Ca²⁺-sensitivity in the *csg2* mutant included two genes involved in signal transduction, namely the protein kinase *TOR2* and the phosphatidylinositol-4-phosphate 5-kinase *MSS4* (18). How the signaling pathways of Tor2p and Mss4p are connected to Ca²⁺-induced cell death in *csg1* and *csg2* mutants remains to be established. Another model put forward to explain the Ca²⁺-sensitive phenotype is that Ca²⁺ alters the permeability of *csg1* and *csg2* cells, causing an increased influx of toxic ions that leads to cell death. This idea is based on the observation that *csg1* and *csg2* mutants display an increased Ca²⁺-uptake and that the Ca²⁺-sensitive phenotype can be reversed by addition of 0.8 M sorbitol to the growth medium (8). Sorbitol reduces osmotic gradients and has been shown to prevent lysis of mutants with defective cell walls (19).

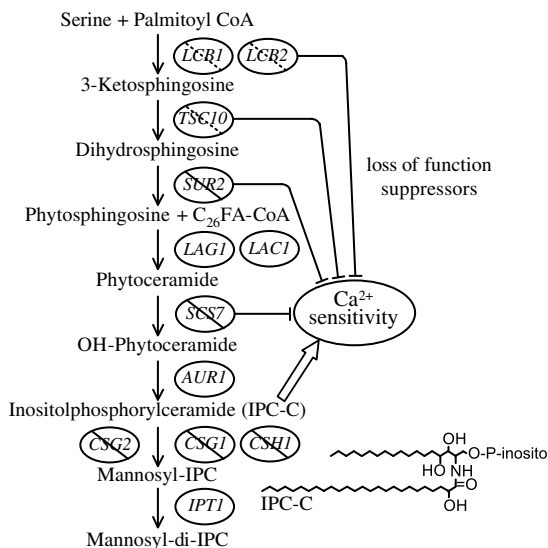


Figure 1. Defects in the yeast sphingolipid biosynthetic pathway affecting Ca²⁺-sensitivity. Pathway intermediates and genes involved at each step are shown. Disruption of genes required for sphingolipid mannosylation (*CSG1*, *CSG2*, *CSH1*) causes accumulation of inositol phosphorylceramide C (IPC-C), which renders cells Ca²⁺-sensitive. The Ca²⁺ sensitivity of IPC-C overaccumulating cells is suppressed by mutations affecting IPC-C structure (*TSC10*, *SUR2*, *SCS7*) or production rate (*LCB1*, *LCB2*).

To gain further insight into the molecular basis of the Ca^{2+} -induced growth defect in IPC-C accumulating cells, we searched for genes whose overexpression restores Ca^{2+} -tolerance in a mutant strain lacking the IPC mannosyltransferases Csg1p and Csh1p. Here we report the isolation and characterization of *HOR7* as a multicopy suppressor of the Ca^{2+} -sensitive phenotype in $\Delta\text{csg1}\Delta\text{csh1}$ cells. Our findings suggest that Hor7p protects $\Delta\text{csg1}\Delta\text{csh1}$ cells from a Ca^{2+} -induced influx of toxic cations by reducing the plasma membrane electric potential.

Experimental Procedures

Strains and plasmids

Unless indicated otherwise, yeast strains were grown at 28°C to mid-logarithmic phase (0.5–1.0 OD_{600}) in synthetic dextrose (SD). Yeast transformations were carried out as described (20). Mutant strains Δcsg1 (JHY075), Δcsh1 (JHY088), $\Delta\text{csg1}\Delta\text{csh1}$ (JHY090), Δipt1 (JHY079) have been described previously (10). The *HIS3* marker in JHY090 was removed by excisive recombination using Cre recombinase, yielding strain JHY101. For deletion of the *HOR7* gene, 450–500 base-pair fragments of the regions flanking the open reading frame were PCR amplified from yeast genomic DNA and cloned into the *NotI/EcoRI* and *SpeI/MluI* sites located on either site of a *loxP-HIS3-loxP* cassette in a pBluescript KS⁻ vector (10). The gene deletion construct was linearized with *NotI* and *MluI* and transformed into EHY227 (*MAT α sec6-4 TPI1::SUC2::TRP1 ura3-52 his3- Δ 200 leu2-3 -112trp1-1*) or JHY101 to generate Δhor7 (JHY161) and $\Delta\text{csg1}\Delta\text{csh1}\Delta\text{hor7}$ (JHY164) strains. Correct integration events were confirmed by PCR. Strains with Pma1p tagged at its N-terminus with one copy of the HA epitope were generated using integration plasmid pRS305 Δ 51 (21). Promoter regions (650 bp) and open reading frames of *CSG1* and *CSH1* were PCR-amplified and ligated into single-copy vector pRS416 (CEN, *URA3*). Promoter regions (650 bp) and open reading frames of *HOR7*, *DDR2* and *YMR252C* were PCR-amplified and ligated into multicopy vector pRS426 (2 μ , *URA3*). To generate a *myc*-tagged version of *HOR7*, nine copies of the *myc* epitope were inserted in the open reading frame between residues 20 and 21 by PCR, using plasmid p9xMYCt-HIS5 (S. Munro, MRC-LMB, Cambridge, UK). *Myc*-tagged *HOR7* was ligated into multicopy vector pRS425 (2 μ , *LEU2*) and expressed in strain SEY6210 (*MAT α ura3-52 his3- Δ 200 leu2-3 112trp1- Δ 901 suc2- Δ 9 lys2-801*) for localization studies.

Multicopy suppressor screen

A YEP13-based yeast genomic DNA library (AB320, ATCC 37323) was transformed into JHY090 ($\Delta\text{csg1}\Delta\text{csh1}$) and transformants were grown on SD plates supplemented with 20 mM CaCl_2 at 28°C. Ca^{2+} -resistant colonies transformed with *CSG1*- or *CSH1*-containing plasmids were identified by colony PCR and discarded. Plasmids rescued from the remaining Ca^{2+} -resistant colonies were isolated, retransformed in JHY090 and screened for their ability to complement the Ca^{2+} -sensitive phenotype. This approach yielded three

overlapping genomic sequences capable of restoring Ca^{2+} tolerance. Complementation experiments with restriction fragments and PCR-amplified open reading frames present in the isolated genomic sequences led to the identification of *HOR7* as a multicopy suppressor of the Ca^{2+} -induced growth defect in JHY090.

Subcellular membrane fractionation

Cells were grown in 500 ml SD medium, harvested, spheroplasted, and then lysed in a hypo-osmotic buffer as described (22). Subcellular membranes were collected at 100,000 g_{av} (60 min, 4°C) and loaded on top of a sucrose gradient prepared in gradient buffer (10 mM Hepes-KOH, pH 7.2, 1 mM EDTA, 0.8 M sorbitol) using the following steps: 0.5 ml 60%, 1 ml 40%, 1 ml 37%, 1.5 ml 34%, 2 ml 32%, 2 ml 29%, 1.5 ml 27% and 1.5 ml 22% (w/w) sucrose. After centrifugation at 130,000 g_{av} in a Beckman SW40Ti rotor (18 hrs, 4°C), 20 x 0.6 ml fractions were collected from the top. Equal volumes per fraction were used to assay for ATPase activity and for Western blot analysis (see below).

Western blot analysis

Myc-tagged *Hor7p* was detected with anti-*myc* rabbit polyclonal (A14) or mouse monoclonal antibody (9E10), and HA-tagged *Pma1p* with anti-HA rabbit polyclonal antibodies (Santa Cruz Biotechnology, CA). Other antibodies were directed against *Gos1p* (22), *Dpm1p* (Molecular Probes, Eugene, OR) and *Sso2p* (S. Keränen, Biotechnology and Food Research, Espoo, Finland). For immunoblotting, all antibody incubations were carried out in PBS containing 5% dried milk and 0.5% Tween-20. After incubation with peroxidase-conjugated secondary antibodies (Biorad, Hercules, CA), blots were developed using a chemiluminescent substrate kit (Pierce, Rockford, USA).

ATPase assay

The protein content of pooled gradient fractions was measured using a Micro BCA Protein Assay Reagent Kit (Pierce, Rockford, IL) with bovine serum albumin as a standard. ATPase assays were performed on 70 μg protein at 30°C in a volume of 25 μl (10 mM Hepes-KOH, pH 7.2, 0.8 M sorbitol, 2 mM ATP, 5 mM MgCl_2). Reactions were stopped after 30 minutes with 175 μl 40 mM H_2SO_4 . Then 50 μl 6 M H_2SO_4 containing 0.001% malachite green was added and after 30 min incubation at room temperature, the absorbance was measured at 595 nm. The specific ATPase activity was calculated from the amount of P_i released after 30 min and expressed as nmol P_i per min per mg of protein.

Immunofluorescence microscopy

Exponentially-grown cells were fixed and mounted on poly-L lysine-coated glass-slides as described previously (22). Antibody incubations were performed in PBS supplemented with 2% dried milk and 0.1% saponin for 2h at room temperature. Anti-*myc* mouse monoclonal antibody 9E10 was used at a dilution of 1:100, and rabbit polyclonal antibody to *Sso2p* at a dilution of 1:200. Goat-anti-mouse fluorescein- and goat-anti-rabbit Cy3-conjugated secondary antibodies (Amersham, Arlington Heights, IL) were used at a dilution of 1:100.

Fluorescence microscopy and image acquisition were carried out using a Leica DMRA microscope (Leitz, Wetzlar, Germany) equipped with a cooled CCD camera (KX85, Apogee Instruments Inc., Tucson, AZ) driven by Image-Pro Plus software (Media Cybernetics, Silver Spring, MD).

Measurement of methylammonium uptake

Cells ($5 \text{ OD}_{600}/\text{ml}$) were incubated in 50 mM glucose, 10 mM MES, pH 6.0 at 2°C . After a 5 min incubation, [^{14}C]methylamine hydrochloride (2 mM and $2.5 \mu\text{Ci}/\text{ml}$ final concentration; Amersham) was added. At the indicated time points, 100 μl aliquots were diluted into 10 ml of ice-cold 20 mM MgCl_2 , filtered through a $0.45 \mu\text{m}$ nitrocellulose filter (Millipore HAWP) and washed twice with 10 ml of the same solution. Filters were transferred to scintillation cocktail and radioactivity measured using a liquid scintillation counter.

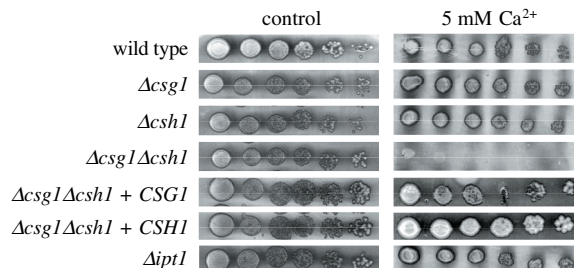
Results

Loss of *Csg1p* and *Csh1p* causes hypersensitivity towards calcium

S. cerevisiae cells have a high tolerance for Ca^{2+} . Thus, cells display normal growth in medium containing up to 100 mM CaCl_2 (data not shown). A screen for genes specifically involved in Ca^{2+} regulation in *S. cerevisiae* revealed *CSG1*, a gene with a critical function in high Ca^{2+} tolerance (Beeler et al., 1994). Subsequent studies showed that *Csg1p* is homologous to *Csh1p*, and that the two proteins function as IPC mannosyltransferases (8–10). To study the effects of Δcsg1 and Δcsh1 mutations on Ca^{2+} sensitivity, cells were grown on SD plates containing 5 mM CaCl_2 at 30°C . As shown in Figure 2, Δcsg1 and Δcsh1 cells were resistant to exogenous Ca^{2+} and displayed normal growth. In contrast, the $\Delta\text{csg1}\Delta\text{csh1}$ double mutant was highly sensitive to Ca^{2+} and did not grow on the medium. Transformation of $\Delta\text{csg1}\Delta\text{csh1}$ cells with the *CSG1* or *CSH1* gene on a single-copy vector fully suppressed the Ca^{2+} -induced growth defect. Deletion of *IPT1*, a gene required for $\text{M}(\text{IP})_2\text{C}$ synthesis (23, 24) had no effect on Ca^{2+} tolerance. Thus, the Ca^{2+} sensitivity of yeast cells correlates with the level of MIPC synthesis rather than $\text{M}(\text{IP})_2\text{C}$ synthesis.

Figure 2. Loss of mannosyltransferases *Csg1p* and *Csh1p* causes hypersensitivity towards calcium.

Serial 3-fold dilutions of exponentially-grown wild type, Δipt1 , Δcsg1 , Δcsh1 , $\Delta\text{csg1}\Delta\text{csh1}$ or $\Delta\text{csg1}\Delta\text{csh1}$ cells transformed with *CSG1* or *CSH1* on a single-copy vector were spotted onto SD plates with or without 5 mM CaCl_2 , as indicated. Plates were scanned after 3 days of incubation at 30°C .



Isolation of *HOR7* as a multicopy suppressor of the Ca^{2+} -induced growth defect in $\Delta\text{csg1}\Delta\text{csh1}$ cells

In the absence of sphingolipid mannosylation, yeast cells accumulate IPC-C. Suppressor mutations that reverse the Ca^{2+} sensitivity of MIPC-deficient cells have been found to either decrease the synthesis of IPC-C or to alter its structure (Figure 1). None of the suppressor mutants synthesized MIPC, indicating that it is the accumulation of IPC-C, rather than the absence of mannosylated sphingolipids, that makes cells Ca^{2+} sensitive. To gain further insight into the molecular basis of the Ca^{2+} -induced growth defect in IPC-C overaccumulating cells, we performed a multicopy suppressor screen aimed at the identification of genes whose overexpression restores Ca^{2+} tolerance in the $\Delta\text{csg1}\Delta\text{csh1}$ mutant. To this end, $\Delta\text{csg1}\Delta\text{csh1}$ cells were transformed with a yeast genomic DNA library on a multicopy vector and transformants that regained tolerance to 20 mM Ca^{2+} were selected. Of the 64,000 transformants screened (6 times the amount required to cover the entire library), 168 grew in the presence of Ca^{2+} . Sixty Ca^{2+} -resistant colonies were picked for further analysis. Colonies transformed with *CSG1*- or *CSH1*-containing plasmids were identified by colony PCR and discarded (49 out of 60). Plasmids rescued from the eleven remaining Ca^{2+} -resistant colonies were retransformed in $\Delta\text{csg1}\Delta\text{csh1}$ cells and screened for their ability to restore Ca^{2+} tolerance. The three plasmids for which this was the case were sequenced. All three had a 25-kb insert derived from the same region in the right arm of chromosome XIII (765,000-790,000 bp), harboring the complete open reading frames of six different genes (Figure 3 A). Complementation studies with restriction fragments of the genomic sequence were used to eliminate four of the six genes as possible suppressors of the Ca^{2+} -induced growth defect in $\Delta\text{csg1}\Delta\text{csh1}$ cells (Figure 3 B). Open reading frames of the remaining two genes were PCR amplified from yeast genomic DNA, ligated into a multicopy expression vector and then screened for their ability to restore Ca^{2+} tolerance. This led to the identification of a gene named *HOR7* whose overexpression suppressed the Ca^{2+} -induced growth defect in $\Delta\text{csg1}\Delta\text{csh1}$ cells (Figure 3 B).

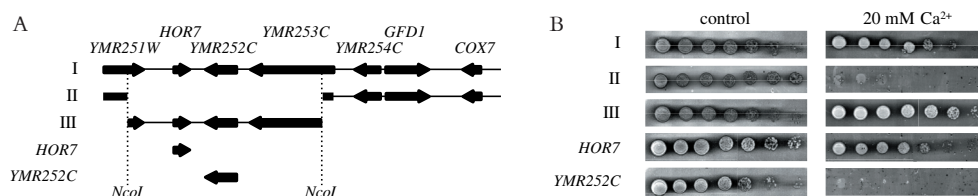


Figure 3. Identification of *HOR7* as a multicopy suppressor of the Ca^{2+} -induced growth defect in $\Delta\text{csg1}\Delta\text{csh1}$ cells. (A) A screen for multicopy suppressors of the Ca^{2+} -induced growth defect in $\Delta\text{csg1}\Delta\text{csh1}$ cells yielded a genomic DNA sequence harboring the complete open reading frames of six different genes (I). *HOR7* was identified by testing restriction fragments (II, III) and PCR-amplified open reading frames for their ability to complement the $\Delta\text{csg1}\Delta\text{csh1}$ Ca^{2+} -sensitive phenotype. (B) Serial 3-fold dilutions of exponentially-grown $\Delta\text{csg1}\Delta\text{csh1}$ cells transformed with genomic DNA fragments (I-III) or PCR-amplified open reading frames (*HOR7*, *YMR252C*) on a multicopy vector were spotted onto SD plates with or without 20 mM CaCl_2 , as indicated. Plates were scanned after 3 days of incubation at 30°C.

HOR7 encodes a small plasma membrane-associated protein

HOR7 was originally identified as one of seven hyperosmolarity-responsive genes co-induced by shifting cells to 1 M NaCl (25). The gene codes for a 59 amino-acid protein of unknown function with a predicted *N*-terminal signal peptide and *C*-terminal membrane span (Figure 4 A). Searching the database for homologous proteins revealed Ddr2p, a 61 amino-acid yeast protein sharing 46% amino acid sequence identity with Hor7p. No additional homologues were found. Ddr2p is encoded by a DNA damage-responsive gene (26). Its expression is also induced by osmotic shock, heat shock and oxidative stress (27). The function of Ddr2p is unknown. In spite of being highly related to Hor7p, overexpression of Ddr2p did not restore Ca^{2+} tolerance in $\Delta\text{csg1}\Delta\text{csh1}$ cells (Figure 4 B). A recent global analysis of protein localization in yeast revealed that Ddr2p is associated with the vacuole (28). To investigate the localization of Hor7p, the protein was tagged with nine copies of the *myc* epitope that were inserted immediately behind the putative signal peptide cleavage site (between residues 20 and 21). Epitope-tagging, whether internally or at the *C*-terminus, abolished the ability of Hor7p to restore Ca^{2+} tolerance in $\Delta\text{csg1}\Delta\text{csh1}$ cells (data not shown). *Myc*-tagged Hor7p expressed in wild type cells migrated as a 37-kDa protein on polyacrylamide gels. Following high-speed centrifugation of a cell lysate, Hor7p-*myc* was found exclusively in the membrane pellet (Figure 5 A). Immunofluorescence microscopy revealed a peripheral staining pattern and extensive co-localization with the plasma membrane-associated syntaxin, Sso2p (Figure 5 B). When cellular membranes were fractionated on an equilibrium sucrose density gradient, the bulk of Hor7p-

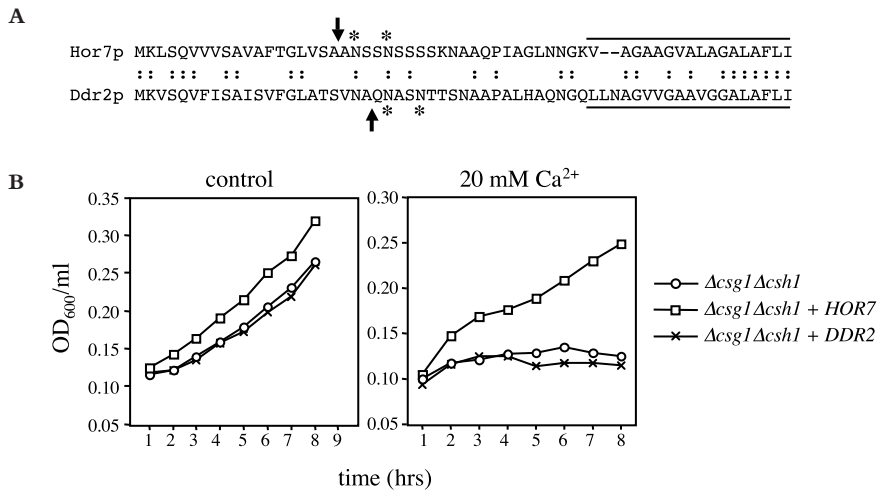


Figure 4. Overexpression of *HOR7*, but not of the homologues gene *DDR2*, suppresses the Ca^{2+} -induced growth defect in $\Delta\text{csg1}\Delta\text{csh1}$ cells. (A) Alignment of the amino acid sequences of Hor7p and Ddr2p. Putative signal peptide cleavage sites are indicated by arrows. Potential transmembrane domains are underlined. Putative *N*-linked glycosylation sites are marked by asterisks. (B) $\Delta\text{csg1}\Delta\text{csh1}$ cells transformed with *HOR7* or *DDR2* on a multicopy vector were grown in SD medium with or without 20 mM CaCl_2 . At the indicated times, 1-ml aliquots were withdrawn for measurement of the OD_{600} .

myc co-migrated with Sso2p and was separated from markers for the endoplasmic reticulum (ER; Dpm1p), Golgi (Gos1p), endosomes (Pep12p) and vacuoles (Vam3p; Figure 5 C and data not shown). Taken together, these results indicate that Hor7p resides at the yeast plasma membrane.

Hor7p contains a putative N-terminal signal sequence and C-terminal membrane span that predict a type I membrane topology where the N-terminus is situated in the lumen/extracellular environment (Figure 5 D). To test this prediction, cells expressing Hor7p-*myc* were spheroplasted and then immunostained with anti-*myc* and anti-Sso2p antibodies either before (pre-stained) or after fixation and permeabilization (post-stained). As expected, post-stained cells were labeled with both antibodies (Figure 5 E, upper panel). In contrast, pre-stained cells were positive for anti-*myc* antibodies, but negative for anti-Sso2p antibodies (Figure 5 E, upper panel). These findings indicate that the N-terminus of Hor7p-*myc* is exposed to the extracellular environment, hence consistent with the topology depicted in Figure 5 D.

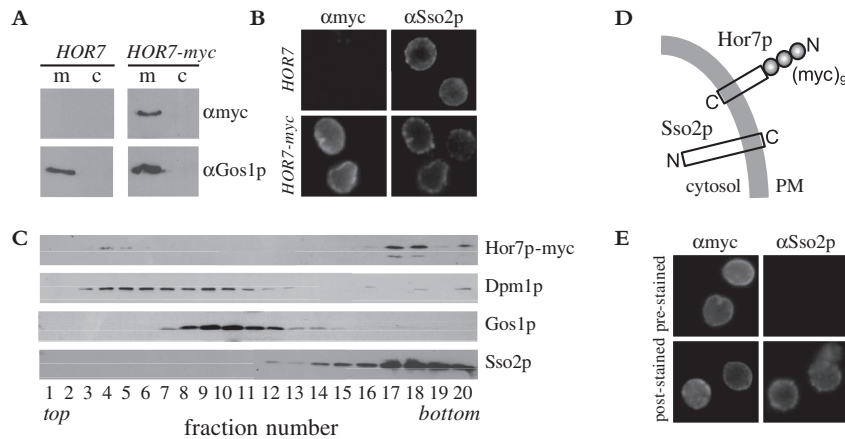
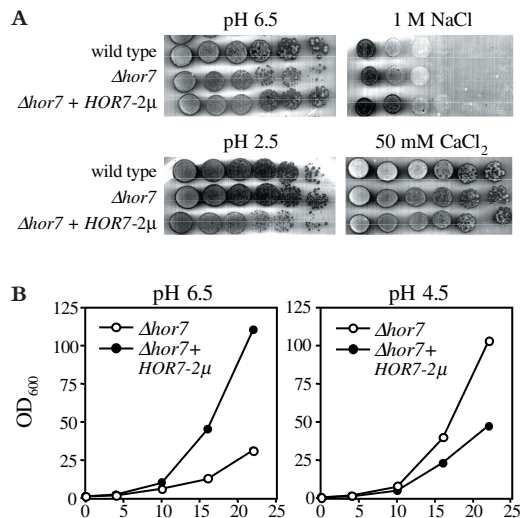


Figure 5. Hor7p localizes at the plasma membrane. (A) Hor7p is membrane-associated. High-speed membrane pellets (100,000 g) were prepared from yeast cells expressing untagged (*HOR7*) or *myc*-tagged *HOR7* (*HOR7-myc*) from a multicopy vector. Membranes (m) and cytosol (c) were analyzed by immunoblotting using anti-*myc* monoclonal and anti-Gos1p polyclonal antibodies. (B) Immunofluorescence micrographs of cells expressing untagged or *myc*-tagged *HOR7* (*HOR7-myc*) from a multicopy vector were co-stained with anti-*myc* monoclonal and anti-Sso2p polyclonal antibodies, as indicated. (C) Subcellular fractionation of Hor7p. A high-speed membrane pellet (100,000 g) prepared from cells expressing *myc*-tagged *HOR7* was fractionated on a sucrose step gradient. Fractions were analyzed by immunoblotting using antibodies against the *myc* epitope, the ER marker Dpm1p, the Golgi marker Gos1p and the plasma membrane marker Sso2p. (D) Schematic view of the (predicted) membrane topologies of *myc*-tagged Hor7p and Sso2p. (E) Immunofluorescence micrographs of cells expressing *myc*-tagged *HOR7* from a multicopy vector and co-stained with mouse monoclonal anti-*myc* and rabbit polyclonal anti-Sso2p antibodies either before (pre-stained) or after fixation and permeabilization (post-stained).

***HOR7* overexpression causes a growth defect at low pH without affecting plasma membrane H^+ -ATPase activity**

To determine the physiological function of Hor7p, the chromosomal copy of *HOR7* was disrupted by homologous recombination. Haploid $\Delta hor7$ and $\Delta csg1\Delta csh1\Delta hor7$ strains were obtained, indicating that Hor7p is not essential under standard growth conditions, i.e. in YEPD or SD medium at 30°C. Hor7p is not required for high salt, high Ca^{2+} or low pH tolerance, since $\Delta hor7$ cells grew as well as wild type on 1 M NaCl, 50 mM $CaCl_2$ or at pH 2.5 (Figure 6 A). However, we noticed that cells overproducing Hor7p from a multicopy vector grew better on 1M NaCl and were more sensitive to low pH than wild type or $\Delta hor7$ cells. While Hor7p-overproducing cells grew better than $\Delta hor7$ cells at pH 6.5, the situation was reversed at pH 4.5 or below (Figure 6 and data not shown). The plasma membrane H^+ -ATPase, Pma1p, plays a key role in the regulation of intracellular pH and yeast cells carrying mutations that reduce Pma1p activity are sensitive to low pH and become resistant to Na^+ (29–31). Pma1p is associated with two small (38 residues) and highly hydrophobic isoproteins, Pmp1 and Pmp2, which are required for maximal ATPase activity (32, 33). Pma1p is one of the most abundant proteins in the yeast plasma membrane and has been estimated to consume as much as one quarter of cellular ATP (34). To investigate whether Hor7p acts as a negative regulator of Pma1p, we determined the rates of MgATP hydrolysis in plasma membranes derived from $\Delta hor7$ cells transformed with *HOR7* on a multicopy plasmid (*HOR7-2 μ*) or with empty vector. To this end, cells were lysed and the plasma membranes separated from intracellular organelles by fractionation on equilibrium sucrose density gradients (Figure 7 A). Of the twenty fractions collected per gradient, the last four high-density fractions contained the bulk of plasma membrane (Pma1p, Sso2p) and were devoid of significant amounts of ER (Dpm1p), Golgi (Gos1p), vacuoles (Vam3p) and endosomes (Pep12p; Figure 7 A and data not shown). Plasma membrane-enriched fractions

Figure 6. *HOR7* overexpression causes a growth defect at low pH. (A) Serial 3-fold dilutions of exponentially-grown wild type, $\Delta hor7$ and $\Delta hor7$ cells transformed with *HOR7* on a multicopy vector (*HOR7-2 μ*) were spotted onto SD plates supplemented with the indicated concentrations of H^+ , NaCl or $CaCl_2$. (B) $\Delta hor7$ and $\Delta hor7$ cells transformed with *HOR7-2 μ* were grown in SD medium supplemented with the indicated concentrations of H^+ . The cultures were kept in log phase by regular dilution in fresh medium. At the indicated times, 1-ml aliquots were withdrawn for measurement of the OD_{600} . Total OD_{600} values for each culture are given. The experiment was repeated twice with similar results.



for each gradient were pooled and then normalized for Pma1p levels by Western blot analysis. As shown in Figure 7 B, there was no significant difference in plasma membrane-associated ATPase activity between Hor7p-deficient and overproducing cells. Hence, it appears unlikely that Hor7p renders cells sensitive to low pH by reducing the activity of plasma membrane H^+ -ATPase.

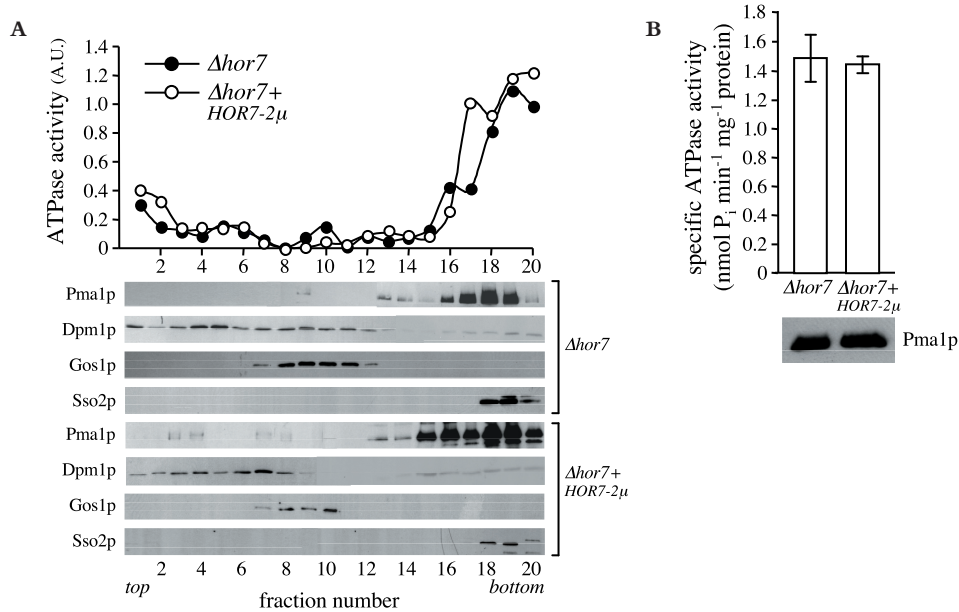


Figure 7. Overexpression or deletion of *HOR7* has no effect on plasma membrane H^+ -ATPase activity. (A) Subcellular fractionation of plasma membrane H^+ -ATPase Pma1p from cells lacking or overexpressing *HOR7*. High-speed membrane pellets (100,000 g) prepared from $\Delta hor7$ cells expressing HA-tagged Pma1p and transformed with empty vector ($\Delta hor7$) or *HOR7* on a multicopy vector ($\Delta hor7 + HOR7-2\mu$) were fractionated on sucrose step gradients. Fractions were collected from the top and analyzed for ATPase activity and by immunoblotting. ATPase activity is expressed in arbitrary units based upon the absorbance measured at 595 nm as described in Experimental Procedures. Immunoblots were stained with anti-HA antibodies to detect HA-tagged Pma1p and with antibodies against Gos1p, Sso2p and Dpm1p. (B) ATPase activity in plasma membrane-enriched fractions derived from Hor7p-deficient ($\Delta hor7$) and Hor7p-overproducing cells ($\Delta hor7 + HOR7-2\mu$). Fractions 16–20 from gradients shown in (A) were pooled, normalized and assayed (70 μ g protein per measurement) for ATPase activity as described under Experimental Procedures. Each bar represents the mean \pm standard deviation of three independent measurements. Immunoblotting with anti-HA antibodies on pooled fractions revealed that both strains contained similar amounts of Pma1p.

***HOR7* overexpression causes a depolarisation of the plasma membrane**

The plasma membrane electric potential maintained by H^+ -ATPase Pma1p has been reported to be a major determinant of toxic cation tolerance (29, 31). Therefore, it is feasible that Hor7p overexpression alters the membrane potential, which might reduce the rate of cation

uptake into the cell and, consequently, the cell's sensitivity to toxic cations. To investigate this possibility, we measured [^{14}C]methylammonium uptake as an indicator of membrane potential (35, 36). As expected, wild type cells preincubated with protonophore CCCP displayed a significant reduction in methylammonium uptake compared to untreated cells (Figure 8). Hor7p-overproducing cells displayed a similar decrease in methylammonium uptake when compared to wild type or Hor7p-deficient cells. Collectively, our results suggest that Hor7p overexpression causes a depolarisation of the plasma membrane through a mechanism independent of Pma1p function.

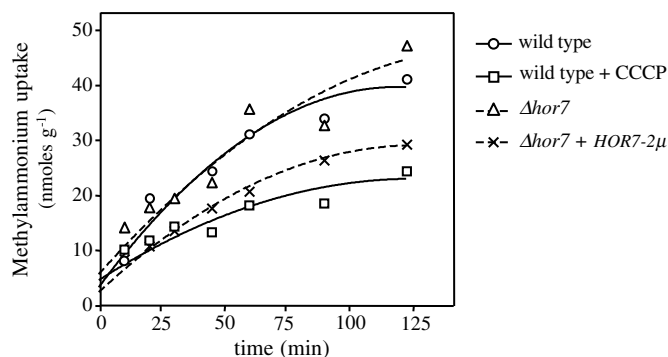


Figure 8. *HOR7* overexpression causes a reduction in methylammonium uptake. Wild type cells incubated with or without 50 μM CCCP, and cells lacking ($\Delta hor7$) or overexpressing *HOR7* from a multicopy vector ($\Delta hor7 + HOR7-2\mu$) were analyzed for [^{14}C]methylammonium uptake. At the indicated times, 100 μl aliquots of cells incubated with [^{14}C]methylammonium were collected, filtered and washed as described in Experimental Procedures. Filters were transferred to scintillation cocktail and radioactivity was counted. The experiment was repeated twice with similar results.

Discussion

Yeast mutants defective in IPC mannosylation accumulate IPC-C, which renders cells Ca^{2+} -sensitive. These mutants provide a positive selection for IPC-C synthesis mutants since the latter are suppressors of the Ca^{2+} -sensitive phenotype. How IPC-C induces Ca^{2+} -sensitivity is not well understood. In here we identified *HOR7* as a multicopy suppressor of the Ca^{2+} -induced growth defect in cells lacking the IPC mannosyltransferases *Csg1p* and *Csh1p*. Our findings suggest that Hor7p causes a depolarisation of the plasma membrane that may counteract a Ca^{2+} -induced influx of toxic cations in IPC-C overaccumulating cells.

Our multicopy suppressor screen on 60.000 transformed $\Delta csg1\Delta csh1$ colonies yielded *HOR7* as the only non-IPC mannosyltransferase-encoding gene capable of restoring high Ca^{2+} -tolerance. *HOR7* was originally identified as one of seven hyperosmolarity-responsive genes whose transcript levels are increased over 10-fold by 1 M NaCl or 1.5

M sorbitol (25). *HOR7* encodes a 59-amino acid protein with a predicted signal sequence and C-terminal membrane span. Membrane fractionation analysis and immunofluorescence microscopy of cells expressing epitope-tagged Hor7p revealed that the protein resides in the plasma membrane with its N-terminus facing the cell surface, hence consistent with a type I membrane topology. Hor7p shares 49% sequence identity with Ddr2p, a 61-amino acid yeast protein encoded by a DNA damage- and hyperosmolarity-responsive gene (37). However, unlike *HOR7*, *DDR2* was unable to serve as a multicopy suppressor of the Ca^{2+} -induced growth defect in $\Delta\text{csg1}\Delta\text{csh1}$ cells. A global protein localization study revealed that Ddr2p is not associated with the plasma membrane but with the yeast vacuole (28). Hence, it is feasible that Hor7p and Ddr2p perform identical functions at different locations within the cell.

Even though Hor7p is induced in response to high salt and serves as a multicopy suppressor of the Ca^{2+} -induced growth defect in $\Delta\text{csg1}\Delta\text{csh1}$ cells, disruption of the corresponding gene had no effect on high salt or high Ca^{2+} tolerance. Overexpression of Hor7p, on the other hand, conferred an increased resistance to Na^+ and sensitivity to low pH. Moreover, Hor7p-overproducing cells displayed a decreased uptake of methylammonium, an indicator of the plasma membrane potential (35, 36). The latter finding suggests that Hor7p overexpression causes a depolarization of the plasma membrane. Plasma membrane depolarization, low pH sensitivity and an increased Na^+ resistance have previously been reported for yeast strains bearing mutations in the plasma membrane H^+ -ATPase, Pma1p (29, 31). This activity is required for cytosolic pH homeostasis as well as for maintaining the electrochemical potential that drives transport of multiple nutrients and ions across the yeast plasma membrane (35, 38, 39). Pma1p function is dependent on Pmp1p and Pmp2p, two small (38 residues) and highly hydrophobic isoproteins whose removal causes a drastic reduction in the rate of plasma membrane-associated ATP hydrolysis (33). A role for Hor7p as negative regulator of Pma1p might explain the reduced methylammonium uptake, low pH sensitivity and increased Na^+ tolerance of Hor7p-overproducing cells. However, this possibility is unlikely given our finding that cells lacking or overexpressing Hor7p display similar rates of ATP hydrolysis in their plasma membranes. Hence, it appears that Hor7p causes a depolarization of the plasma membrane through a mechanism independently of Pma1p. It is possible that Hor7p induces a depolarizing proton leak, or mediates the proton leak itself. This would be consistent with the low pH sensitivity of Hor7p-overproducing cells. A similar function has previously been attributed to Pmp3p, a small 55 residue hydrophobic polypeptide found in the yeast plasma membrane with high sequence similarity to a family of plant polypeptides that are induced by high salinity (40). Whereas removal of Pmp3p causes a hyperpolarization of the plasma membrane (40), loss of Hor7p had no obvious effect on the membrane potential (this study). Further analysis of the proton permeability of Hor7p-deficient and -overproducing cells will be required to understand the precise role of Hor7p in the regulation of the plasma membrane potential.

Ca^{2+} has previously been proposed to induce an irreversible alteration in the plasma membrane of *csg1* and *csg2* yeast mutants that increases the influx of Ca^{2+} and perhaps other toxic cations, resulting in cell death (8). Our data suggest that Hor7p restores high Ca^{2+} -

tolerance in IPC mannosyltransferase-deficient yeast by counteracting the Ca^{2+} -induced influx of toxic cations through a depolarisation of the plasma membrane. Whether Ca^{2+} affects the ion permeability of the plasma membrane via an IPC-C dependent signaling pathway or by directly interacting with cell surface-exposed IPC-C remains an open issue. Hence, future studies will be necessary to identify the Ca^{2+} target that initiates Ca^{2+} -induced cell death in IPC-C overaccumulating yeast.

Acknowledgements

We are grateful to Amy Chang, Sean Munro and Sirkka Keränen for generously providing plasmids and antibodies, and to Maurice Jansen for technical assistance. Q.L. is supported by a grant from the Meelmeijer foundation, and J.H. by a grant from the Royal Academy of Arts and Sciences.

References

1. Dickson, R. C. (1998) *Annu. Rev. Biochem.* **67**, 27-48
2. Holthuis, J. C., Pomorski, T., Raggars, R. J., Sprong, H., and Van Meer, G. (2001) *Physiol. Rev.* **81**, 1689-1723
3. Edidin, M. (2003) *Annu. Rev. Biophys. Biomol. Struct.* **32**, 257-283
4. Haak, D., Gable, K., Beeler, T., and Dunn, T. (1997) *J. Biol. Chem.* **272**, 29704-29710
5. Dunn, T. M., Haak, D., Monaghan, E., and Beeler, T. J. (1998) *Yeast* **14**, 311-321
6. Nagiec, M. M., Nagiec, E. E., Baltisberger, J. A., Wells, G. B., Lester, R. L., and Dickson, R. C. (1997) *J. Biol. Chem.* **272**, 9809-9817
7. Dickson, R. C., and Lester, R. L. (1999) *Biochim. Biophys. Acta* **1426**, 347-357
8. Beeler, T. J., Fu, D., Rivera, J., Monaghan, E., Gable, K., and Dunn, T. M. (1997) *Mol. Gen. Genet.* **255**, 570-579
9. Uemura, S., Kihara, A., Inokuchi, J., and Igarashi, Y. (2003) *J. Biol. Chem.* **278**, 45049-45055
10. Lisman, Q., Pomorski, T., Vogelzangs, C., Urli-Stam, D., de Cocq van Delwijnen, W., and Holthuis, J. C. (2004) *J. Biol. Chem.* **279**, 1020-1029
11. Zhao, C., Beeler, T., and Dunn, T. (1994) *J. Biol. Chem.* **269**, 21480-21488
12. Beeler, T., Gable, K., Zhao, C., and Dunn, T. (1994) *J. Biol. Chem.* **269**, 7279-7284
13. Mandala, S. M., Thornton, R., Tu, Z., Kurtz, M. B., Nickels, J., Broach, J., Menzeleev, R., and Spiegel, S. (1998) *Proc. Natl. Acad. Sci. U.S.A.* **95**, 150-155
14. Mao, C., Saba, J. D., and Obeid, L. M. (1999) *Biochem. J.* **342 Pt 3**, 667-675
15. Skrzypek, M. S., Nagiec, M. M., Lester, R. L., and Dickson, R. C. (1999) *J. Bacteriol.* **181**, 1134-1140
16. Fishbein, J. D., Dobrowsky, R. T., Bielawska, A., Garrett, S., and Hannun, Y. A. (1993) *J. Biol. Chem.* **268**, 9255-9261
17. Nickels, J. T., and Broach, J. R. (1996) *Genes Dev.* **10**, 382-394
18. Beeler, T., Bacikova, D., Gable, K., Hopkins, L., Johnson, C., Slife, H., and Dunn, T. (1998) *J. Biol. Chem.* **273**, 30688-30694
19. Cid, V. J., Duran, A., del Rey, F., Snyder, M. P., Nombela, C., and Sanchez, M. (1995) *Microbiol. Rev.* **59**, 345-386

20. Elble, R. (1992) *Biotechniques* **13**, 18-20
21. Ziman, M., Chuang, J. S., and Schekman, R. W. (1996) *Mol. Biol. Cell* **7**, 1909-1919
22. Holthuis, J. C., Nichols, B. J., Dhruvakumar, S., and Pelham, H. R. (1998) *Embo J.* **17**, 113-126
23. Dickson, R. C., Nagiec, E. E., Wells, G. B., Nagiec, M. M., and Lester, R. L. (1997) *J. Biol. Chem.* **272**, 29620-29625
24. Leber, A., Fischer, P., Schneiter, R., Kohlwein, S. D., and Daum, G. (1997) *FEBS Lett.* **411**, 211-214
25. Hirayama, T., Maeda, T., Saito, H., and Shinozaki, K. (1995) *Mol. Gen. Genet.* **249**, 127-138
26. McClanahan, T., and McEntee, K. (1984) *Mol. Cell Biol.* **4**, 2356-2363
27. Treger, J. M., Schmitt, A. P., Simon, J. R., and McEntee, K. (1998) *J. Biol. Chem.* **273**, 26875-26879
28. Huh, W. K., Falvo, J. V., Gerke, L. C., Carroll, A. S., Howson, R. W., Weissman, J. S., and O'Shea, E. K. (2003) *Nature* **425**, 686-691
29. McCusker, J. H., Perlin, D. S., and Haber, J. E. (1987) *Mol. Cell Biol.* **7**, 4082-4088
30. Nass, R., Cunningham, K. W., and Rao, R. (1997) *J. Biol. Chem.* **272**, 26145-26152
31. Withee, J. L., Sen, R., and Cyert, M. S. (1998) *Genetics* **149**, 865-878
32. Navarre, C., Ghislain, M., Leterme, S., Ferroud, C., Dufour, J. P., and Goffeau, A. (1992) *J. Biol. Chem.* **267**, 6425-6428
33. Navarre, C., Catty, P., Leterme, S., Dietrich, F., and Goffeau, A. (1994) *J. Biol. Chem.* **269**, 21262-21268
34. Ambesi, A., Miranda, M., Petrov, V. V., and Slayman, C. W. (2000) *J. Exp. Biol.* **203 Pt 1**, 155-160
35. Vallejo, C. G., and Serrano, R. (1989) *Yeast* **5**, 307-319
36. Mulet, J. M., Leube, M. P., Kron, S. J., Rios, G., Fink, G. R., and Serrano, R. (1999) *Mol. Cell Biol.* **19**, 3328-3337
37. Kobayashi, N., McClanahan, T. K., Simon, J. R., Treger, J. M., and McEntee, K. (1996) *Biochem. Biophys. Res. Commun.* **229**, 540-547
38. Goffeau, A., and Slayman, C. W. (1981) *Biochim. Biophys. Acta* **639**, 197-223
39. Serrano, R. (1984) *Curr. Top. Cell Regul.* **23**, 87-126
40. Navarre, C., and Goffeau, A. (2000) *Embo J.* **19**, 2515-2524

Chapter 5

Loss of yeast *trans*-Golgi P-type ATPases Drs2p and Dnf3p disrupts aminophospholipid asymmetry in Pma1p-containing secretory vesicles*

* Lisman Q., Alder-Baerens N., Luong, L., Pomorski T., and Holthuis J.C.M. (2004)
Manuscript in preparation

Summary

Eukaryotic plasma membranes generally display asymmetric lipid distributions with the aminophospholipids concentrated in the cytoplasmic leaflet. This arrangement is likely maintained by aminophospholipid translocases (APLTs) that use ATP hydrolysis to catalyze a fast inward movement of phosphatidylserine and phosphatidylethanolamine (PE) across the bilayer. The identity of APLTs has not yet been established but prime candidates are members of the P4 subfamily of P-type ATPases. The yeast *Saccharomyces cerevisiae* contains five P4 ATPases localized to different organelles, namely Dnf1p and Dnf2p to the plasma membrane, Drs2p and Dnf3p to the *trans*-Golgi, and Neo1p to compartments of the endosomal system. Previous work revealed that loss of Dnf1p and Dnf2p disrupts aminophospholipid transport across the plasma membrane and causes an increased aminophospholipid exposure at the cell surface. Here we show that post-Golgi secretory vesicles destined for the cell surface have an asymmetric aminophospholipid arrangement with the bulk of PE (up to 80%) located in the cytoplasmic leaflet. Strikingly, removal of Drs2p and Dnf3p proved sufficient to abolish this lipid asymmetry. Our findings indicate that aminophospholipid asymmetry is not a unique feature of the plasma membrane and that P4 ATPases serve a general function as regulators of the transbilayer lipid arrangement in the late secretory pathway of yeast.

Introduction

Numerous cell types, including yeast, exhibit a non-random distribution of phospholipids across their plasma membranes (1, 2). In general, the inner leaflet consists predominantly of aminophospholipids phosphatidylserine (PS) and phosphatidylethanolamine (PE), whereas sphingolipids are enriched in the outer leaflet. Loss of this asymmetric lipid arrangement gives rise to several physiological events, ranging from blood coagulation to the recognition and clearance of apoptotic cells. Yet how lipid asymmetry is established and what significance it has for the functioning of individual cells is not well understood.

It has been postulated that lipid asymmetry is generated and maintained by ATP-driven lipid transporters or translocases (1). The use of short-chain lipid analogues has led to the discovery of an aminophospholipid translocase (APTL) that catalyzes a fast, inwardly directed transport of PS and PE across the plasma membrane (3). This activity, first described in human erythrocytes and later demonstrated in many nucleated cell types, is thought to be responsible for the selective accumulation of aminophospholipids in the inner leaflet of the plasma membrane. A prime candidate APLT is ATPase II (4). Cloning of the gene encoding ATPase II from bovine chromaffin granules revealed it to be a member of a previously unrecognized subfamily of P-type ATPases, the P4 ATPases (5). A block in the non-endocytic uptake of NBD-labeled PS in yeast cells in which the homologous gene, *DRS2*, was disrupted has been taken as evidence for a role of P4 ATPase as APLTs (5, 6) even though other groups have reported no dependency on Drs2p for aminophospholipid translocation (7, 8). Subsequent findings have shed further light on potential causes of this disparity. First, Drs2p was found to be associated with the *trans*-

Golgi rather than the plasma membrane (9). Second, the yeast plasma membrane contains two other P4 ATPases, namely Dnf1p and Dnf2p (10, 11). Third, loss of Dnf1p and Dnf2p abolishes the inward translocation of NBD-PE, -PS and -PC across the yeast plasma membrane and causes an increased cell surface exposure of endogenous PE (11).

Drs2p plays a critical role in membrane traffic from the *trans*-Golgi to the plasma membrane and is required for the formation of clathrin-coated vesicles involved in cell surface delivery of the periplasmic enzymes invertase and acidic phosphatase (9, 12). Moreover, a recent analysis of strains carrying all possible viable combinations of null alleles for genes encoding P4 ATPases revealed that Drs2p, Dnf1p, Dnf2p and Dnf3p constitute an essential protein family with overlapping functions in membrane traffic between the Golgi and endosomal/vacuolar system (10). Together with a defect in lipid transport and altered lipid distribution across the plasma membrane, cells lacking Dnf1p and Dnf2p display a cold sensitive defect in the internalization step of endocytosis (11). Collectively, these findings suggest that by regulating the transbilayer lipid arrangement, P4 ATPases seem to fulfil a requirement in the formation of intracellular transport vesicles.

In the present study, we demonstrate that post-Golgi secretory vesicles (SVs) have an asymmetric lipid distribution with PE accumulated in the cytoplasmic leaflet. Strikingly, loss of the *trans*-Golgi P4 ATPases Drs2p and Dnf3p is sufficient to disrupt SV-associated lipid asymmetry. Our finding that $\Delta drs2\Delta dnf3$ cells are defective in the biogenesis of invertase-containing SVs but still form SVs containing the plasma membrane H⁺-ATPase Pma1p indicates that the functional link between P4 ATPase-dependent lipid transport and vesicle biogenesis is not absolute.

Experimental Procedures

Strains and plasmids

Unless indicated otherwise, yeast strains were grown at 25°C to mid-logarithmic phase (0.5–1.0 OD₆₀₀) in synthetic dextrose (SD) medium. Yeast transformations were carried out as described (13). All mentioned gene deletion phenotypes were characterized in the strain EHY227 (*MAT α sec6-4 TPI1::SUC2::TRP1 ura3-52 his3- Δ 200 leu2-3 -122trp1-1*). For deletion of *DRS2* and *DNF3*, 450–550 base-pair fragments of the promoter and ORF 3'-end of each gene were amplified by PCR from yeast genomic DNA and cloned on either site of a *loxP-HIS3-loxP* cassette in a pBluescript KS⁻ vector, as described (14). The deletion constructs were linearized with *NotI* and *MluI* and then transformed into EHY227 (*MAT α sec6-4 TPI1::SUC2::TRP1 ura3-52 his3- Δ 200 leu2-3 -122 trp1-1*). A double deletion was performed sequentially in EHY227 by repeated use of the *loxP-HIS3-loxP* cassette and subsequent removal of the *HIS3* marker by excisive recombination using Cre recombinase (15), yielding the $\Delta drs2\Delta dnf3$ (TPY143) strain. In each case, the correct integration or excision event was confirmed by PCR. In each strain analysed, Pma1p was tagged at its amino-terminus with one copy of the HA epitope using integration plasmid pRS305 Δ 51, as described (16).

Subcellular membrane fractionation

Exponentially grown *sec6-4* or *sec6-4Δdrs2Δdnf3* cells were inoculated into 500 ml SD medium and then grown for 14–16 h at 25°C to 0.7 OD₆₀₀/ml. Next, half of the culture was shifted to 38°C for 90 min to allow accumulation of SVs, and the other half grown at 25°C. Spheroplasting, cell lysis and collection of membrane pellets enriched in SVs were performed essentially as described (17) except that SVs were collected on a 60% Nycodenz (w/w) cushion in lysis buffer (0.8 M sorbitol, 10 mM triethanolamine, 1 mM EDTA, pH 7.2). SVs were resuspended in 1.5 ml lysis buffer adjusted to 30% Nycodenz (w/w) and then loaded at the bottom of an 11 ml linear 12–22% Nycodenz (w/w)/0.8 M sorbitol gradient. Following centrifugation at 100,000 *g*_{av} for 16 h at 4°C in a Beckman SW41Ti rotor, 0.6-ml fractions were collected from the top of the gradient. Fraction densities were determined by reading refractive indices on a Bausch and Lomb refractometer. Equal amounts per fraction were subjected to immunoblotting and analyzed for ATPase and invertase enzyme activities as described below.

Enzyme assays and immunoblotting

ATPase assays were performed on 10-fold diluted fractions at 30°C in a final volume of 25 μl (10 mM Hepes-KOH, pH 7.2, 0.8 M sorbitol, 2 mM ATP, 5 mM MgCl₂). Reactions were stopped after 30 minutes with 175 μl 40 mM H₂SO₄. Then 50 μl 6 M H₂SO₄ containing 0.001% malachite green was added and after 30 min incubation at room temperature, the absorbance was measured at 595 nm. For determining invertase activity, fractions were diluted 10–20 fold and assayed by the method described by Goldstein and Lampen (18), and the absorbance was measured at 540 nm. HA-tagged Pma1p was detected with anti-HA rabbit polyclonal antibodies (Santa Cruz Biotechnology, CA). For immunoblotting, all antibody incubations were carried out in PBS containing 5% dried milk and 0.5% Tween-20. After incubation with peroxidase-conjugated secondary antibodies (Biorad), blots were developed using a chemiluminescent substrate kit (Pierce, Rockford, USA).

Immuno-isolation of secretory vesicles

Immuno-isolations of Pma1p-HA-containing SVs were performed using magnetic Dynabeads protein G (DynaL Biotech GmbH, Hamburg, Germany) loaded with mouse monoclonal anti-HA antibody, 12CA5 (Boehringer-Mannheim, Germany). Beads were incubated for 40 min at room temperature with 0.36 μg 12CA5 antibody/μl bead-slurry. For immuno-isolation of Pma1p-containing SVs, a 500 μl reaction was prepared in lysis buffer (0.8 M sorbitol, 10 mM triethanolamine, 1 mM EDTA, pH 7.2, protease inhibitors) containing 200 μl of antibody-loaded Dynabead slurry, 5 mg/ml BSA and 100–200 μl of Nycodenz gradient PM-ATPase peak fraction obtained by fractionation of SV-enriched membranes prepared from 1 g of 38°C-shifted cells. The reactions were rotated gently at 4°C for 2 h. Next, beads and supernatant were separated by centrifugation for 2 min at 500 *g*. The supernatants were subjected to high-speed centrifugation (100,000 *g*_{av}, 1 h, 4°C) and membrane pellets were resuspended in 200 μl lysis buffer. Beads were washed twice for 30 min in 1 ml of 0.5% BSA-containing lysis buffer, twice in lysis buffer, and then resuspended in 200 μl lysis buffer.

Per sample, 25 μ l was used for Western blot analysis, and 175 μ l was used for lipid analysis.

TNBS labeling of secretory vesicle-enriched membranes

Sec6-4 and *sec6-4 Δ Drs2 Δ Dnf3* were grown overnight in SD medium at 25°C to 0.7 OD₆₀₀/ml. Half of the culture was shifted to 38°C for 90 min, the other half grown at 25°C. Cells were lysed by vortexing with glass beads in 1.5 ml of KHCO₃-buffer (120 mM KHCO₃, 15 mM KCl, 5 mM NaCl, 0.8 mM CaCl₂, 2 mM MgCl₂, 1.6 mM EGTA, protease inhibitors, pH 8.5). Lysates were spun at 500 g_{av} for 10 min at 4°C. Next, 2.5 ml of supernatant was mixed with 2.5 ml of 2x labelling buffer (KHCO₃-buffer containing 10 mM trinitrobenzene sulphonic acid (TNBS, Sigma) or 10 mM 1-Fluoro-2,4-dinitrobenzene (FDNB, Sigma), pH 8.5) and incubated at room temperature with periodic mixing. After 45 min of labeling, samples were centrifugated at 13,000 g in a Beckman MLS50 rotor for 20 min at 4°C. To terminate labeling, the supernatant was added to 15 ml of stop buffer (0.93 M sorbitol, 500 mM glycylglycine, 100 mM citric acid, pH 5.0) on ice, and samples were centrifugated at 100,000 g_{av} for 90 min at 4°C in a Beckman SW41Ti rotor. Per strain, SVs were resuspended in 1.5 ml, adjusted to 26% Nycodenz (w/w) and then loaded at the bottom of an 11 ml linear 12–22% Nycodenz (w/w)/0.8 M sorbitol gradient. Following centrifugation at 100,000 g_{av} for 16 h at 4°C in a Beckman SW41Ti rotor, 0.6-ml fractions were collected from the top of the gradient. Equal volumes per fraction were used for Western blot analysis, total phosphate determination, and lipid analysis.

Intactness of secretory vesicles

Intactness of SVs isolated from 38°C–shifted *sec6-4* or *sec6-4 Δ Drs2 Δ Dnf3* cells was monitored by measuring the accessibility of newly synthesized NBD-IPC accumulated in the SV lumen to extraction by BSA. To this end, exponentially grown cells were harvested and resuspended at 33 OD₆₀₀/ml SD medium supplemented with 4% glucose and pre-incubated for 20 min at 25°C or 38°C. Then, 30 nmol NBD-hexanoyl-sphingosine (C₆-NBD-ceramide, Molecular Probes) from an ethanolic stock were added. After 10 min, BSA (final concentration of 2% w/v) was added to extract NBD-lipid from the cell surface. After 20 min, BSA-containing media were collected and cells subjected to a second back-exchange incubation on ice in medium containing 2% (w/v) BSA, followed by lipid analysis of cells and pooled media. For probing the accessibility of NBD-IPC in SVs, NBD-ceramide-labeled cells were disrupted by vortexing 10 times for 30 s with glass beads (425–600 nm) in 0.5 ml of ice-cold lysis buffer (120 mM potassium glutamate, 15 mM KCl, 5 mM NaCl, 2 mM MgCl₂, 2 mM EGTA, 20 mM Hepes-KOH, pH 7.2) containing protease inhibitors (1 mg/ml aprotinin, 1 mg/ml leupeptin, 1 mg/ml pepstatin A, 5 mg/ml antipain, 1 mM benzamidin, 1 mM phenylmethylsulfonyl fluoride). Glass beads and cell debris were removed by centrifugation at 700 g_{av} for 10 min. Then, BSA (final concentration of 2% w/v) was added, and the sample incubated for 10 min on ice. After BSA treatment, the sample (3 ml) was loaded on top of a 2-ml 0.4 M sucrose cushion in lysis buffer and centrifuged (MLS-50, 90 min, 40,000 rpm, 4°C). The BSA-containing top fraction, the sucrose, and the membrane pellet were isolated, and their short-chain NBD-lipid composition was analysed by TLC.

Lipid analysis

NBD-lipids were extracted from media by addition of chloroform:methanol (1:2.2, v/v) to give a single phase and from cells by resuspending pelleted cells directly in 4.4 ml of a 1:2.2:1 mixture of chloroform:methanol:water and vortexing for 6 min with glass beads (425–600 nm). After centrifugation (3000g, 10 min), the supernatants were dried and subjected to butanol/water partitioning (2:1, v/v). Lipids in the butanol phase were separated by one-dimensional TLC on silica gel 60 plates (Merck, Darmstadt, Germany) in chloroform/methanol/4 M ammonium hydroxide (9:7:2, v/v). Fluorescent lipid spots were visualized under UV light, scraped off, re-extracted in chloroform:methanol:water (1:2.2:0.1, v/v) and quantified fluorometrically. In some cases, fluorescent lipid spots were quantified on a FLA-3000 Fuji Imaging System (Raytest, Straubenhardt, Germany) equipped with a 488 nm laser and a 515 nm long pass emission filter. Image analysis was performed using Aida Image Analyser 3.24 software (Raytest, Straubenhardt, Germany). For phospholipid analysis, lipids were extracted as described (19), using 20 mM acetic acid in the aqueous phase, and separated by two-dimensional TLC (I: chloroform/methanol/25% aqueous ammonium hydroxide, 65:25:4; II: chloroform/acetone/methanol/acetic acid/water, 50:20:10:10:5). Lipid spots stained by iodine were scraped and quantitated by phosphate determination (20). Phospholipids were identified by comparison with commercial standards (Sigma).

Results

***Δdrs2Δdnf3* cells display a specific defect in the biogenesis of invertase-containing SVs**

The finding that the late Golgi of yeast harbors two candidate APLTs, namely Drs2p and Dnf3p, suggests that aminophospholipid asymmetry is not a unique feature of the plasma membrane and may already be established at the level of the Golgi. To investigate this possibility, we disrupted the *DRS2* and *DNF3* genes in the late secretory mutant *sec6-4* and analyzed the transbilayer distribution of aminophospholipids in post-Golgi SVs that accumulate at the non-permissive temperature. The *sec6-4* strain harbors a temperature-sensitive mutation in a component of the exocyst protein complex required for polarized fusion of SVs with the plasma membrane (21). The *sec6-4* mutant grows like wild-type cells at 25°C, but growth ceases at 38°C and cells accumulate two populations of SVs that can be separated by equilibrium isodensity centrifugation on Nycodenz gradients, namely a light density population containing the major plasma membrane ATPase, Pma1p, and a higher density population containing the periplasmic enzymes invertase and acidic phosphatase (17).

Previous work revealed a critical role for Drs2p in the formation of the high-density class of invertase-containing SVs (12). To study the effect of a simultaneous loss of Drs2p and Dnf3p on secretory vesicle formation, *sec6-4* and *sec6-4Δdrs2Δdnf3* cells were grown in SD medium at 25°C and then shifted to 38°C for 90 min, lysed and subjected to a 13,000 x g spin to remove most of the ER, nuclei, vacuoles, mitochondria and plasma membrane.

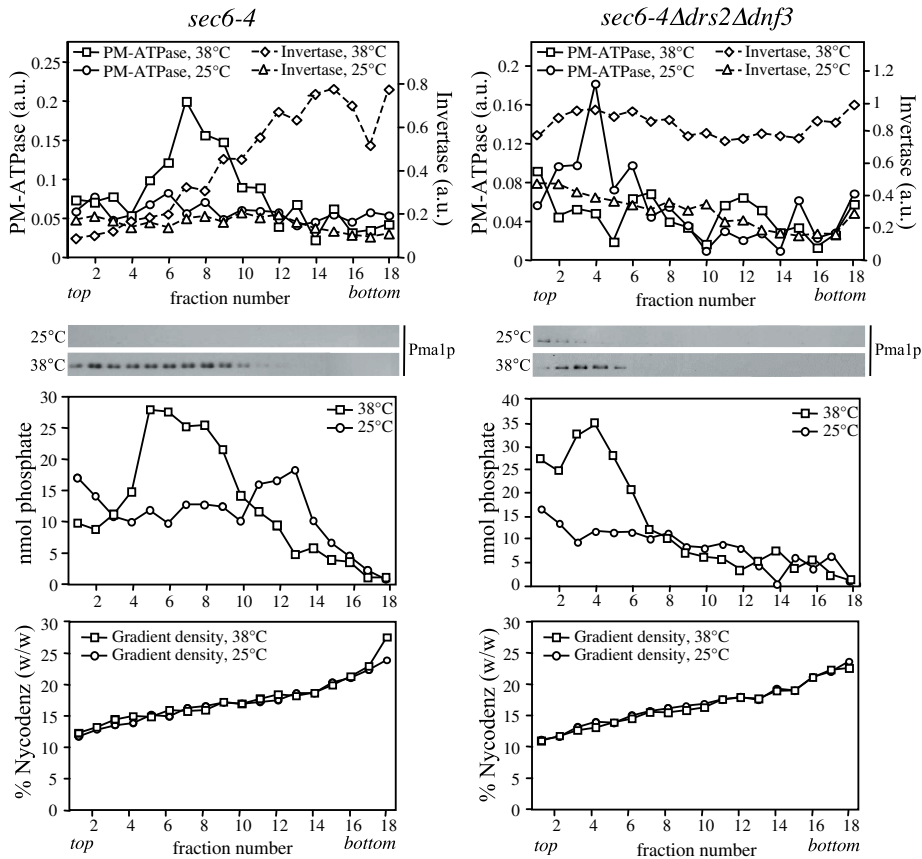


Figure 1. *Δdrs2Δdnf3* cells display a specific defect in the formation of invertase-containing SVs. Membrane pellets (100,000 *g*) enriched in SVs were prepared from 38°C-shifted and 27°C-grown cells, loaded on the bottoms of linear 12–22% Nycodenz/0.8 M sorbitol gradients, and then floated to equilibrium by centrifugation. Fractions were collected from the top and analyzed for enzyme activities and by immunoblotting. Enzyme activities are expressed in arbitrary units (a.u.) based on the absorbance measured at 595 nm (PM-ATPase) or 540 nm (invertase) as described under Experimental Procedures. Immunoblots were stained with a monoclonal antibody against the HA epitope to detect HA-tagged Pma1p. The lipid phosphorus content was determined according to Rouser *et al.* (20), and fraction densities were measured by reading refractive indices on a Bausch and Lomb refractometer.

Next, high-speed (100,000 *x g*) membrane pellets enriched in SVs were collected and loaded at the bottom of a linear 12–22% Nycodenz gradient in 0.8 M sorbitol. As shown in Figure. 1 (*left panel, top*), gradient fractionation of membranes from 38°C-shifted *sec6-4* cells resulted in two peaks of enzyme activities that were absent when fractionation was performed on 25°C-grown cells: a low density peak containing ATPase activity and a higher density peak containing invertase activity. Western blot analysis revealed that Pma1p co-fractionates with the lower density membranes, confirming that the detected ATPase activity is due

to this protein. Using a phosphorus assay, a peak comprising the bulk of phospholipids (> 80% of total) was found to coincide with the ATPase peak in gradients of 38°C-shifted cells (Figure 1, *left panel, middle*; see also Figure 5). This phospholipid peak was absent in gradients of 25°C-grown cells. Hence, of the two classes of SVs accumulating in 38°C-shifted *sec6-4* cells, the low-density Pma1p-containing vesicles are by far the most abundant, outnumbering the high-density invertase-containing vesicles at least four times. In fact, counting vesicular profiles in electronmicrographs of negatively stained membranes derived from plasma membrane ATPase and invertase peak fractions suggested that the low-density vesicles are about ten-fold more abundant than the high-density ones (data not shown).

Gradients of 38°C-shifted *sec6-4Δdrs2Δdnf3* cells lacked the high-density invertase peak and only contained a low density ATPase peak harboring the bulk of phospholipids (Figure 1, *right panel, top*). Even though 38°C-shifted *sec6-4Δdrs2Δdnf3* cells contained elevated levels of membrane-associated invertase activity in comparison to 25°C-grown cells, this activity was found evenly spread throughout the gradient. These results are in line with the recent finding that loss of Drs2p perturbs formation of the high-density SVs that carry invertase and acidic phosphatase to the cell surface (12). Moreover, our data indicate that formation of the more abundant, low-density class of Pma1p-containing SVs is essentially independent of Drs2p and Dnf3p.

Loss of Drs2p and Dnf3p reduces the TNBS-reactive pool of PE in SV-enriched membranes

A comparison of the phospholipid content between high-speed membrane pellets prepared from equal amounts of 38°C-shifted and 25°C-grown *sec6-4* or *sec6-4Δdrs2Δdnf3* cells indicated that in each case, 60-70% of the phospholipids in the 38°C pellet was derived from SVs (data not shown). Therefore, an initial analysis of the aminophospholipid topology in SVs was carried out on high-speed membrane pellets of 38°C-shifted *sec6-4* and *sec6-4Δdrs2Δdnf3* cells. To this end, the SV-enriched membrane pellets were treated with TNBS, a membrane-impermeable compound reacting with the primary amines in the head group of PE and PS. Next, lipids were extracted, separated by TLC and the percentage of TNBS-reacted PE (TNP-PE) relative to total PE was calculated based on the phosphate content of scraped PE spots. Within the first 30 min of incubation, PE in SV-enriched membrane pellets from 38°C-shifted *sec6-4* cells displayed a significantly higher rate of TNBS labeling than PE in pellets from 38°C-shifted *sec6-4Δdrs2Δdnf3* cells (Figure 2 A). Over the next 30 min, the levels of TNP-PE formed stabilized and after 60 min comprised approximately 70% and 60% of the total PE in *sec6-4*- and *sec6-4Δdrs2Δdnf3*-derived membrane pellets, respectively. These strain-dependent differences in PE labeling could not be ascribed to changes in the overall phospholipid composition of SV-enriched membranes (Figure 3). Moreover, the differential PE labeling was abolished when membrane pellets were either sonified prior to TNBS treatment or reacted with FDNB, a membrane-permeable derivative of TNBS (Figure 2 B, C).

We next investigated whether the observed differences in PE labeling could be due to differences in vesicle intactness. As approach, *sec6-4* and *sec6-4Δdrs2Δdnf3* cells were shifted

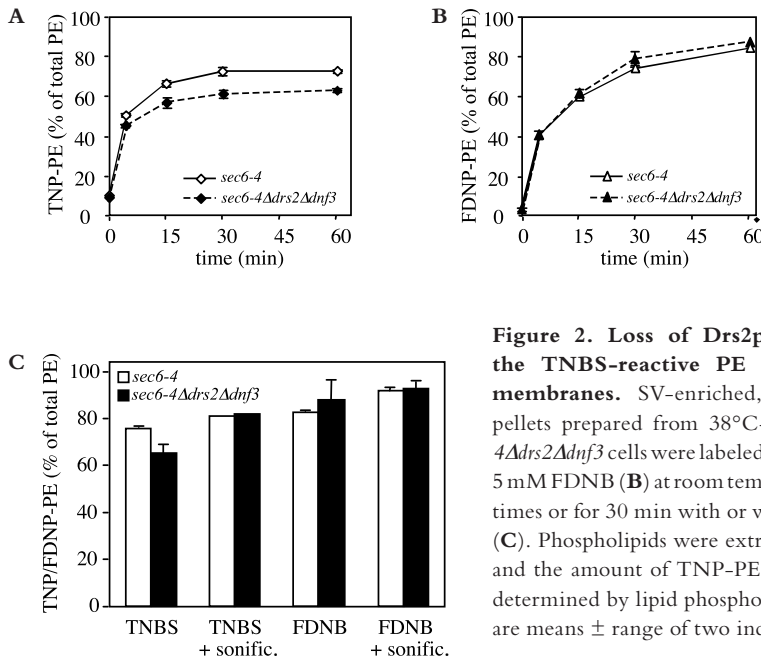


Figure 2. Loss of Drs2p and Dnf3p reduces the TNBS-reactive PE pool in SV-enriched membranes. SV-enriched, high-speed membrane pellets prepared from 38°C-shifted *sec6-4* and *sec6-4Δdrs2Δdnf3* cells were labeled with 5 mM TNBS (A) or 5 mM FDNB (B) at room temperature for the indicated times or for 30 min with or without prior sonification (C). Phospholipids were extracted, separated by TLC and the amount of TNP-PE, FDNP-PE and PE was determined by lipid phosphorus analysis. Data shown are means ± range of two independent experiments.

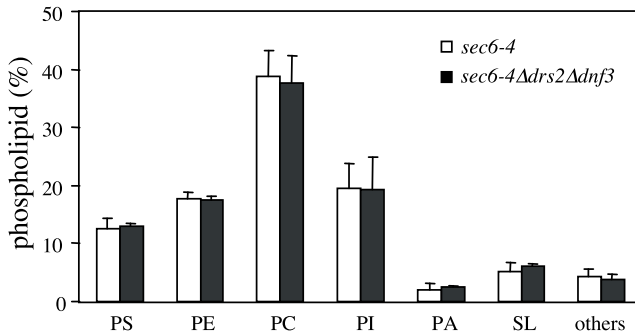


Figure 3. Loss of Drs2p and Dnf3p does not affect the overall phospholipid composition of SV-enriched membranes. Membrane pellets (100,000 g) enriched in SVs were prepared from 38°C-shifted *sec6-4* and *sec6-4Δdrs2Δdnf3* cells. Phospholipids were extracted, separated by TLC and determined by lipid phosphorus analysis. Each bar represents the mean ± range of two independent experiments.

to 38°C and then labeled with the short-chain fluorescent ceramide analogue, C6-NBD ceramide. This compound is converted into C6-NBD inositolphosphorylceramide (NBD-IPC) by an IPC synthase active in the Golgi lumen (22). In wild type cells grown at 38°C, newly synthesized NBD-IPC is efficiently transported to the cell surface from where it can be extracted by BSA added to the culture medium. In 38°C-shifted *sec6-4* or *sec6-4Δdrs2Δdnf3* cells, on the other hand, NBD-IPC is prevented from reaching the cell surface and becomes trapped intracellularly (Figure 4 A). In post-nuclear supernatants of NBD-IPC accumulating *sec6-4* cells, the majority of membrane-associated NBD-IPC (70%) was

protected from BSA extraction. There was no significant change in the percentage of BSA-resistant NBD-IPC when extraction was performed on post-nuclear supernatants of NBD-IPC accumulating *sec6-4Δdrs2Δdnf3* cells, regardless of whether or not supernatants were pre-incubated with TNBS (Figure 4 B and data not shown). Hence, the above differences in PE labeling are unlikely due to differences in vesicle intactness or spontaneous lipid flip-flop rates. Instead, our findings suggest that SVs formed in *sec6-4Δdrs2Δdnf3* cells contain a reduced level of PE in their cytoplasmic leaflet compared to SVs formed in *sec6* cells.

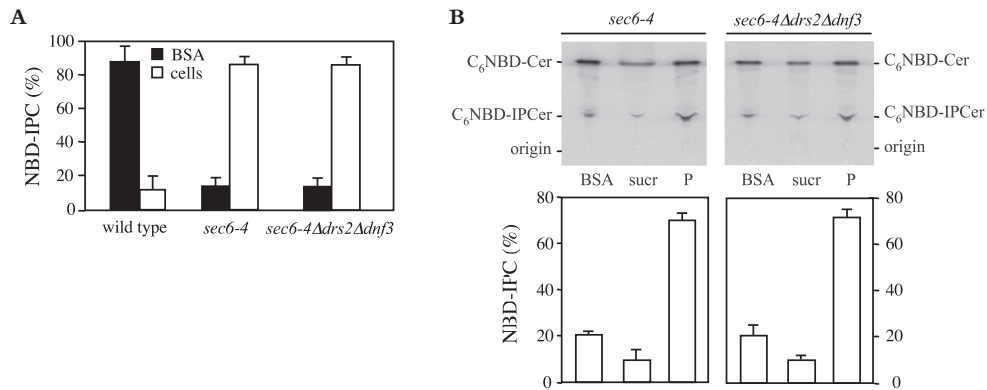


Figure 4. SVs isolated from *sec6-4* and *sec6-4Δdrs2Δdnf3* cells are largely intact. (A) Wild type, *sec6-4* and *sec6-4Δdrs2Δdnf3* cells were shifted to 38°C and then metabolically labeled with C₆-NBD-ceramide. After 10 min, 2% BSA was added to the medium to extract NBD-lipids appearing on the cell surface. Cells and medium were separated by centrifugation and lipids extracted separated by TLC. NBD-labeled lipids were detected with a PhosphorImager and quantified with AIDA software. Each bar represents the mean ± S.D. of four independent experiments. (B) *Sec6-4* and *sec6-4Δdrs2Δdnf3* cells were labeled with 30 nmol C₆-NBD-ceramide at 38°C. After 10 min, BSA was added. Cells were washed in BSA-containing medium and lysed. After removal of cell debris by centrifugation (700 *g*_{av}), BSA was added and the sample incubated for 10 min on ice. Next, BSA incubated membranes were loaded on top of a sucrose cushion, and after centrifugation three fractions were collected from the top: a BSA fraction (BSA), sucrose fraction (sucr) and pellet (P). Lipids were extracted and separated by TLC. NBD-labeled lipids were detected with a PhosphorImager and quantified with AIDA software. Each bar represents the mean ± range of two independent experiments

Loss of *Drs2p* and *Dnf3p* disrupts PE transbilayer asymmetry in *Pma1p*-containing SVs

To obtain more detailed information on the transbilayer PE arrangement in SVs and its potential regulation by P4 P-type ATPases, SV-enriched membrane pellets of 38°C-shifted *sec6-4* and *sec6-4Δdrs2Δdnf3* cells were treated with TNBS and then fractionated by equilibrium isodensity centrifugation on linear Nycodenz gradients. Fractions were analyzed for plasma membrane ATPase activity, phospholipid content and the percentage of TNBS-reactive PE. As observed previously (Figure 1), gradients of 38°C-shifted *sec6-4* and *sec6-4Δdrs2Δdnf3* cells contained overlapping plasma membrane ATPase and phospholipid

peaks that were absent in gradients of 25°C-grown cells (Figure 5, *top* and *middle panels*). In gradients of 38°C-shifted *sec6-4* cells, there was a strong and positive correlation between plasma membrane ATPase levels and the percentage of TNBS-reactive PE, with the latter rising from 50% in ATPase-deficient fractions to nearly 80% in ATPase peak fractions (Figure 5, *left panel, bottom*). In gradients of 38°C-shifted *sec6-4Δdrs2Δdnf3* cells, on the other hand, no such correlation was observed and the percentage of TNBS-reactive PE was close to 50% in both ATPase-deficient and peak fractions (Figure 5, *right panel, bottom*; see also Figure 6 A). This Drs2p/Dnf3p-dependent change in the TNBS-reactive PE pool was also observed when the analysis was performed on Pma1p-containing SVs immunoprecipitated from the ATPase peak fractions (Figure 6). Together, these results indicate that PE is primarily concentrated in the cytoplasmic leaflet of Pma1p-containing SVs and that maintenance of this PE asymmetry requires Golgi-associated P4 P-type ATPases.

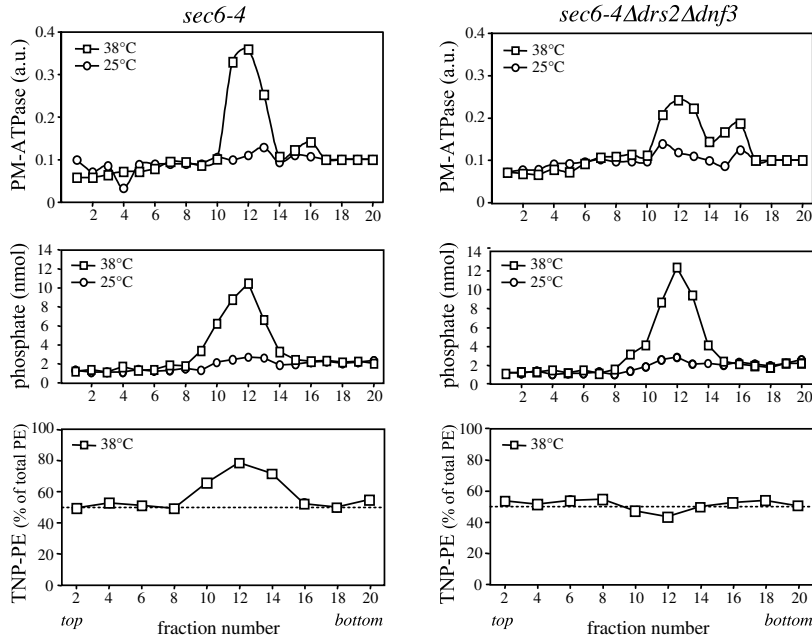


Figure 5. Gradient fractionation of TNBS-labeled SV-enriched membranes isolated from *sec6-4* and *sec6-4Δdrs2Δdnf3* cells. SV-enriched membranes prepared from 38°C-shifted or 25°C-grown cells were labeled with 5 mM TNBS for 45 min at room temperature. Next, membranes were centrifugated at 13,000 *g* for 20 min at 4°C. To terminate labeling, the supernatant was diluted 3-fold in glycyglycine-containing stop buffer and membranes collected by high-speed (100,000 *g*_{av}) centrifugation. Membranes were resuspended in 1.5 ml 26% Nycodenz (w/w), loaded at the bottom of a 11 ml linear 12–22% Nycodenz (w/w)/0.8 M sorbitol gradient and then floated to equilibrium by centrifugation. 0.6 ml fractions were collected from the top and equal amounts were analyzed for enzyme assays, phosphate determination and lipid extraction. Lipids were separated by TLC and the amount of TNP-PE and PE was determined by lipid phosphorus analysis. Density profiles were similar for all gradients (not shown).

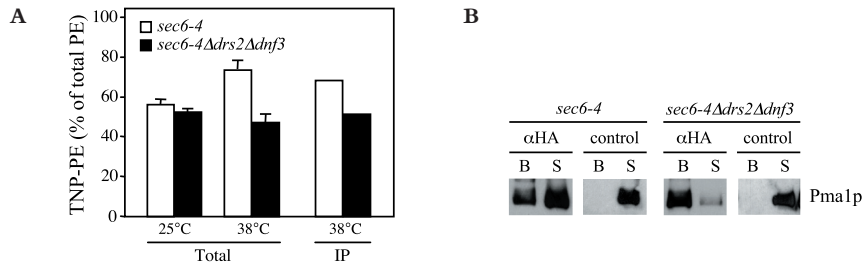


Figure 6. Loss of Drs2p and Dnf3p causes a decrease in the TNBS-reactive PE pool of Pma1p-containing SVs. (A) TNBS-labeled SV-enriched membranes derived from *sec6-4* and *sec6-4Δdrs2Δdnf3* cells were fractionated as in Figure 5 and the percentage of TNP-PE of total PE determined in plasma membrane ATPase peak fractions (Total) or in immuno-isolated Pma1p-containing SVs (IP). (B) Western blot analysis of SVs containing HA-tagged Pma1p immuno-isolated from plasma membrane ATPase peak fractions using anti-HA antibodies (α HA) bound to magnetic Dynabeads protein G. Immuno-isolation with beads lacking antibody served as control. B: beads; S: supernatant.

Discussion

We previously showed that removal of P4 P-type ATPases Dnf1p and Dnf2p abolishes inward aminophospholipid transport across the yeast plasma membrane and causes an increased aminophospholipid exposure at the cell surface (11). In the present study, we have shown that post-Golgi SVs display an asymmetric transbilayer arrangement of PE and that this lipid asymmetry is abolished upon removal of the *trans*-Golgi P4 ATPases Dnf3p and Drs2p. We conclude that aminophospholipid asymmetry is not a unique feature of the plasma membrane and that P4 P-type ATPases likely function as general regulators of the transbilayer lipid arrangement in the late secretory pathway of yeast.

Whether P4 P-type ATPases are directly responsible for aminophospholipid transport remains to be established. This will require reconstitution of purified ATPases in chemically defined liposomes. Dnf1p and Dnf2p do not strictly qualify as APLTs since their removal affects ATP-dependent translocation of both NBD-PS, -PE and -PC from the exoplasmic to the cytoplasmic leaflet of the plasma membrane (11). In a recent study, a temperature-conditional Drs2p mutant was used to show that this protein is required for the ATP-dependent translocation of NBD-PS from the luminal to the cytoplasmic leaflet of the yeast *trans*-Golgi (23). Remarkably, the Drs2p-dependent translocase activity was head-group specific with a strong preference for NBD-PS. In fact, no Drs2p-dependent translocase activity could be detected when NBD-PE or -PC was used. This would imply that Drs2p functions as a PS-specific translocase. If so, the establishment of PE asymmetry in post-Golgi secretory vesicles would require Dnf3p and not Drs2p. At present, the precise contribution of Drs2p and Dnf3p in creating asymmetric aminophospholipid arrangements in the late secretory pathway remains to be established.

Several lines of evidence point to a functional link between P4 ATPase-dependent lipid

transport and the biogenesis of intracellular transport vesicles. Concurrent with a block in aminophospholipid transport across the plasma membrane, cells lacking Dnf1p and Dnf2p exhibit a cold-sensitive defect in the internalization step of endocytosis (11). In addition, deletion of *DRS2* is synthetically lethal with mutations in the genes for ADP-ribosylation factor 1 (*ARF*) and clathrin heavy chain (*CHC1*; Ref. 9), and perturbs the formation of a high-density class of post-Golgi SVs that carry acidic phosphatase and invertase to the cell surface (12). Using a late secretion mutant in yeast, we observed that simultaneous loss of Drs2p and the *trans*Golgi P4 ATPase Dnf3p specifically affects biogenesis of the invertase-containing SVs. Our finding that removal of Drs2p and Dnf3p suffices to eliminate PE asymmetry in, but does not block formation of the lower density class of Pma1p-containing secretory vesicles indicates that the functional link between P4 ATPase-dependent lipid transport and vesicle biogenesis is not absolute.

The apparent specificity of Drs2p for NBD-PS transport suggests that Drs2p-catalyzed translocation of PS to the cytosolic leaflet of the Golgi is required for the formation of invertase-containing SVs. However, PS-deficient yeast cells produce these vesicles normally (23). Moreover, Drs2p is still required for SV formation when PS is absent. Collectively, these results strongly suggest that Drs2p is capable of pumping some other substrate across the Golgi membrane that may play a more critical role in secretory vesicle formation. Our previous finding that Drs2p contributes independently of Dnf1p and Dnf2p to an asymmetric distribution of PE across the plasma membrane (11) together with the present finding that loss of Drs2p and Dnf3p disrupts PE asymmetry in post-Golgi SVs urges for a re-evaluation of the role of Drs2p in PE transport.

Acknowledgements

We thank Gerrit van Meer and Maarten Egmond for valuable discussions and critical reading of the manuscript. Q.L. is supported by a grant from the Meelmeijer foundation, and J.H. by a grant from the Royal Academy of Arts and Sciences.

References

1. Devaux, P. F. (1991) *Biochemistry* **30**, 1163-1173
2. Cerbon, J., and Calderon, V. (1995) *Biochim. Biophys. Acta* **1235**, 100-106
3. Seigneuret, M., and Devaux, P. F. (1984) *Proc. Natl. Acad. Sci. U.S.A.* **81**, 3751-3755
4. Zachowski, A., Henry, J. P., and Devaux, P. F. (1989) *Nature* **340**, 75-76
5. Tang, X., Halleck, M. S., Schlegel, R. A., and Williamson, P. (1996) *Science* **272**, 1495-1497
6. Gomes, E., Jakobsen, M. K., Axelsen, K. B., Geisler, M., and Palmgren, M. G. (2000) *Plant. Cell* **12**, 2441-2454
7. Siegmund, A., Grant, A., Angeletti, C., Malone, L., Nichols, J. W., and Rudolph, H. K. (1998) *J. Biol. Chem.* **273**, 34399-34405
8. Marx, U., Polakowski, T., Pomorski, T., Lang, C., Nelson, H., Nelson, N., and Herrmann, A. (1999) *Eur. J.*

- Biochem.* **263**, 254-263
9. Chen, C. Y., Ingram, M. F., Rosal, P. H., and Graham, T. R. (1999) *J. Cell Biol.* **147**, 1223-1236
 10. Hua, Z., Fatheddin, P., and Graham, T. R. (2002) *Mol. Biol. Cell* **13**, 3162-3177
 11. Pomorski, T., Lombardi, R., Riezman, H., Devaux, P. F., van Meer, G., and Holthuis, J. C. (2003) *Mol. Biol. Cell* **14**, 1240-1254
 12. Gall, W. E., Geething, N. C., Hua, Z., Ingram, M. F., Liu, K., Chen, S. I., and Graham, T. R. (2002) *Curr. Biol.* **12**, 1623-1627
 13. Elble, R. (1992) *Biotechniques* **13**, 18-20
 14. Lisman, Q., Pomorski, T., Vogelzangs, C., Urli-Stam, D., de Cocq van Delwijnen, W., and Holthuis, J. C. (2004) *J. Biol. Chem.* **279**, 1020-1029
 15. Sauer, B. (1987) *Mol. Cell Biol.* **7**, 2087-2096
 16. Ziman, M., Chuang, J. S., and Schekman, R. W. (1996) *Mol. Biol. Cell* **7**, 1909-1919
 17. Harsay, E., and Bretscher, A. (1995) *J. Cell Biol.* **131**, 297-310
 18. Goldstein, A., and Lampen, J. O. (1975) *Methods Enzymol.* **42**, 504-511
 19. Bligh, E. G., and Dyer, W. J. (1959) *Can. J. Med. Sci.* **37**, 911-917
 20. Rouser, G., Fkeischer, S., and Yamamoto, A. (1970) *Lipids* **5**, 494-496
 21. TerBush, D. R., Maurice, T., Roth, D., and Novick, P. (1996) *Embo J.* **15**, 6483-6494
 22. Levine, T. P., Wiggins, C. A., and Munro, S. (2000) *Mol. Biol. Cell* **11**, 2267-2281
 23. Natarajan, P., Wang, J., Hua, Z., and Graham, T. R. (2004) *Proc. Natl. Acad. Sci. U.S.A.* **101**, 10614-10619

Chapter 6

Summarizing discussion

In an environment of glycerolipids, sphingolipids and sterols tend to cluster spontaneously into lipid microdomains, which are believed to act as protein sorting platforms (**Chapter 1**). This self-organizing behaviour of sphingolipids is thought to be due to their long saturated fatty acids and sugar-containing headgroups. Interestingly, sphingolipids are primarily synthesized in the Golgi, thus separated from glycerolipid and sterol production in the ER (1). The Golgi plays a key role in the organization of membrane traffic, and serves as a filter between the glycerolipid-rich ER and sphingolipid/sterol-rich plasma membrane. Therefore, an attractive possibility would be that the self-organizing behaviour of sphingolipids is exploited by the Golgi to boost its performance as the central sorting station of the cell. To test this possibility, we stripped sphingolipids of structural features that are considered important for microdomain formation and studied the effect this had on the sorting capacity of the Golgi in the yeast *Saccharomyces cerevisiae*. Apart from representing a transition point in membrane lipid composition, the Golgi is also a site where lipids adopt an asymmetric distribution across the bilayer. We decided to investigate the significance of this lipid asymmetry in relation to Golgi function.

Primary function of Csg1p and Csh1p as sphingolipid mannosyltransferases

At the onset of our studies, little was known about the enzyme(s) responsible for mannosylating the sphingolipid headgroups in yeast. Three structurally unrelated genes had been implicated in IPC mannosylation: the GDP-mannose importer *VRG4*, which was found to be essential (2), and the *CSG1* and *CSG2* genes, mutation of which causes a reduction in MIPC synthesis, but does not completely eliminate it (3, 4).

In **Chapter 2** we identified Csh1p, a protein with close homology to Csg1p, and observed that loss of both Csg1p and Csh1p completely blocks synthesis of mannosylated sphingolipids. Both proteins are localized to the Golgi, share a region of homology with the yeast mannosyltransferase Och1p, and contain a conserved DXD motif which is part of a catalytic site found in known glycosyltransferases (5). Detergent extracts of $\Delta csg1\Delta csh1$ cells were found to be devoid of IPC mannosyltransferase activity. This result argues in favour of Csg1p and Csh1p being mannosyltransferases, rather than an involvement of both of these proteins in delivery of GDP-mannose or IPC to the transferase-containing compartment. As IPC represents a mixture of molecules that differ in hydroxylation state (6), a possible explanation for yeast having two independent mannosyltransferases might be that they differ in substrate specificity. Now that Csg1p and Csh1p had been identified as IPC mannosyltransferases, a next challenge was to determine the function of Csg2p in MIPC synthesis.

Regulatory role for Csg2p in sphingolipid mannosylation

Results suggesting that Golgi-localized Csg1p and Csh1p form a complex with Csg2p (6) were challenged by observations that Csg2p, when overexpressed, localizes to the ER (7, 8). Could it be that association in a (transient) complex is necessary for efficient export of newly-synthesized Csg1p and Csh1p from the ER to the Golgi? In **Chapter 3** we tested this possibility and found that loss of Csg2p does not prevent Csg1p and Csh1p from reaching the Golgi. So, what does Csg2p actually do?

Csg2p contains a Ca^{2+} -binding domain (3, 7). Based on the observation that Ca^{2+}

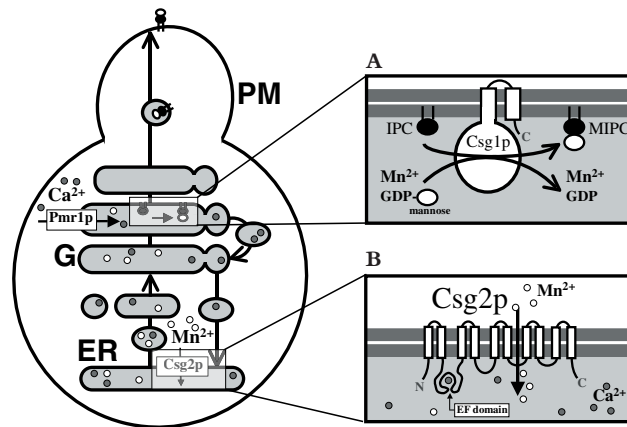


Figure 1. Model for Pmr1p-through-Csg2p controlled Mn^{2+} transport into the lumen of early secretory organelles. (A) The catalytic site of the IPC mannosyltransferase Csg1p is exposed to the Golgi lumen (Chapter 2). GDP-mannose forms a quaternary complex with Mn^{2+} , IPC and the Csg1p catalytic site. (B) Csg2p contains an EF-hand Ca^{2+} -binding domain, here positioned in the lumen. Ca^{2+} pumped by Pmr1p regulates the supply of Mn^{2+} ions required for this reaction by activating Csg2p-mediated Mn^{2+} transport. PM, plasma membrane; G, Golgi; ER, endoplasmic reticulum; IPC, inositol phosphorylceramide; MIPC, mannosyl-IPC; GDP, guanosine-diphosphate.

stimulates the conversion of IPC to MIPC, Uemura *et al.* (6) proposed that IPC mannosyltransferase activity may be regulated by Ca^{2+} through Csg2p. Results from our *in vitro* IPC mannosyltransferase assay showed that Csg2p is not directly required for MIPC synthesis. Moreover, we observed that Ca^{2+} has no influence on this reaction. A burning question therefore remained: How does Csg2p participate in sphingolipid mannosylation? A homology search showed that Csg2p shares a region of homology with the permease component of a bacterial ABC-type Mn^{2+}/Zn^{2+} transport system. Furthermore, it has been reported that protein mannosyltransferases in the Golgi usually require divalent metal ions for activity, with a high preference for Mn^{2+} over other metal ions (5, 9). We found that IPC mannosylation *in vitro* requires Mn^{2+} and that Mn^{2+} uptake into the lumen of intracellular organelles is perturbed in *Δcsg2* cells.

Up until now, Pmr1p was viewed as a Golgi-associated Ca^{2+}/Mn^{2+} P-type ATPase responsible for maintaining the intralumenal Ca^{2+} and Mn^{2+} concentrations in the early secretory pathway of yeast (10–13). However, our data raise an alternative scenario. We suggest that the Mn^{2+} content of the Golgi is determined, at least in part, by Csg2p-mediated Mn^{2+} transport into the ER lumen, and propose the following working model (Figure 1): Pmr1p pumps Ca^{2+} into the lumen of the Golgi, which via retrograde vesicle transport enters the lumen of the ER. Ca^{2+} 'switches on' Csg2p via its Ca^{2+} -binding domain, thereby 'opening' the manganese channel which enables Mn^{2+} to reach the lumen of the ER, followed by vesicular transport to the Golgi lumen. In the Golgi, GDP-mannose forms a quaternary complex with Mn^{2+} , IPC and Csg1p (14, 15). As it has been reported that *E. coli*

GDP-mannose mannosylhydrolase (GDPMH) requires one divalent cation per active site (14) to promote catalysis by facilitating the departure of the GDP leaving group, we propose that also in the case of yeast IPC mannosyltransferases, Mn^{2+} is a co-factor and binds to the active site of the enzyme. It may be clear that the challenging prospect of Mn^{2+} uptake being controlled by Pmr1p through Csg2p is currently under investigation.

Protein versus sphingolipid mannosylation

Our results demonstrated that invertase mannosylation occurs independently of Csg1p and Csh1p, and that the defect in $\Delta csg1\Delta csh1$ cells is sphingolipid specific. In contrast, in $\Delta pmr1$ cells protein mannosylation is affected (10). We were therefore surprised to find that loss of Csg2p apparently did not affect protein mannosylation. An explanation might be that transferases involved in sphingolipid mannosylation require higher levels of Mn^{2+} than can be provided by Pmr1p when Csg2p is absent, whereas transferases involved in protein mannosylation still operate at low Mn^{2+} levels.

Lack of sphingolipid mannosylation is coupled to Ca^{2+} sensitivity

Because of the different hydroxylation states of ceramide, there are five species for each sphingolipid in yeast (6). Cells defective in MIPC synthesis accumulate IPC-C. This renders cells Ca^{2+} sensitive through a mechanism that is not well understood. In order to get a better insight into this process we searched for genes overexpression of which restores Ca^{2+} tolerance in MIPC-deficient yeast cells (**Chapter 4**). A multicopy suppressor screen yielded the gene *HOR7*, originally identified as one of seven hyperosmolarity-responsive genes (16). *HOR7* is the only non-IPC mannosyltransferase-encoding gene capable of restoring tolerance to high Ca^{2+} levels. We found that Hor7p encodes a small (59 residues), type I plasma membrane-associated protein, overexpression of which causes a growth defect at low pH. Our first guess was therefore: Can *HOR7* be a negative regulator of Pma1p, the major plasma membrane H^+ -ATPase? Our results showed that this was not the case. It is feasible that Hor7p overexpression alters the membrane potential, thereby reducing the rate of cation uptake into the cell, and consequently the sensitivity of the cell to toxic cations. This possibility was tested by measuring [^{14}C]methylammonium uptake as an indicator of membrane potential (17, 18). We observed that Hor7p-overproducing cells indeed display a decrease in uptake, and conclude that Hor7p overexpression causes a depolarization of the plasma membrane through a mechanism independent of Pma1p function. As depicted in Figure 2, we propose that Hor7p induces a depolarizing proton pore. This would probably require oligomerization, as it is unlikely that a 59-amino acid protein with a single membrane span forms the proton pore itself. Further analysis will be necessary to understand the mechanism by which Ca^{2+} affects the ion permeability of the plasma membrane of cells lacking mannosylated sphingolipids. One possibility is that Ca^{2+} causes lipid-packing defects via direct interaction with IPC-C. An attractive hypothesis is that sphingolipid mannosylation is required to protect the cells from such interactions that would undermine the barrier function of the plasma membrane.

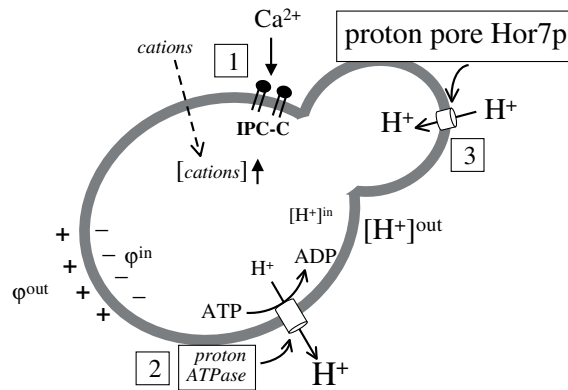


Figure 2. Model for Hor7p function. [1] Ca^{2+} interacts directly with cell-surface exposed IPC-C, which accumulates in IPC mannosyltransferase-deficient yeast. This interaction causes a lipid-packing defect, thereby increasing the ion permeability of the plasma membrane. [2] H^{+} -ATPase Pma1p maintains the plasma membrane electric potential ($\Delta\phi$) and is a major determinant of toxic cation tolerance. [3] Hor7p forms a proton pore, thereby depolarizing the plasma membrane through a mechanism independent of Pma1p function. This would help reducing a Ca^{2+} -dependent influx of toxic cations.

The role of mannosylated sphingolipids in Golgi function

Our finding that $\Delta\text{csg1}\Delta\text{csh1}$ cells exhibit a specific and complete block in sphingolipid mannosylation offered a tool to explore whether this sphingolipid-specific head group modification serves a role in organizing membrane traffic to the plasma membrane. Yeast harbours two transport routes from the Golgi to the plasma membrane, mediated by two classes of post-Golgi secretory vesicles that differ in density and protein content. One class mediates delivery of Pma1p while the other one carries the secretory enzyme invertase among its cargo (19). In **Chapter 2** we showed that blocking sphingolipid mannosylation has no effect on the sorting of cargo proteins into these distinct classes of secretory vesicles. Gas1p, a GPI-anchored protein sorting of which is believed to be depending on microdomains (rafts), segregates together with Pma1p from the invertase route. As the two classes of secretory vesicles were generated at a similar rate in wild type and $\Delta\text{csg1}\Delta\text{csh1}$ cells, we concluded that mannosylated sphingolipids are fully dispensable for their biogenesis. As cells that cannot make IPC are not viable, it remains to be seen whether IPC-enriched microdomains play a role in vesicle biogenesis and protein sorting at the late Golgi.

Although glycosphingolipids have been implicated in protein sorting to the plasma membrane in mammalian cells (**Chapter 1**), our data indicate that glycosphingolipids are not generally required in sorting of secretory proteins.

P-type ATPase-controlled aminophospholipid asymmetry in the Golgi

Members of the P4 subfamily of P-type ATPases are prime candidate aminophospholipid translocases. Previous findings have shown that removal of the yeast plasma membrane P4 ATPases Dnf1p and Dnf2p abolishes inward aminophospholipid transport across the plasma

membrane, and causes an increased cell surface exposure of endogenous PE, and a delay in the internalization step of endocytosis. Both the accumulation of PE at the cell surface and the defect in endocytosis were enhanced by removal of *trans*-Golgi P4 P-type ATPase Drs2p (20). As Dnf3p also localizes to the *trans*-Golgi, it was tempting to speculate that, like Dnf1p and Dnf2p in the plasma membrane, Drs2p and Dnf3p control the transbilayer aminophospholipid distribution in the *trans*-Golgi. In **Chapter 5** we found that post-Golgi secretory vesicles display an asymmetric arrangement of PE, with the bulk concentrated in the cytoplasmic leaflet. This lipid asymmetry was abolished upon removal of Drs2p and Dnf3p (Figure 3). We conclude that aminophospholipid asymmetry is regulated by P4 ATPases at multiple levels along the secretory pathway.

Recent work suggests that Drs2p functions as a PS-specific translocase (21). If this is indeed the case, then the establishment of PE asymmetry in post-Golgi vesicles would require Dnf3p and not Drs2p. However, the precise contribution of Drs2p and Dnf3p in aminophospholipid asymmetry remains to be established.

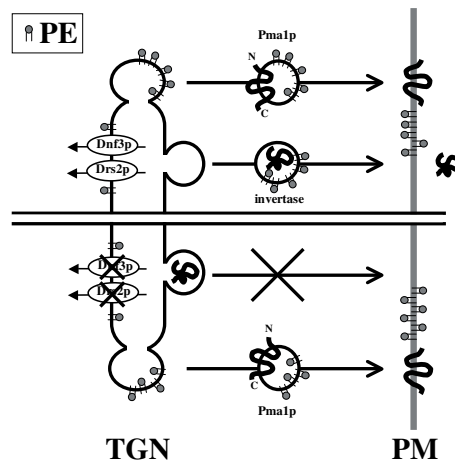


Figure 3. Model for Drs2p and Dnf3p function in lipid asymmetry and vesicle biogenesis. At the Golgi, loss of Drs2p and Dnf3p abolishes aminophospholipid asymmetry across the membrane of post-Golgi secretory vesicles, and inhibits budding of invertase-transporting secretory vesicles. PM, plasma membrane; TGN, *trans*-Golgi network; PE, phosphatidyl ethanolamine; Pma1p, plasma membrane H⁺-ATPase.

Link between aminophospholipid asymmetry and post-Golgi secretory vesicle formation

Several lines of evidence point to a functional link between P4 ATPase-dependent lipid transport and the biogenesis of intracellular transport vesicles. For example, $\Delta dnf1\Delta dnf2$ cells exhibit a cold-sensitive defect in budding of endocytic vesicles whereas $\Delta drs2$ cells are defective in formation of clathrin-coated secretory vesicles that carry invertase and acidic phosphatase to the cell surface (22). Our data indicated that simultaneous loss of Drs2p

and Dnf3p eliminates PE asymmetry in, but does not block formation of, the low-density, Pma1p-containing class of post-Golgi secretory vesicles. These results indicate that the requirement for P4 ATPase-dependent lipid pumping in vesicle formation is not absolute, and that there are fundamental differences in the mechanisms by which the two classes of post-Golgi secretory vesicles are formed.

Concluding remarks

Taken together, we found that two independent mannosyltransferases are responsible for synthesis of mannosylated sphingolipids in the Golgi. Moreover, we discovered that involvement of Csg2p in IPC mannosylation is indirect: our evidence suggests that Csg2p forms a manganese channel, mediating luminal uptake. We saw that the sensitivity to high Ca^{2+} levels displayed by yeast mutants defective in IPC mannosylation can be suppressed by a single membrane-spanning 59-amino acid protein called Hor7p. Hor7p reduces the membrane potential without regulating Pma1p, suggesting that it may form a proton pore. Our results exclude a role for mannosylated sphingolipids in protein sorting in the late Golgi of yeast. We provided evidence that P-type ATPases Drs2p and Dnf3p play a role in post-Golgi vesicle biogenesis and lipid asymmetry. Further yeast studies on the mechanism of Csg2p and Drs2p/Dnf3p are currently being carried out. Approaching glycosphingolipid function in yeast, it is imaginable that a certain amount of inositol-sphingolipid is necessary for proper cell function and that mannosylation forms a tool that protects the cell from the damaging effects caused by overaccumulation of IPC(-C). I expect that further exploitation of the yeast system will continue to elicit a lot of excitement in the field of proteins, lipids and their role in sorting.

References

1. Levine, T. P., Wiggins, C. A., and Munro, S. (2000) *Mol. Biol. Cell* **11**, 2267-2281
2. Dean, N., Zhang, Y. B., and Poster, J. B. (1997) *J. Biol. Chem.* **272**, 31908-31914
3. Beeler, T., Gable, K., Zhao, C., and Dunn, T. (1994) *J. Biol. Chem.* **269**, 7279-7284
4. Beeler, T. J., Fu, D., Rivera, J., Monaghan, E., Gable, K., and Dunn, T. M. (1997) *Mol. Gen. Genet.* **255**, 570-579
5. Wiggins, C. A., and Munro, S. (1998) *Proc. Natl. Acad. Sci. U.S.A.* **95**, 7945-7950
6. Uemura, S., Kihara, A., Inokuchi, J., and Igarashi, Y. (2003) *J. Biol. Chem.* **278**, 45049-45055
7. Takita, Y., Ohya, Y., and Anraku, Y. (1995) *Mol. Gen. Genet.* **246**, 269-281
8. Huh, W. K., Falvo, J. V., Gerke, L. C., Carroll, A. S., Howson, R. W., Weissman, J. S., and O'Shea, E. K. (2003) *Nature* **425**, 686-691
9. Nakajima, T., and Ballou, C. E. (1975) *Proc. Natl. Acad. Sci. U.S.A.* **72**, 3912-3916
10. Durr, G., Strayle, J., Plemper, R., Elbs, S., Klee, S. K., Catty, P., Wolf, D. H., and Rudolph, H. K. (1998) *Mol. Biol. Cell* **9**, 1149-1162
11. Strayle, J., Pozzan, T., and Rudolph, H. K. (1999) *Embo J.* **18**, 4733-4743
12. Cronin, S. R., Rao, R., and Hampton, R. Y. (2002) *J. Cell Biol.* **157**, 1017-1028
13. Sorin, A., Rosas, G., and Rao, R. (1997) *J. Biol. Chem.* **272**, 9895-9901

14. Legler, P. M., Lee, H. C., Peisach, J., and Mildvan, A. S. (2002) *Biochemistry* **41**, 4655-4668
15. Lobsanov, Y. D., Romero, P. A., Sleno, B., Yu, B., Yip, P., Herscovics, A., and Howell, P. L. (2004) *J. Biol. Chem.* **279**, 17921-17931
16. Hirayama, T., Maeda, T., Saito, H., and Shinozaki, K. (1995) *Mol. Gen. Genet.* **249**, 127-138
17. Vallejo, C. G., and Serrano, R. (1989) *Yeast* **5**, 307-319
18. Mulet, J. M., Leube, M. P., Kron, S. J., Rios, G., Fink, G. R., and Serrano, R. (1999) *Mol. Cell Biol.* **19**, 3328-3337
19. Harsay, E., and Bretscher, A. (1995) *J. Cell Biol.* **131**, 297-310
20. Pomorski, T., Lombardi, R., Riezman, H., Devaux, P. F., van Meer, G., and Holthuis, J. C. (2003) *Mol. Biol. Cell* **14**, 1240-1254
21. Natarajan, P., Wang, J., Hua, Z., and Graham, T. R. (2004) *Proc. Natl. Acad. Sci. U.S.A.* **101**, 10614-10619
22. Gall, W. E., Geething, N. C., Hua, Z., Ingram, M. F., Liu, K., Chen, S. I., and Graham, T. R. (2002) *Curr. Biol.* **12**, 1623-1627

Abbreviations

ABC	ATP-binding cassette
ADP	adenosine diphosphate
ALP	alkaline phosphatase
ATP	adenosine triphosphate
BSA	bovine serum albumine
CCCP	carbonyl cyanide <i>p</i> -chlorophenylhydrazone
Cer	ceramide
CPY	carboxypeptidase Y
DMB-	N-(4,4-difluoro-5,7-dimethyl-4-bora-3a,4a-diaza-s-indacene-3-pentanoyl)
EDTA	ethylenediaminetetraacetic acid
Endo H	Endoglycosidase H
ER	endoplasmic reticulum
GalCer	galactosylceramide
GlcCer	glucosylceramide
GPI	glycosylphosphatidylinositol
GSH	glutathione (reduced)
HEPES	4-(hydroxyl)-1-piperazine-ethanesulfonic acid
IPC	inositol phosphorylceramide
LacCer	Lactosylceramide
M(IP) ₂	Cmannosyl-di-IPC
MIPC	mannosyl-IPC
NBD-	N-6(7-nitro-2,1,3-benzoxadiazol-4-yl) amino hexanoyl
PC	phosphatidylcholine
PCR	polymerase chain reaction
PE	phosphatidylethanolamine
PI	phosphatidylinositol
pmf	proton motive force

Abbreviations

PNS	postnuclear supernatant
PS	phosphatidylserine
SDS-PAGE	sodium dodecyl sulfate - polyacrylamide gel electrophoresis
SM	sphingomyelin
SV	secretory vesicle
TGN	<i>trans</i> -Golgi network
TLC	thin layer chromatography
TX-100	Triton X-100

Nederlandse samenvatting

Inleiding

Om het ontstaan en verloop van een ziekte te kunnen begrijpen en beïnvloeden, is het noodzakelijk dat celbiologen fundamenteel onderzoek verrichten om te leren hoe de cel, de kleinste eenheid van leven, functioneert en 'ziek' dan wel 'beter' kan worden.

Mensen hebben meer dan een biljoen cellen, waarvan de meeste gespecialiseerd zijn in een bepaalde functie. Afhankelijk van hun functie leven ze kort tot zeer lang (een mensenleven). Veel micro-organismen bestaan echter slechts uit één cel, die alle eigenschappen draagt die nodig zijn om te overleven. Grofweg zijn cellen op te vatten als ballonnetjes gevuld met een stroperige vloeistof, waarbij de ballon de 'membraan' is (Fig. 1). In de cel bevinden zich organellen ('organen'), elk met een eigen functie, die eveneens omgeven worden door een membraan die de binnenkant van het organel (het lumen) scheidt van de celvloeistof (het cytoplasma).

De celmembraan is opgebouwd uit verschillende typen vetten (lipiden) en een scala aan eiwitten. Membraanlipiden pakken samen tot een dubbellaag (bilaag) waarbij hun wateroplosbare kopgroepen naar buiten zijn gekeerd terwijl de wateronoplosbare vetzuurstaarten naar elkaar toe zijn gericht. Ze hebben een semi-vloeibaar karakter en vormen als het ware een tweedimensionale 'zee', waarin zich de eiwitmoleculen bevinden. Op grond van hun structuur kunnen membraanlipiden verdeeld worden in drie hoofdklassen: glycerolipiden, (glyco-)sfgingolipiden en cholesterol.

Welke belangrijke processen spelen zich nu af in welk organel? Het kunnen beantwoorden van deze vraag staat hoog op de agenda van ons onderzoeksprogramma. De celkern bevat het erfelijk materiaal, het DNA. In opdracht van de kern worden eiwitten gemaakt op ribosomen die zich los in het cytoplasma of op het endoplasmatisch reticulum (ER) bevinden. Het ER is een ingewikkeld netwerk van membranen. In het ER worden membraanlipiden gemaakt, of voorlopers daarvan. Bij glycosfingolipiden bijvoorbeeld, wordt pas in het Golgi, het centrale sorteringsstation van de cel, de suiker ('glyco') aan

de kopgroep toegevoegd. Het Golgi modificeert derhalve de halffabrikaten van het ER en sorteert en verdeelt ze over hun verschillende eindbestemmingen. Van het Golgi kunnen zich namelijk verschillende transportblaasjes afsnoeren die zich verplaatsen naar het juiste organel of naar de plasmamembraan. Met deze membraanstructuren versmelten zij, onder uitscheiding van hun inhoud naar het lumen van het betreffende organel of naar de buitenzijde van de cel. Hoe een eiwit in het juiste transportblaasje terecht komt hangt af van de lipidenstelling van het stukje Golgi-membraan waarvan zich het blaasje afsnoert. Als er bij sortering in het Golgi-apparaat fouten optreden, worden eiwitten en lipiden niet, of naar de onjuiste eindbestemming, getransporteerd waardoor de cel 'ziek' wordt en zijn functie niet meer kan uitoefenen. Hoe de samenstelling van een membraan tot stand komt, is daarom een brandende vraag waar vele wetenschappers het antwoord op proberen te vinden.

Sfingolipiden hebben de bijzondere eigenschap om, in een omgeving van glycerolipiden, met cholesterol spontaan samen te klitten tot sfingolipide-cholesterol complexen die als vloten rondrijven in de 'zee' (qua verhouding zou je beter 'zwembad' kunnen zeggen) van overige membraanlipiden in de plasmamembraan. De engelse term voor zo'n complex is dan ook 'raft' (Fig. 1). De indicatie dat rafts specifieke eiwitten aantrekken en daarmee een belangrijke rol in sortering spelen, heeft tot logische modellen geleid. Direct bewijs voor de betrokkenheid van sfingolipiden bij eiwitsortering ontbreekt echter. Fundamenteel onderzoek heeft de betrokkenheid van rafts bij het ontstaan van verschillende ziektes aangetoond. Met andere woorden: fundamenteel onderzoek is nodig om tot de ziektebron te komen.

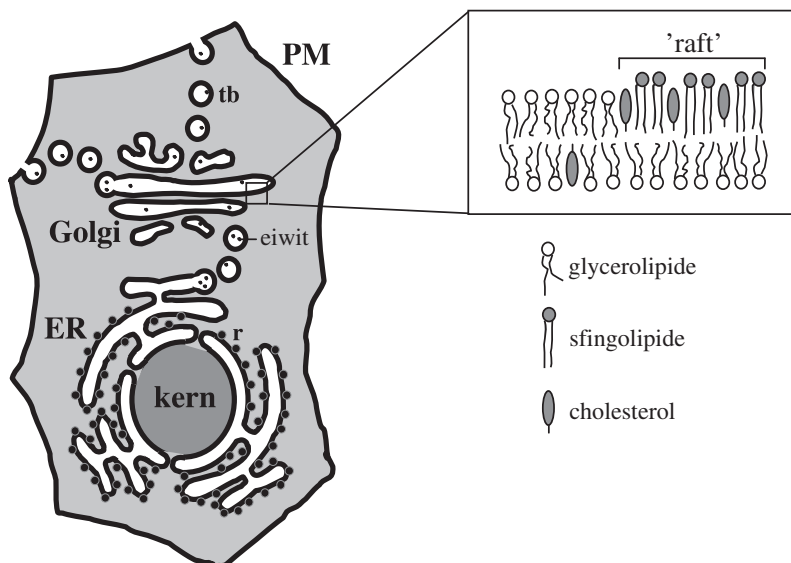


Figure 1. Schematische weergave van een cel. PM, plasmamembraan; ER, endoplasmatisch reticulum; tb, transportblaasje; r, ribosoom; raft, sfingolipide-cholesterol complex. Alle zwarte lijnen stellen membranen voor, m.a.w. lipide bilagen.

Het centrale doel in mijn onderzoek was om, naast het effect dat verandering van de membraanlipidensamenstelling heeft, het effect van verandering van de transbilag-lipidendistributie op de functie van het Golgi te bestuderen.

Het onderzoek

Aangezien de plasmamembraan sterk verrijkt is in glycosfingolipiden t.o.v. membranen van organellen, hebben we allereerst gekeken naar de wijze waarop deze lipiden vanuit het Golgi naar de plasmamembraan vervoerd worden. Aangezien een dier veel verschillende glycosfingolipiden produceert en de gist *Saccharomyces cerevisiae* zijn simpelste sfingolipide, inositolfosforylceramide (IPC), omzet in slechts twee gesuikerde vormen, besloten wij deze gist als modelsysteem te gebruiken. Het grote voordeel van gist is dat het relatief makkelijk is om de sfingolipide-structuur te wijzigen door 'genetische manipulatie' (aanpassen van het erfelijk materiaal om nieuwe gewenste eigenschappen te introduceren), aangezien belangrijke genen die betrokken zijn bij sfingolipide-synthese bekend zijn. Tevens heeft gist net als dierlijke cellen twee transportroutes die van het Golgi naar het plasmamembraan lopen.

Aan het begin van ons onderzoek was er weinig bekend over de enzymen die betrokken zijn bij de mannosylering van de sfingolipide-kopgroep (het toevoegen van een 'mannose'-residu, een suiker). In Hoofdstuk 2 vonden wij dat door de Golgi-enzymen Csg1p en Csh1p samen uit te schakelen de cel helemaal geen glycosfingolipiden meer kan maken en concluderen we dat gist twee onafhankelijke mannosyltransferases bezit. De reden waarom gist er twee heeft is nog onduidelijk.

In Hoofdstuk 3 tonen we aan dat het *CSG2*-gen betrokken is bij transport van mangaan-ionen naar het lumen van het ER. Uit eerder onderzoek was reeds gebleken dat dit gen, naast *CSG1*, betrokken is bij de productie van glycosfingolipiden. Vandaar dat wij graag wilden weten op welke wijze Csg2p (het eiwit waarvoor het *CSG2*-gen codeert) functioneert. Onze vondst verklaart waarom cellen die het *CSG2*-gen niet hebben, slechts heel weinig glycosfingolipiden kunnen maken: Csg1p en Csh1p hebben beide mangaan nodig om hun werk te kunnen doen. Zij bevinden zich allebei in het lumen van het Golgi, dus als mangaan daar niet wordt afgeleverd komt glycosfingolipide-synthese op non-actief te staan. Het feit dat Csg2p in de ER-membraan zit compliceert de zaak: wij denken dat er in het Golgi een calcium-pomp zit, die er voor zorgt dat calcium via transportblaasjes in het lumen van het ER terecht komt, daar het enzym Csg2p activeert, dat vervolgens zijn mangaankanaal opent. Hierdoor komt mangaan in het lumen van het ER terecht en vervolgens via transportblaasjes in het lumen van het Golgi, alwaar het Csg1p en Csh1p in hun behoefte voorziet.

Cellen die geen glycosfingolipiden maken kunnen niet, zoals gewone gistcellen, groeien in aanwezigheid van calcium. Deze Ca^{2+} -gevoeligheid wordt veroorzaakt door de ophoping van IPC. In Hoofdstuk 4 laten we zien dat de Ca^{2+} -gevoeligheid kan worden opgeheven door 'overexpressie' van het zogenaamde *HOR7* gen. Een mogelijke verklaring is, dat dit gen ervoor zorgt dat er 'gaatjes' in de plasmamembraan ontstaan, waardoor H^+ -ionen naar binnen kunnen lekken. Hierdoor neemt de membraanpotential af, zodat Ca^{2+} en andere schadelijke kationen

buiten de cel blijven. De *HOR7*-overexpresserende cellen hebben weliswaar een verlaagde pH, maar kunnen hierdoor wel groeien in de aanwezigheid van calcium.

Terug naar de glycosfingolipiden. Onze vondst in Hoofdstuk 2 dat *Δcsg1Δcsh1* cellen geen glycosfingolipiden kunnen maken, bood ons gereedschap om te onderzoeken of de suikerkopgroep een rol speelt in eiwitsortering naar de plasmamembraan. Wij vonden echter dat in gist, in tegenstelling tot wat gepubliceerd is over dierlijke cellen, de afwezigheid van glycosfingolipiden geen nadelige gevolgen heeft voor eiwitsortering van de door ons bestudeerde eiwitten tot gevolg had. Glycosfingolipiden blijken dus niet betrokken te zijn bij eiwitsortering in het Golgi, een resultaat waarmee we echter het mechanisme waarmee post-Golgi transportblaasjes worden gevormd, onopgehelderd lieten.

Om inzicht te krijgen in bovenstaand mechanisme, gaan we in Hoofdstuk 5 in op het fenomeen 'lipiden-asymmetrie', d.w.z. dat de buitenste laag van de plasmamembraan een andere lipidenamenstelling heeft dan de binnenste laag. Deze asymmetrie wordt in stand gehouden door 'actieve' lipide-translocatoren, ATPases (d.w.z. enzymen die ATP omzetten in energie), van welke de identiteit onbekend is. Wij tonen aan dat gistcellen zonder de ATPases Drs2p en Dnf3p niet in staat zijn om de lipiden-asymmetrie van hun post-Golgi transportblaasjes op weg naar de plasmamembraan te handhaven. De afwezigheid van lipiden-asymmetrie in de plasmamembraan heeft invloed op de opname van voedseldeeltjes (dit proces wordt endocytose genoemd) en brengt daarmee de gezondheid van de cel in gevaar.

En.... is er nu een duidelijk antwoord gekomen op de centrale vraagstelling?? In de afgelopen vier jaar heb ik membraanlipiden bestudeerd. Mijn werk laat zien dat glycosfingolipiden in gist geen rol spelen bij eiwitsortering in het Golgi. Verder heb ik een functie kunnen toekennen aan een aantal eiwitten: Csg2p, Hor7p en het Drs2p/Dnf3p-duo. Wat betreft de rol van glycosfingolipiden blijft er onduidelijkheid. Het is niet ondenkbaar dat een gistcel een bepaalde hoeveelheid sfingolipiden nodig heeft om goed te kunnen functioneren en dat omzetting in glycosfingolipiden dient om de cel te beschermen tegen schadelijke effecten die veroorzaakt worden door ophoping van IPC.

Deze samenvatting laat zien dat wetenschappelijk onderzoek niet altijd datgene oplevert waarop bij aanvang is ingezet. Echter, een aantal nieuwe inzichten die voortkomen uit dit werk hebben ons weer stappen vooruit gebracht. Het moge duidelijk zijn dat de toekomst nog veel spannend (gist-)werk te bieden heeft!

Dankwoord

Wat een mooie en spannende tijd heb ik achter de rug! En wat zijn het veel mensen die mij de afgelopen jaren hebben gemotiveerd en gesteund. Ik had het dankwoord kunnen reduceren tot één pagina, maar dacht: "Nee, dat doe ik niet. Ik doe lekker uitgebreid. Ik doe lekker sentimenteel." Want er is toch al zo weinig sentiment in de wereld.

Lieve Joost, het klinkt dramatisch (maar dat past bij ons): zonder jou was het me nooit gelukt om op deze manier te promoveren. Jij durfde het aan om mijn begeleider te worden, terwijl ik met mijn technische achtergrond een hoop biologische basiskennis miste. Je hebt enorm geïnvesteerd en mij ingewijd in de wereld der celbiologie. Dank voor al je briljante ideeën (ook al was het soms best frustrerend dat ze bijna altijd beter waren dan die van mezelf...!), je geduld, je humor en je vertrouwen. Ik schreef drie jaar geleden niet voor niets in de Elsevier influx achter 'Leermeester': *Joost Holthuis. Een briljante wetenschapper en een leuke vent met humor*. Ik wens jou, Laurence, Pierre en Margot het allerbeste toe en hoop dat onze paden in de toekomst nog vele malen zullen kruisen.

Lieve Gerrit, wat was het een feest om onderzoek te doen binnen een groep met jou als afdelingshoofd. Al die jaren heb je, naast het (actief!) overdragen van je wetenschappelijke kennis en enthousiasme én je liefde voor een pilsje, gezorgd voor een constant positieve sfeer binnen onze groep. Dat vind ik een enorme prestatie en daar ben ik je zeer dankbaar voor. Ook al was je niet altijd direct bij mijn onderzoek betrokken, daar waar ik hulp bij je zocht (o.a. bij het schrijven van de discussie), stond je klaar.

Dear Sophie, how I have missed you the past half year! Thanks for your friendship and for the many times that I was allowed to complain about my experiments, or science in general... You are one of the kindest persons I have ever met. And one of the strongest. I wish you lots of happiness for the future with Geoffrey and the lovely Sarah.

Lieve Hein, wat geniet ik van het feit dat jij weer terug bent. Drie jaar geleden waren Sophie en ik jouw paranimfen en toen verliet je ons om voor twee jaar naar Dresden te gaan... Ik vind het geweldig om te zien wat een inspirator je bent voor Jasja, David, Sandra, Suzanne en Sylvia. En zelfs voor mij maakte je tijd om mee te denken als ik vast-, en Joost

in z'n scherm- zat. Gaan we snel met Marwyske en Lodewijk naar Lille?

Lieve Maarten, wat is het samengaan van Gerrits groep met de jouwe een verrijking geweest. Niet alleen in wetenschappelijk opzicht, maar tevens de rust die jij uitstraalt en je immer luisterend oor zijn mede verantwoordelijk voor eerder genoemde positieve werksfeer. Dank voor al je hulp (o.a. bij het schrijven van de discussie en samenvatting) en dank voor onze leuke gesprekken over de keuzes die een mens in dit leven moet, of mag, maken.

Lieve Klazien, David en Patricia, lieve roomies, dank voor jullie hulp, geduld en gezelligheid! Klaas, heerlijk om met jou over Joost te roddelen (en met hem weer over jou) en fijn dat ik af en toe even wat stoom bij je mocht afblazen. En David, we waren leuke 'Assistenten in Afdeling' voor elkaar! Ik vond het (bijna) elke dag een genoegen jullie te zien, te horen en te ruiken; hopelijk was dit wederzijds.

Lieve Dorothy, wat kan ik zeggen? Met jou waren het heerlijke én bevlogen jaren en ik geloof er dankzij jou nog steeds heilig in dat het succes van een experiment afhankelijk kan zijn van de afwezigheid van 'het boze oog'...

Dear Thomas, Sigrún and Antje, 'out of sight' does not mean 'out of mind'. At least, not in your case. I have nothing but good memories of the time that you were in the lab. Thanks very much for all your help and friendship, and I'm looking forward to visiting you (again).

Lieve Jasja, Joep, Cécile, Ruud, Suzanne, Nanette, Jessica, Fred, Dirk, Seléne en Martin: ook al deelden we geen kamer, heel veel dank voor jullie hulp en gezelligheid! Lieve Janneke, Dick en Rob: ook jullie veel dank voor alle hulp en de leuke gesprekken. Dear Guillaume, Sandra, and Sylvia: it was short, but it was nice... Thanks for all the fun in and outside the lab!

En dan de lieve hardwerkende studenten... William, als 'mijn eerste' was jij enkele malen getuige van mijn sporadisch licht ongenueanceerd taalgebruik, maar gelukkig liet je je niet afschrikken. Hoofdstuk 2 is een mooi resultaat van onze gebundelde krachten. Alfred, als 'mijn laatste' was jij helaas eveneens getuige van mijn sporadisch licht ongenueanceerd taalgebruik. Jij liet je wél afschrikken en was na drie maanden spoorloos verdwenen. De laatste keer dat je gezien bent, is in een zweefvliegtuig boven Vianen... Waar je ook bent, wees trots op ons hoofdstuk 3.

Lambert, mijn lievelingsstudent, mijn 'stille wateren hebben diepe gronden'... Ongelooflijk hoe goed, hard en zelfstandig jij gewerkt hebt: heel veel dank voor deze meer dan prettige samenwerking en ik voorspel jou een grote toekomst. Tot slot Maurice, de toffe gozer. Dank dat jij de laatste experimenten voor hoofdstuk 2 bij elkaar hebt gepipetteerd. Ik bewonder je keuze om na je Australië-avontuur, nu voor een toekomst samen met Katja in Finland te kiezen en wens jullie veel succes en geluk. En gozer, dank voor alle gein.

Dear Nele, during our collaboration, the distance Utrecht-Berlin formed a handicap. Nevertheless, you showed me that every handicap can be overcome, as long as you're determined enough. Thanks very much for all your hard work and I think we can be very proud of chapter 5.

Ook mijn oud-collega's uit het AMC wil ik hartelijk danken voor de leuke tijd die ik de eerste twee jaar van mijn onderzoek dankzij hen heb gehad. Lieve Trees en Ilse, jullie in

het bijzonder dank ik voor alle hulp en de interesse die jullie toonden, ook na mijn vertrek naar Utrecht.

Lieve Rutger, dank voor jouw aandeel in hoofdstuk 3 én dank voor je vrolijke glimlach! Lieve Renske, ik zal onze lunch-dates missen. Heel veel succes met jouw laatste loodjes.

Lieve Ingrid, zonder jou was de lay-out van mijn proefschrift nooit zo strak geworden. Heel veel dank voor je tijd en je geduld. Ook veel dank voor de vele keren dat Jan, Aloys en jij mij uit de brand hebben geholpen met publicatie-PDFjes én voor onze leuke chimpansee-gesprekken!

En toen was er licht. En leven. Buiten het lab. Godzijdank...:

Lieve Bumpertjes, lieve Forte- en OD-babes, lieve nous-sommes-sept-vriendinnen, dank voor de heerlijke afleiding waar jullie voor zorgden! Wat heb ik jullie verwaarloosd het afgelopen jaar en wat verheug ik me op de inhaalslag.

Lieve Joos, gekkie, op de Kerkstraat is het promotie-idee gaan leven. Dank voor je luisterend oor, je wijze raad en je aanmoediging. Lieve Beel, zo'n smaakvolle en originele omslag kan alleen van jouw hand komen. Enorm veel dank voor alle tijd en energie die je hierin hebt gestoken.

Lieve Diet, ook al ben je steeds in Verwegistan, je bent nimmer uit mijn gedachten! En lieve Ot, ik verheug me op weer een ouderwets Haags (of Velps, of Brezzo's...) bakkie met jou!

Lieve Cleo en Mach, mijn allerliefste paranimfen, tranen krijg ik in mijn ogen als ik denk aan alle steun, advies en liefde die jullie mij de afgelopen tijd hebben gegeven. Ik prijs mijzelf enorm gelukkig dat ik jullie op 17 december aan mijn zijde heb.

Lieve Paul en Willemijn, jullie vormen het levende bewijs dat schoonfamilie die attent, warm en als thuis is, wel degelijk bestaat.

Lieve pap en mam, dank voor jullie geweldige steun en vertrouwen en even onder ons: jullie zijn natuurlijk altijd mijn échte inspiratoren geweest! Lieve Job en Herm, lieve broers, ook al zijn jullie trots (daar ga ik gewoon maar even vanuit), jullie zullen nooit zo trots zijn als ik op jullie ben.

Lieve oma, ook al hebt u nooit begrepen waarom een vrouw zonodig hoogopgeleid moet zijn, toch zijn we het over één ding eens: een optimist heeft de halve wereld.

Lieve Lody, met jou is mijn wereld een dansfeest.

Quirine

Curriculum Vitae

Catherine Quirine Lisman werd geboren op 2 april 1974 te Oss. Zij sleet haar eerste levensjaren in het Gelderse Rozendaal en behaalde in 1992 het Atheneum Dipoma aan het Rijnlands Lyceum te Oegstgeest. Datzelfde jaar begon zij de studie Scheikundige Technologie aan de Technische Universiteit Delft en slaagde in 1998 voor haar ingenieursexamen.

Eind 1998 vertrok zij naar West-Afrika, om vijf maanden vrijwilligerswerk te doen in een ziekenhuis en in een chimpansee-rehabilitatiecentrum. In 1999 werkte zij bij Merck Sharp & Dohme B.V. en in 2000 startte zij haar promotieonderzoek bij de afdeling Celbiologie en Histologie van de faculteit Geneeskunde aan de Universiteit van Amsterdam en bij de afdeling Membraan Enzymologie van de faculteit Scheikunde aan de Universiteit Utrecht. Het in dit proefschrift beschreven onderzoek werd uitgevoerd onder leiding van Dr. J.C.M. Holthuis en Prof. Dr. G.F.B.P. van Meer.

Sinds oktober 2004 is Quirine werkzaam bij de afdeling Chemische Wetenschappen van de Nederlandse Organisatie voor Wetenschappelijk Onderzoek in Den Haag.



Publications

van Meer G. and **Lisman Q.** (2002) Sphingolipid transport: rafts and translocators. *Journal of Biological Chemistry* 277, 25855-8.

Lisman Q., Pomorski T., Vogelzangs C., Urli-Stam D., de Cocq van Delwijnen W., and Holthuis J.C.M. (2004) Protein sorting in the late Golgi of *Saccharomyces cerevisiae* does not require mannosylated sphingolipids. *Journal of Biological Chemistry* 279, 1020-9.

Lisman Q., Alferts, A.P., Staffhorst R., and Holthuis J.C.M. (2004) Sphingolipid mannosylation in yeast requires Csg2p-dependent manganese transport into the lumen of early secretory organelles. *Manuscript in preparation.*

Lisman Q., Urli-Stam D., and Holthuis J.C.M. (2004) *HOR7*, a multicopy suppressor of the Ca^{2+} -induced growth defect in sphingolipid mannosyltransferase-deficient yeast. *Journal of Biological Chemistry* 279, 36390-6.

Lisman Q., Alder-Baerens N., Luong, L., Pomorski T., and Holthuis J.C.M. (2004) Loss of the yeast *trans*-Golgi P-type ATPases Drs2p and Dnf3p disrupts aminophospholipid asymmetry in Pma1p-containing secretory vesicles. *Manuscript in preparation.*

